School of Engineering

Leak Detection in Gas Transmission Pipelines

Michael R Sullivan

This thesis is presented for the Degree of
Master of Engineering (Mechanical Engineering)
of
Curtin University of Technology

February 2003

Declaration

This thesis contains no material which has been accepted for the award of any other degree or diploma in any university.

To the best of my knowledge and belief this thesis contains no material previously published by any other person except where due acknowledgment has been made.

Signature: .....

Date: .....30/05/04.....

SUMMARY

This dissertation applies a commercial flow simulation software package together with common signal processing techniques to the task of accurately detecting leakage in a large commercial gas pipeline. The techniques developed significantly improved the ability to produce accurate, reliable and stable leak detection predictions for the gas transmission pipeline studied and can be applied generally to other pipelines as well. Recommendations for minimum pipeline requirements to implement successful leak detection are also detailed.

There are several commercial software packages available that perform some form of leak detection via system modelling. However, due to the commercial aspects of these products, vendors do not publish the detailed methods of leak detection. This thesis identifies the fundamental techniques required to have accurate and reliable leak detection on a gas transmission pipeline, whilst taking into account the lack of measurement data typically encountered on most gas pipelines.

The investigation confirmed that a mass balance technique could be successfully used to produce stable leak detection results for compressible flow in gas transmission pipelines. This leak detection [using mass balance] can be achieved without flow measurement along the pipeline, instead, using only pressure and temperature measurements. Although it is recognized that flow measurement data will greatly improve the ability to detect leaks, the focus of this work is on pipelines where this flow measurement data at intermediate points along the pipeline is not available. It was also demonstrated the reliability of the leak detection was improved by the application of on-line signal processing techniques at various stages of the data processing. It was clear early into the investigation that the majority of the errors within the leak detection model were created by random errors from the input field data. These non-systematic errors from the measurement data that included pressure and temperature, produced interference with model output. This interference resembled random "white" noise that was removed by a combination of well established data filtering techniques.

The most appropriate process of calculating leak detection flow was determined after analysing the results of different techniques applied to large quantities of actual pipeline operating data. The validation of the on-line techniques developed provides a valuable resource for those wishing to implement similar leak detection schemes elsewhere. Furthermore a software environment was chosen which incorporated an open input and output platform for data that could be interfaced with any operating system. Therefore these techniques can be applied to the numerous Supervisory Control and Data Acquisition (SCADA) systems in operation throughout the gas transmission industry, to provide a low cost solution to leak monitoring.

ACKNOWLEDGMENTS

The author would like to thank Dr David Devenish for his guidance throughout the development of this thesis.

David Moss, Manager of AGL Pipelines (WA) Pty Ltd is thanked for his support and encouragement during this industry project.

The freedom permitted by the management of Goldfields Gas Transmission Pty Ltd, to perform analysis on system data from the pipeline is greatly appreciated.

Finally, the author would like to thank his wife, who has tolerated the long hours of her husband being away from home.

DEDICATION

to Mum

"Never regard study as a duty, but as the enviable opportunity to learn to know the liberating influence of beauty in the realm of the spirit for your own personal joy and to the profit of the community to which your later work belongs."

Albert Einstein

CONTENTS

LIST OF FIGURES

LIST OF TABLES

NOTATION

The notation for quantities used generally throughout the thesis is listed below. Other notation that is used in a limited context is defined as it is introduced within the text.

a	Weights for weighted average
A	Cross sectional area of pipeline section
$\dot{B}$	Rate of gas leak (TJ/day)
B	Total amount of gas leak over a given time period (TJ)
D	Internal diameter of pipe section (mm)
f_c	Cut off frequency for low pass filter (Hz)
f	Friction factor
k	Constant of proportionality
L	Energy of gas within pipeline section. Also known as linepack (TJ)
n	Number of samples
P	Pressure at a point along a pipeline section (MPag)
$\overline{P}$	Average pipeline section pressure (MPag)
R	Gas Constant (KJ/kg.K)
Re	Reynold's number
$\overline{T}$	Average pipeline section temperature (K)
t	Time (day)
U	Unaccounted gas over a given period from energy balance (TJ)
V	Volume of pipeline section (m^3)
$\dot{W}$	Energy flow rate into or out of a pipeline section (TJ/day)
W	Accumulated energy from into or out of a pipeline section (TJ)
Z	Distance along a pipeline section (km)
ε	Surface roughness (mm)
ρ	Gas density (kg/m^3)
σ	Standard deviation or uncertainty of sample

1.0 INTRODUCTION

1.1 General

The ability for prompt and reliable detection of uncontrolled releases of gas, commonly referred to as leaks in long gas transmission pipelines has been an elusive goal in the industry. Uncontrolled release of gas into the atmosphere has both an economic and environmental impact as noted by Tollefson (1972) on both pipeline operators and the community. Often these incidents have to be reported to the pipeline regulatory authority in the country the pipeline is located. The early detection of leaks can prevent both environmental hazards and financial loss. Leak detection can be classified in the following main categories:

- positive detection;
- inferred detection.

Positive detection relates to ways, either by physical detection such as operators or the general public detecting a gas odour or dead vegetation, or by employing sensors that such as fibre optic cables that will alarm if a rupture or gas quantities are detected within proximity to a sensor as outlined by Bowles and Morrow (1996) and Zhang (1996). This method explicitly confirms the presence of a leak without the reliance on related observations or measurements. Inferred detection employs the use of related measurements to infer the presence of a leak within a region. This can include the use of a mathematical model to perform a mass balance on sections within a pipeline, the examination of pressure rates of change or pulses at measured intervals. These methods are only as accurate as the data used, and cannot explicitly confirm the presence of a leak alone, but are a useful tool for monitoring possible leaks. This thesis investigates applying signal processing techniques to a model simulating a gas transmission pipeline in order to obtain reliable leak detection information from the model.

In long transmission-lines, it is often not feasible to install gas detection equipment at suitable intervals to provide a reliable gas detection system. At above ground

stations such as compressors and processing facilities, this method is feasible and is often employed successfully. However, the majority of gas pipelines are buried and range from a few hundred to a few thousand kilometres in length, thus making this process impractical to implement. Most existing gas transmission pipelines typically only monitor pressure and temperature at intervals along the pipeline length. Ideally gas flow measurement at these points would be used in an on-line model to infer the presence of a leak. Since main line flow measurement is sparse on the Goldfields Gas Pipeline (as with most gas transmission pipelines), it will be investigated whether reliable leak detection can be achieved with pressure and temperature measurements alone at these locations. In addition to lack of measured data for the model, measurement errors due inherent uncertainty from the measuring equipment introduce further uncertainty into the model results. Due to uncertainty present in all input data from both systematic and non-system errors, "false" leaks may be inferred and more importantly, genuine leaks may be undetected. The effect of field measurement uncertainty on leak detection is described by Turner (1987) and Wike (1993). Thus when no actual leaks are present, the leak flow output from the model should always be zero, however due to the inherent inaccuracies in measurement for both dynamic and physical data, this is unlikely to occur.

The mathematical model uses conservation of mass equations to solve for unknowns at each node including pressure and temperature, based on the physical information supplied to the model. Therefore when field data such as pressure and temperature are used in the model, the conservation of mass condition is compromised due to firstly, inaccuracies in measurement of the field data, and secondly, discrepancies between the model and actual pipeline. The magnitude of the conservation of mass imbalance is commonly referred to as a leak flow. Due to the inherent uncertainty of field measurements, the leak flow values will contain non-systematic errors or noise. In addition to non-systemic errors there can be systematic errors present such as errors in calibration or faults with the measuring equipment. Systematic errors can be eliminated by the calibration of the model by adjusting physical quantities such as the pipeline roughness of a section. Non-systematic errors cannot be eliminated easily as they are random and can only be described in terms of a normal distribution about a mean, which can be considered the "true" value. For this reason, signal

processing techniques are applied to reduce the effect of non-systematic errors, enabling the correct magnitude of leak flows and their locations to be identified.

Any uncertainty with real time field measured data will have an impact on the accuracy of the model. Therefore if it is not possible to reduce the uncertainty of an input measurement, a method must be developed that will address these uncertainties on both the measured inputs, and leak flow outputs of the model. Some other sources of uncertainty common to all pipelines are instrument repeatability, dead-band filtering, time stamp error, changes in fluid properties, and even changes in the physical characteristics of the pipeline system itself. These data uncertainties combine to conceal a leak from detection, because if a leak does not cause a measurement to change by more than its uncertainty, that measurement cannot be used to infer the presence of a leak as illustrated by Wike (1993).

The preceding areas are addressed by this thesis through research and testing with actual pipeline data obtained from the Goldfields Gas Transmission (GGT) Natural Gas Pipeline of Western Australia. The mathematical model was developed using a commercial package called FlowTran, owned and marketed by William J Turner Pty Ltd. The data filtering techniques and subsequent program code are developed separately within a Microsoft Visual Basic / Excel ™ environment, examples of which are illustrated by Rakesh (1997). A standard Microsoft Excel ™ interface is supplied with FlowTran, and this was used as the basis of all program development.

This research is an emerging field within the gas pipeline industry. With more stringent greenhouse gas regulations, it is imperative that emissions are identified quickly. In this study, the feasibility of implementing a leak detection system using mathematical modelling is investigated. Limitations of the system are identified, and recommendations for minimum system requirements to produce accurate results are made. Accuracy is defined in this report by two parameters, the smallest leak flow rate detectable, and the number of time this can be detected without false alarms under normal operating conditions.

1.2 Previous Work in the Area of Leak Detection

The successful implementation of reliable leak detection systems by means of on-line mathematical modelling is still an emerging area in the field of gas transmission pipelines. This is due to many of the commercial software packages not having been validated by actual operating data and published in the public domain. There are numerous published works for on-line modelling and real time simulations of gas transmission pipelines, which include Graham *et al.* (1989), Turner and Mudford (1992) and Zhang (1996). However there are no publications with specific emphasis on leak detection in gas transmission pipelines and results using actual operating data. The more common publications relate to process optimisation and prediction of events.

There are works that relate to leak detection techniques other than on-line modelling. These include work by Schwendeman (1987) for monitoring and leak detection of underground liquid hydrocarbon storage systems, Hardy (1978) whose work outlined various physical detection systems, and Butler (1982) who covered the leak detection options for liquid hydrocarbon transmission pipelines. It should be noted that the implementation of leak detection has been more successful in liquid pipelines compared to gas pipelines. This is due to liquids not undergoing compressible flow during transportation, which greatly reduces the complexity of flow and density calculations. In addition to the computational simplicity of incompressible flow, because a liquid hydrocarbon leak is more dangerous than a gas hydrocarbon leak, more levels of safety management are commonly employed. Methods of containment and automatic control of leaks are described by Bowles and Morrow (1996).

The work of Wike (1993) and Zhang (1996) utilised actual pipeline data. However Wike's papers related to proprietary software, therefore the leak detection techniques were omitted from the public domain. Zhang focused on the operating data from liquid pipelines where success was experienced with the implementation. The most significant published work for a leak detection technique utilising on-line modelling of a gas transmission pipeline is by Turner (1987), which was preceded by a more

comprehensive article including leak location estimation, Turner and Mudford (1988) although published later. These papers were both approached theoretically, making assumptions for the uncertainty of real time data.

The basis of the leak detection methodology proposed by Turner and Mudford (1988) is the utilisation of a mass balance on individual pipeline sections. The pipeline section is typically designated the portion between two pressure or flow measurements. This is developed in more detail later in Section 3.5. Since compressible flow allows significant changes of mass within a pipeline section, large differences between flow into and flow out of a pipeline section may occur during transient conditions, even without the presence of a leak. Thus it is a requirement for an accurate transient model of the pipeline system, to avoid the generation of false leaks caused by devices such as compressors during intermittent operation.

Turner and Mudford (1988) acknowledged a significant component of systematic and random measurement noise exists on all measured quantities. These measurement errors lead to errors in the calculated pipeline section imbalances. The systematic errors can be eliminated by comparing the model against measurement data and adjusting quantities such as pipe wall roughness to negate the difference. The non-systematic or random measurement error was reduced by averaging a pipeline section leak flow over several measurement periods, which is discussed in further detail in Chapter 5. Statistical analysis was then employed to investigate the propagation of noise, and hence determine an acceptable leak detection threshold. An algorithm for determining the location of a leak along a pipeline section was introduced, however an alternative technique is introduced in this work that allows the estimation of leak location within a pipeline section if pressure and flow are available at the end points of the section. Turner and Mudford's algorithm was based on the ratio of leak flow between adjacent pipeline sections. The algorithm employed in this work, makes the assumption that some form of flow measurement is present at each end of a section where a leak exists. The behaviour of these flows can then be used to estimate the leak location.

Turner and Mudford initially tested their leak detection process against noise free simulated measurement data with induced leaks ranging from 2% to 50% of pipeline flow. After this was simulated, measurement noise was introduced by specifying a standard error for a measurement and multiplying this by a series of normally distributed, pseudo-random numbers that have a standard deviation of unity and a mean of zero. The standard error assumed for pressure measurement was 20 kPa, which agrees well with the allowable error of a calibrated pressure transmitter. The noise for flow and temperature measurements was set to zero, which is optimistic even though the impact of these measurements on leak flow is less than pressure.

Turner (1987) introduced the use of moving weighted averages and quantifying the optimal number of measurement periods to average the leak flow results to obtain reliable information. He concluded that his method provides a factor of three reduction in threshold for leak detection averaged over fifty measurement periods compared to no averaging. The derivation of equations relating leak sensitivity to the number measurement periods is listed in Section 4.4. The compromise with filtering data to reduce the leak detection threshold is the introduction of a time delay in the detection of the true leak magnitude, and this time delay is proportional to the number of measurements averaged. It should be noted that in both Turner's works, the data filtering was applied only to the output of the model, namely the leak flows. The only processing of input data was the limitation of these values to ±3.5 standard deviations. The possibility of filtering the input data to the model in the same manner as the output data was not considered extensively. This concept is introduced in the course of this present work.

1.3 Present Objectives and Outline of Content

Given the lack of public domain reporting of leak detection studies, this thesis seeks to continue the work of Turner and Mudford by introducing real measurement data to the simulations. The model output using real data was analysed to investigate the effects of several techniques to increase the model sensitivity to leaks, whilst reducing measurement noise. Since the averaging process employed by Turner was

effectively a simple filter in the time domain, it was decided to investigate other forms of filtering in both the time and frequency domains. A range of applications were examined which have been illustrated in texts including Oppenheim (1978) and Stanley (1975) to determine the most appropriate filter for the given behaviour of the model output.

For testing of techniques, sample pipeline sections were used with a set of test data. Off-line testing of several signal processing techniques including averaging and low pass filters, were performed to verify which produced the most reliable results. This enabled the different filters to be compared against the same input data, which would not be possible if the signal processing techniques were tested against on-line data. Once the most suitable techniques for providing reliable leak data were determined, the implementation of the online model was commenced.

The successful implementation of an on line leak detection system can be summarised into four main processes that have to be completed:

a) develop a mathematical model which represents the physical pipeline;
b) implement real time data exchange between the model and the Supervisory Control And Data Acquisition (SCADA) system;
c) develop signal processing techniques to process both input data and leak flows from the model and remove the effects of measurement noise;
d) compare and validate each signal processing technique by conducting a simulated real time leak test on the pipeline;
e) evaluate possible improvements to such areas as input data and model.

Stage (a) was addressed with the development of a mathematical model using SIROGAS to represent the actual pipeline. This included the accurate representation of compressors, pipe section lengths and elevations. This was then tested against actual data from the pipeline to tune certain parameters such as pipeline surface roughness and ground temperatures.

Stage (b) was completed by implementing the transfer of measured data between the SCADA system and the external PC on which the model was running by the use of File Transfer Protocol (FTP). This is outlined in more detail in Section 2.3. The model then was tested over extended time periods to verify the reliability of data exchange. The validity of the results from the model is reliant on the frequency and quality of the data being received from the SCADA system. Stages (a) and (b) were part of the system implementation and on-line model development, and are discussed in more detail in Chapter 3.

Stage (c) was necessary to increase the clarity of results once measurement noise was introduced to the model input data. Using the results from the test pipeline sections, the optimum combination of data filters was applied to the online model. Each filter was then evaluated by its ability to firstly, remove random measurement noise, and secondly, the ability of the filter to respond to a step response induced by a leak for the test pipeline sections. This is outlined in Chapter 5 describing the output data analysis.

Once the optimum filter was selected, stage (d) of the project concluded with the estimation of simulated leaks induced via the input data. Leaks of constant magnitude were created by manipulating the input data. The resultant model output was then examined to determine the length of time before the correct magnitude of each leak was detected. The achievable leak detection threshold was also determined for each pipeline section examined. The performance of each filter was examined to determine the most appropriate technique, with the results listed in Chapter 6.

After analysis of the results, recommendations for the improvement of the model performance were made in Chapter 7. These improvements were then proposed for implementation on the GGT Pipeline.

2.0 BACKGROUND

2.1 GGT Pipeline

The purpose of transmission pipelines is to safely and economically transport product from producer to consumer. The product can range from oil to natural gas to water or slurry transportation of minerals. The data collection for the purpose of this study was obtained from the GGT natural gas pipeline. The GGT pipeline traverses two thirds of WA, taking natural gas from the northwest shelf and transporting it to Kalgoorlie in the Goldfields region. It is nearly 1400 kilometres long and delivers over 1100 tonnes of natural gas per day.

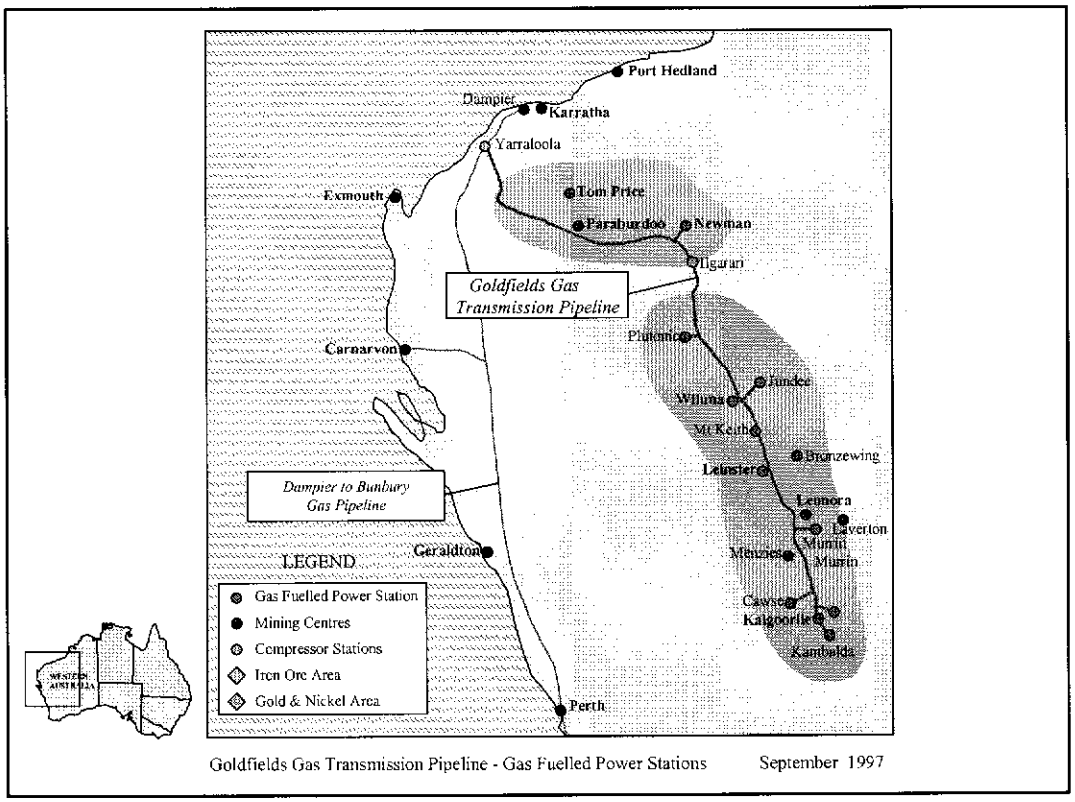

Figure 2.1. The GGT Pipeline

An overview of the pipeline is shown in Figure 2.1. It illustrates that the pipeline is the second largest gas pipeline to be built in Western Australia, the Epic Energy Dampier to Bunbury Natural Gas Pipeline (DBNGP) being the largest. It can be seen from the diagram, that the pipeline traverses some remote locations of the state. Thus, any uncontrolled release of gas could go undetected for days or weeks.

Typical operating data from the pipeline is transmitted via satellite from the field Remote Terminal Units (RTU's) to the control centre located in Perth. Therefore information critical to the leak detection model such as pressure, temperature and gas composition is telemetered at one minute intervals to the SCADA system at the control centre.

The entire pipeline model representing the GGT pipeline consists of smaller pipeline sections determined by locations where pressure and temperature data are measured. Due to the amount of input and output data being processed, pipeline sections will be treated individually. Of particular note are the three pipeline sections Anaconda to Leonora, Ned's Creek to Wiluna and Jeedamya to Cawse that are examined later. These sections and the completed network model are described in further detail in Chapter 3. These sections are too small to be shown in detail on Figure 2.1.

2.2 FlowTran and Sirogas

FlowTran is the Windows based graphical interface part of the SIROGAS program. SIROGAS is a computer program for simulating the transient and steady state behaviour of fluid in complex pipe networks containing devices such as compressors and regulators by employing a one dimensional finite difference method. At each time step, the program provides a semi implicit solution of the system equations. The numerical procedures used in SIROGAS were developed by Turner and Maguire (1993) in an earlier computer program, NAIAD, for the cooling water networks of nuclear power reactors. SIROGAS was developed in Fortran, which is noted for its computational speed, whereas FlowTran was developed in a Windows environment, providing all the associated benefits of a multi-layered graphical system.

A piping system such as the GGT pipeline model is known as a network and is made up of flow paths and devices that join flow paths together. The main dependent variables within each flow path can be summarised as follows:

- Gas composition
- Mass flow rate
- Fluid pressure
- Fluid temperature
- Flow path surface temperature
- Flow path wall or ground temperature a nodes

In calculating the steady state and transient behaviour of compressible gas in a complex flow network, SIROGAS treats the flow network as a set of one-dimensional flow paths each of which begins and ends at a connection. Flow paths can consist of uniform round pipes, complex tubes of varying shape and area, or even banks of tubes such as those used in heat exchangers. The basic conditions are that fluid mass can only enter or leave the flow path at the ends, and that momentum and energy can pass through the flow path walls or directly into the fluid, and also be moved with the fluid through the ends. Nodes are placed at the start, finish and any required intermediate positions in each flow path so that an implicit finite difference method can be used for each flow path. The typical nodal spacing used in the GGT pipeline model was 1 km. A justification of this spacing is provided in Chapter 3.

Flow path connectors provide boundary conditions to the model and simulate actual devices. These may include preset pressure or flow regulation, or pressure increases simulating compression. There are various types of connection that are available for the construction of a network model with SIROGAS, and include pressure regulation, flow regulation and compression. Boundary conditions may include flows, pressures and temperatures (at supply and demand points), set points (for compressors, regulators, etc) and ground temperatures.

The user can generate more complex devices by using any combination of the above standard connections. To begin a transient calculation, the following initial conditions must be specified at every node:

- mass flow rate
- pressure

- temperature
- enthalpy

In addition to flow rate, pressure and temperature, the state of all connections must be determined. For example, this may include the operating point of a compressor, or the flow through a regulator. These initial conditions are obtained prior to a transient calculation by either a steady-state calculation or by reading dynamic values from a previous SIROGAS calculation on the same network, referred to as a restart calculation. The SIROGAS steady-state section consists of a series of steady-state calculations for individual flow paths or for all flow paths in the network.

If the network steady state option is used, the steady state is calculated corresponding to the flow, pressure and temperature boundary conditions appropriate to the network. This is performed within SIROGAS by running a transient simulation of the network beginning from a state of low flow, equal pressure and equal temperature at all nodes, uniform composition and gravity set to zero. This is termed the global state. The values of all boundary conditions, wall temperature and set points are changed from their global values to their required initial values using a cosine variation over a user specified period. These values are then held constant until a steady state is reached or until a limit placed on the calculation is reached. The transient calculation can now be commenced from this initial steady state. If more than one steady state calculation is performed in SIROGAS, the last one is used as the initial state for the transient.

Three parameters must be specified in the set of data for each flow path calculation which include pressure and temperature at one node, and either pressure at another node or mass flow rate in the flow path. This is demonstrated later when each flow path (pipeline section) is examined in isolation from the entire pipeline network, as pressure and temperature are defined at each end point. The finite difference equations are derived from the equations of conservation of mass, momentum and energy for the gas mixture, and the energy equation for the pipe wall. These equations, together with the boundary conditions and the connection equations, fully define the system.

The conditions throughout the network at the end of each time step are determined from the initial conditions at the start of the time step together with the boundary conditions. The time step in an off-line model (where conservation of mass is preserved and measured pressures are not imposed) will vary to limit the maximum change in values. However, in an on-line model the time step is constrained to the period between field data updates of parameters including pressure and temperature. This is once every minute for the GGT pipeline.

2.3 SCADA System and Data Collection

The leak detection model must be interfaced with the existing SCADA system on the GGT pipeline. As described earlier, the SCADA system utilises satellite communications to transfer information from the pipeline to the control centre. The reliability of this can be affected by weather and atmospheric conditions. This was a consideration when developing the data exchange between the SCADA system and the leak detection model. Figure 2.2 outlines the transferral of data within the GGT pipeline SCADA system.

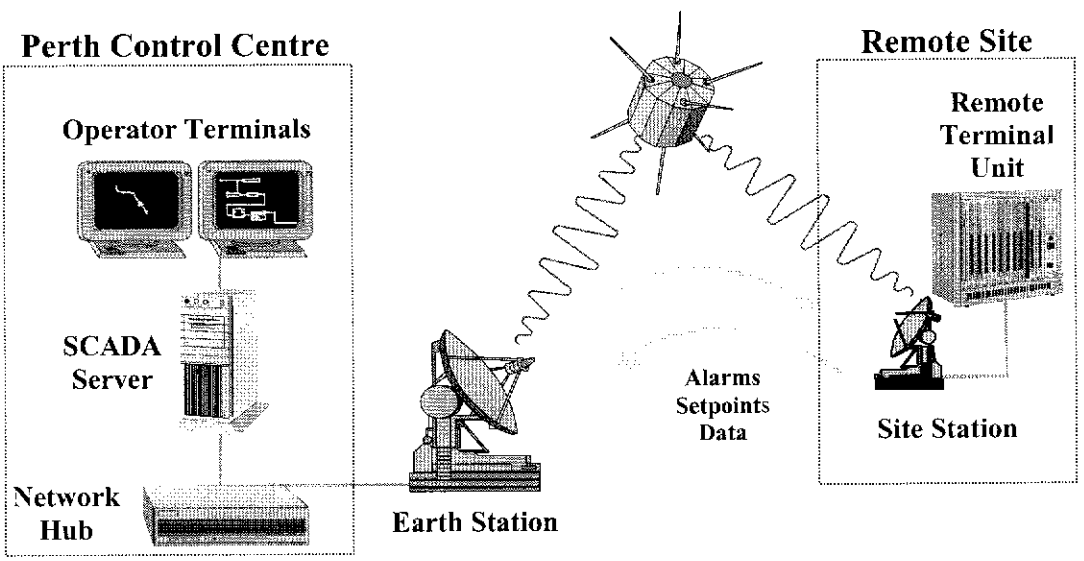

Figure 2.2 The SCADA System

Examples of typical applications interfacing with SCADA technology available are outlined by Reith *et al.* (1990). The SCADA system primarily performs the following functions:

1. Provide the operator with the ability to perform basic control duties, i.e. opening and closing valves remotely, starting and stopping compressors.
2. Generate alarms when parameters are outside normal operating conditions.
3. Provide a historic database of information gathered from the pipeline, which can be displayed as data or on trends.

Item (3) was utilised by the model, as some of the information gathered from the pipeline is required to be the input for simulation at each time period. Data required by the model is collected and stored by the SCADA system at one minute intervals from measurement devices located on the pipeline. Thus when model requests new data for the next simulation period, this is retrieved from the historical database on the SCADA system. The final on-line model required a method of transferring data between the flow modelling software, and the SCADA database. The method selected was File Transfer Protocol (FTP) between the SCADA database and the network personal computer that executes the model using SIROGAS.

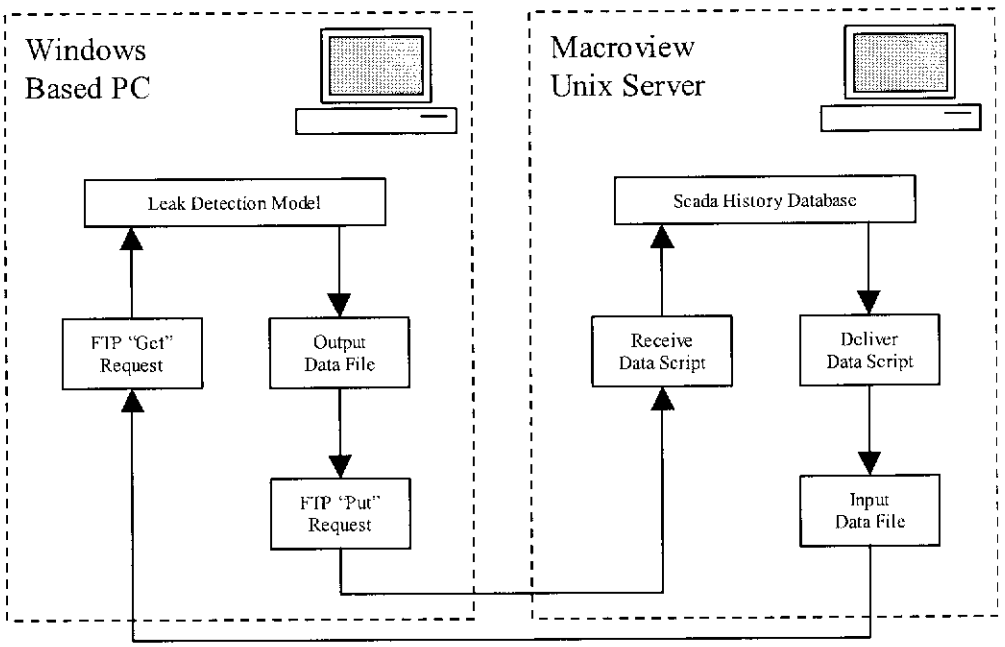

Figure 2.3 FTP Overview

FTP was chosen due to the robustness of the process, and ability to transfer data quickly between the SCADA server on a Unix platform, and the Windows based computer. A script was written on the SCADA server that created a text file each minute containing all the required dynamic inputs to the model such as pressure and temperature. The computer running the model then transfers this file each minute using FTP, which is then read into the model. If the file is not available for transfer, the model then waits and retries at the next simulation period. The transfer of data between the SCADA system and the model is illustrated in Figure 2.3.

Due to the diversity of SCADA systems available in the market place, there may be a wide range of effective methods to transfer data between a SCADA system and the model. For example many SCADA vendors offer standard data transfer protocols with their systems such as Dynamic Data Exchange (DDE), Open Database Connectivity (ODBC) and Object Linking and Embedding (OLE). Therefore it is more useful to describe the general process for implementation of the leak detection model.

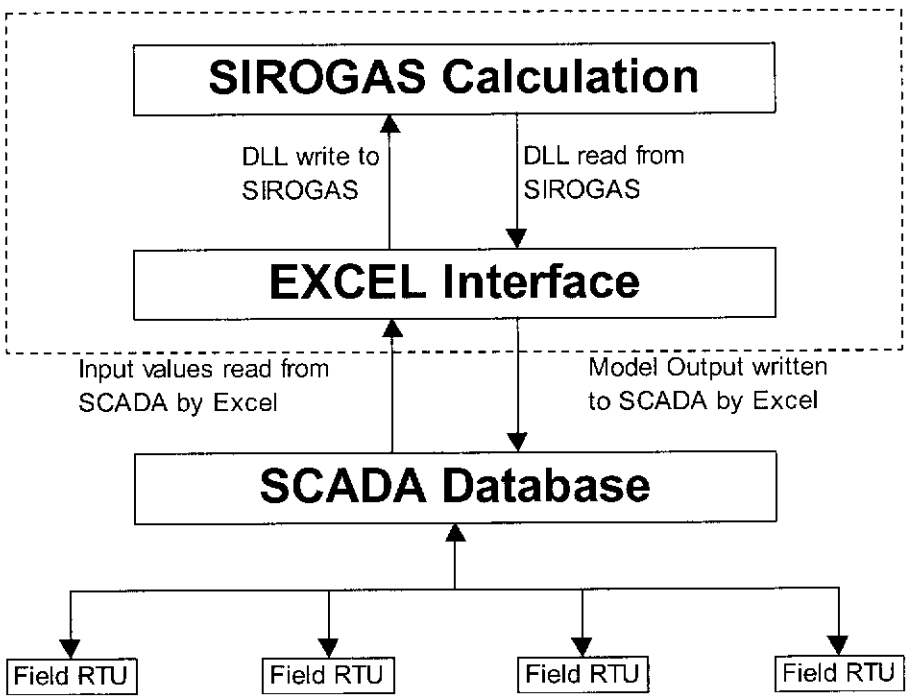

Figure 2.4 System Overview

Figure 2.4 outlines the overall process and requirements for a leak detection model using SIROGAS via Excel. The main advantage of using Excel as the central platform controlling the leak detection model is that the Visual Basic code within Excel is compatible with a variety of different applications such as SCADA and SIROGAS. The Visual Basic code calls standard Dynamic Link Libraries (DLL's) developed within SIROGAS, which enable inputs and outputs to be exchanged with the Fortran code in SIROGAS without needing to start the FlowTran interface. In this implementation, the FTP process to transfer data is controlled using Visual Basic, but other forms of data transfer can be controlled in the same manner. The Visual Basic code developed to control the model is listed in Appendix A.

The actual pipeline data used for the simulation was extracted from the SCADA system into an Excel spreadsheet. This included all pressure, temperature, flow, compressor set points and gas composition data. Eight days of one minute samples were collected for later use in this thesis, which provided 11,520 input data points for each pipeline section within the model.

3.0 PIPELINE MODEL DEVELOPMENT

3.1 Entire Pipeline Network

The first step in creating an on-line model is to develop and test a FlowTran input file off-line. This was done by using the graphical interface of FlowTran to physically replicate the features of the GGT pipeline to best represent the field conditions. There was a range of standard FlowTran devices that were used as mentioned in Chapter 2. An example of the graphical display for the GGT pipeline model is illustrated below.

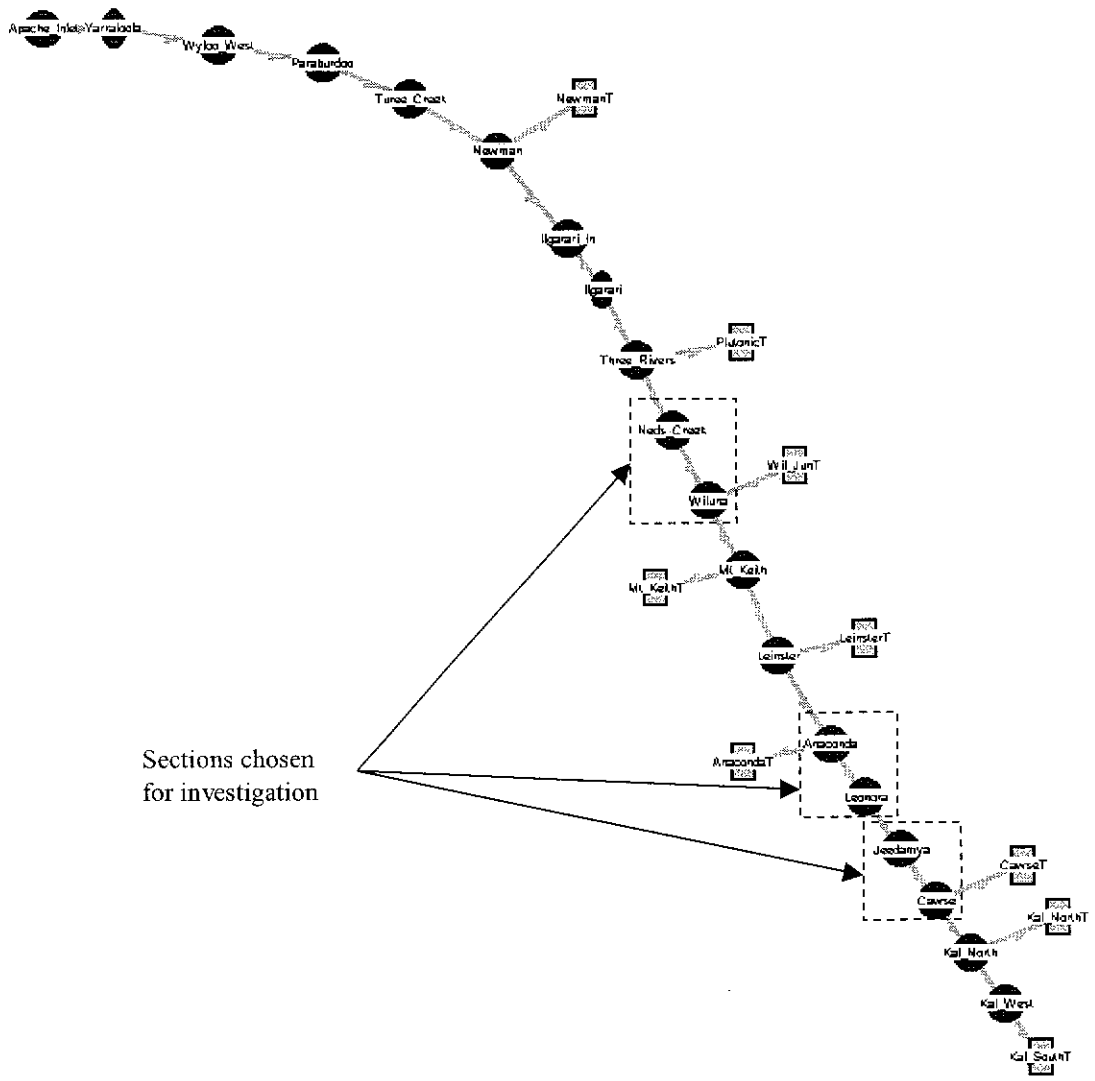

Figure 3.1 GGT Pipeline Network

The inputs and outputs of this model are defined to meet the data exchange requirements from the SCADA database. Table 3.1 provides a description of each point in the model and how it relates to the corresponding pipeline facility.

Pipeline Facility Type	Facility Names	Corresponding FlowTran Device	Available Inputs
Pipeline Inlet – Gas received from offshore production.	Apache	Known Pressure junction - A known pressure junction is a junction at which a known pressure and optionally temperature is maintained instead of mass and energy conservation. Composition of gas leaving the connection is determined by conservation of mixture masses. This junction can be used when a measured pressure and optionally temperature is available.	Gas Composition, flow rate, pressure and temperature.
Main Line Valve (MLV) – Remotely operated valve for isolating pipeline sections. Pressure and temperature also measured.	Three Rivers, Mt Keith, Anaconda, Leonora, Cawse, Kal North and Kal West.	Known Pressure junction – As above.	Pressure.
Scraper Station – Remotely operated valve for isolating pipeline sections. Pressure and temperature also measured, and provision for future compressor station.	Wyloo West, Paraburdoo, Turee Creek, Newman, Ned's Creek, Wiluna, Leinster and Jeedamya.	Known Pressure junction – As above.	Pressure and temperature.
Compressor Station – Gas pressure increased to boost pipeline capacity.	Yarraloola and Ilgarari.	Compressor Unit - A compressor unit connection simulates a single compressor unit. It is represented in SIROGAS by a single flow controlled connection that is at the junction of two pipes: the end of the inlet pipe, and the start of the outlet pipe.	Compressor unit performance curves, discharge pressure set point.
Delivery Station – Outlet flow from pipeline to customer.	NewmanT, PlutonicT, WilJunT, Mt KeithT, LeinsterT, AnacondaT, CawseT, Kal NorthT, Kal SouthT	Flow Regulator - A flow regulator connects to a single pipe to simulate a demand and/or supply point.	Gas flow rate.

Table 3.1 Model Device Overview

The model was configured to accept SCADA data at each time step. This data included outlet flows, pipeline pressures and temperatures, compressor set points. Thus all the boundary conditions to the SIROGAS simulation are provided at each time step from the SCADA data. Each of the physical devices on the pipeline was mapped to a FlowTran device, using methodology as illustrated by Rasins (1997).

One boundary condition is that of the composition of the gas entering the inlet of the pipeline, this gas replaces the assumed steady state value of composition as the on-line model progresses. Thelen (1995) and Van der Hoeven (1998) investigated the tracking of gas composition through gas pipelines, with particular emphasis on blending different gas composition streams. It was also verified that all components of the gas mixture were in the gaseous phase when the composition was supplied to FlowTran as previously investigated by Thelen (1995) and Van der Hoeven (1998), as not to falsely introduce two phase flow. The FlowTran input file defining all the necessary parameters in the final on-line implementation is listed in Appendix B.

3.2 Pipeline Sections

The entire pipeline network consists of many smaller components and devices. A pipeline section can be defined as the flow path adjoining two known pressures. There are sixteen pipeline sections in the GGT network model, two of which contain compressor devices. These pipeline sections can be seen in Figure 3.1 and include the flow paths Wyloo West to Paraburdoo and Ilgarari In to Three Rivers for example. Effectively each of these sections can be modelled in isolation since the pressures and temperatures are known at each end, from the measured field data. The only reason to create an entire network model is to track any gas composition changes from one pipeline section to the next. These changes have an effect on fluid properties such as enthalpy and density, which in turn can affect the integrity of the model.

For the purposes of this investigation, the pipeline sections chosen for analysis were modelled in isolation, where each pipeline section consisted of a separate model with

only two known pressure devices joined by a flow path that represented the physical characteristics of each section. When this method is employed, the composition of the gas cannot be tracked along the GGT pipeline, therefore the average composition for the eight day data collection period was used. Since gas composition did not vary substantially over the time period the data was collected, the impact on the density calculation is minimal, and therefore this approximation is valid. This made data handling and presentation of results more convenient.

Pipeline Section	Linepack (TJ)	Average Flow (TJ/day)	Residence Time (Days)
Ilgarari In to Ilgarari	0.013	85.198	0.000
Apache Inlet to Yarraloola	2.648	99.611	0.027
Anaconda to Leonora	3.548	33.887	0.105
Kal North to Kal West	3.586	23.145	0.155
Three Rivers to Ned's Creek	14.720	70.317	0.209
Turee Creek to Newman	22.078	81.624	0.270
Newman to Ilgarari In	23.083	75.494	0.306
Mt Keith to Leinster	22.321	58.408	0.382
Cawse to Kal North	11.951	30.734	0.389
Wiluna to Mt Keith	29.691	66.857	0.444
Ilgarari to Three Rivers	41.387	85.198	0.486
Leonora to Jeedamya	16.276	31.477	0.517
Ned's Creek to Wiluna	47.655	71.507	0.666
Yarraloola to Wyloo West	72.113	99.611	0.724
Paraburdoo to Turee Creek	68.371	81.860	0.835
Leinster to Anaconda	43.131	49.624	0.869
Wyloo West to Paraburdoo	77.981	81.206	0.960
Jeedamya to Cawse	36.140	34.253	1.055

Table 3.2 Residence Times for Pipeline Sections

Each pipeline section was ranked in order of residence time. The residence time was defined as the time interval required to replace the entire contents (linepack) for a given pipeline section. The ratio of a section linepack measured in Terajoules, to the typical flow through that section measured in Terajoules per day, provided a residence time in days for each section. Table 3.2 shows the residence times for each

pipeline section in order from lowest to highest. The residence time provides a measure of whether linepack or flow will dominate. By choosing three pipeline sections with different residence times, the effect of leak detection performance can be assessed for a range of conditions.

The three pipeline sections chosen from the entire pipeline network for detailed analysis have important physical properties for the model listed in Table 3.3. The sections were chosen to provide diversity in both size and typical flow, and thus demonstrate the prediction of leaks for a certain range of conditions. The lowest residence times belong to Ilgarari In to Ilgarari and Apache Inlet to Yarraloola. These however were not used, as these are not true pipeline sections, only short sections of pipe on the suction side of each compressor to provide an accurate suction pressure. Therefore Anaconda to Leonora was chosen as the pipeline section with the shortest residence time, Jeedamya to Cawse was chosen for the longest residence time, and Wiluna to Mt Keith was chosen as a pipeline section with a residence time between the lowest and highest.

Pipeline Section	**Length (km)**	**Diameter (mm)**
Anaconda to Leonora	11.10	345
Ned's Creek to Wiluna	124.40	345
Jeedamya to Cawse	112.19	345

Table 3.3 Pipeline Section Data

3.3 Test Pipeline Section

For most of the initial investigation, a test pipeline section was used to examine the effects of a leak on a section, and to determine the best method to verify the presence of a leak. The test section consisted of two known pressure junctions joined by a flow path of length 100 km and diameter 394.4 mm and is shown in Figure 3.2 (a). These dimensions were chosen to representative of a typical pipeline section on the GGT pipeline network. To generate input data for the pipeline test section model,

another model was created that consisted of a flow path that represented the test pipeline section with a junction inserted along the length so that a simulated leak flow could be extracted. The junction could be relocated along the 100 km flow path to simulate the effects of leaks at different locations. In addition to the flow path representing the test pipeline section, there were two identical flow paths, one upstream and one downstream of the pipeline test section. These represent adjacent pipeline sections that would be present in the entire GGT pipeline network. This model can be seen in Figure 3.2(b). Since the simulated leak was conducted over relatively short time periods, it was assumed that the outer boundary pressures of the neighbouring sections remained constant as they are a large distance from the pipe section being examined. In reality these pressures would be affected by a leak in an adjacent section to a small extent. This model allowed FlowTran to calculate the inlet and outlet pressures and temperatures of the pipeline test section when the leak was present. These values then became the inputs for the model in Figure 3.2(a).

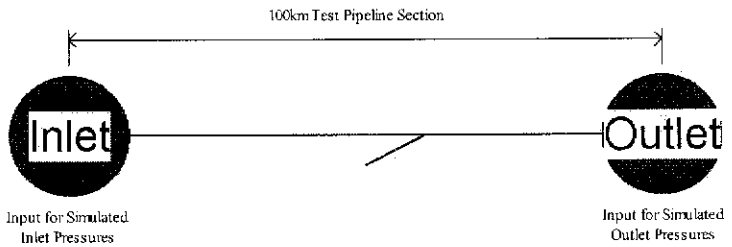

Figure 3.2(a) Model for Pipeline Test Section

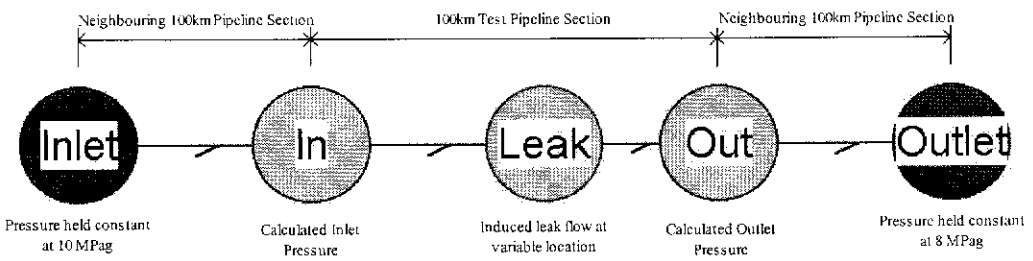

Figure 3.2(b) Model to Generate Data for Pipeline Test Section

3.4 Nodal Spacing

Using the test pipeline section, the effect of nodal spacing on a flow path between two devices was examined. This was done by inducing a rapid transient at the inlet to the section, and observing the resultant effects along the flow path. The steady state conditions for the pipeline section included a constant inlet pressure of 8 MPag, a constant outlet flow of 80 TJ/day and a constant gas temperature of 25°C. The gas temperature is maintained at this value by using a ground temperature of 25°C along the entire pipeline section. It is assumed that the measured temperature data from the GGT pipeline used later is representative of the upstream ground temperature. This assumption is valid for good heat transfer from the ground to the flowing gas, and sufficiently long pipeline sections (greater than 10 km). These parameters are indicative of a typical large section on the GGT pipeline.

From steady state conditions the inlet pressure was increased from 8 MPag to 10 MPag over a time period of one minute, which is extreme for typical operating conditions of most pipelines. However, at compressor or pressure regulating stations, similar conditions can be induced. Therefore any inaccuracies in pressure or flow estimation will directly impact the integrity of the leak detection system.

Figure 3.3 Transient Response to a Step Change

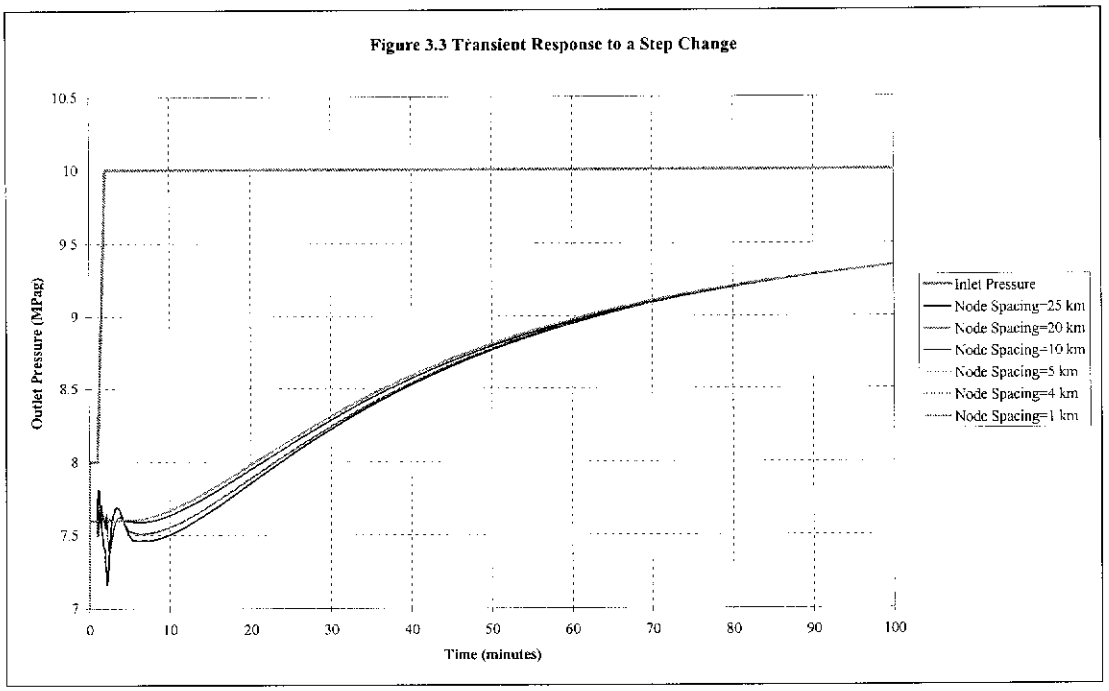

The outlet pressures versus time can be seen in Figure 3.3, for different nodal spacing. Within the first ten minutes after the pressure rise, there is substantial variance between each of the node densities, especially those greater than one node spaced every 4 km along the flow path. There is marginal improvement by reducing the node spacing from 4 km to 1 km. After 90 minutes the number of nodes along the flow path has negligible effect as the system has almost reached steady state conditions once again. Figure 3.2 shows the outlet pressure of the section for increasing node spacing. The gradient of each of the lines is close to zero between a 1 km and 4 km spacing for all time periods. Therefore a nodal spacing of 4 km or closer would be sufficient for use within the model.

Another method of confirming the suitability of the selected nodal spacing is by calculating the Courant Number of the model as discussed by Fletcher (1991). The dimensionless Courant Number provides a measure of the impact of the nodal spacing on the model results, and is defined in Equation 3.1.

$$Courant\ Number = \frac{\dot{W}_{\Delta Z}\,\Delta t}{L_{\Delta Z}} \tag{3.1}$$

This examines for a model time step of Δt the ratio of average flow $\dot{W}$ across a finite segment of pipeline between two nodes ΔZ, to the mass contained within the same segment L. Figure 3.4 lists the Courant Number as a function of time for the first 20 minutes after the transient for the first 10 nodal spaces, with a constant time step of 1 minute to represent the on-line model.

The calculated Courant Number exceeds the value of 1 for the first five nodal spacings. Ideally the Courant Number should be less than 1 for explicit solutions, however since the model is implicit, this result is acceptable. Figure 3.4 demonstrates that the effects of the transient diminish rapidly with distance from the inlet. The effects around devices that create known rapid transients can also be reduced by the use of irregular nodal spacings, by having a finer nodal mesh adjacent to these devices as discussed by Turner and Mudford (1988).

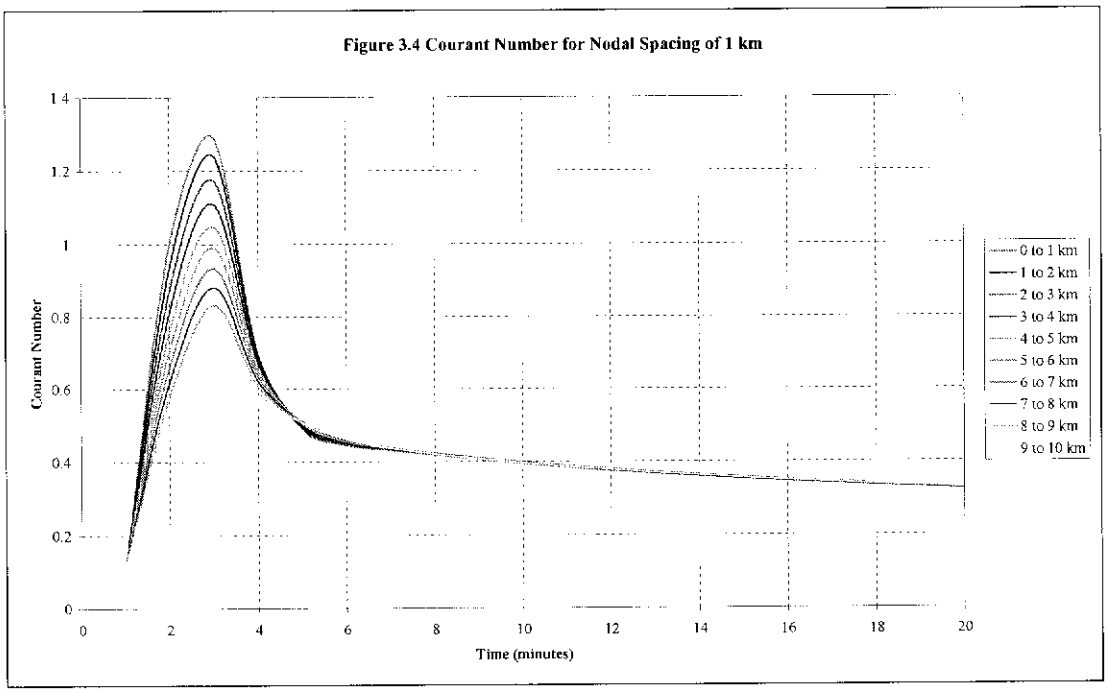

3.5 Compressor Performance

The characteristics of the compressor need to be modelled accurately to provide reliable data such as flow and temperature of the gas leaving the compressor. Any inaccuracies in compressor flow greater than the leak flow threshold would impact the validity of the leak detection results. Wright (1998) and Bryant (1997) demonstrated the benefits of accurate compressor modelling. The compressor performance curves shown in Figure 3.5 were generated using a modelling program supplied by the compressor vendor. These were then verified against pipeline compressor operating data. The curves were then transformed into tables of data for implementation into the FlowTran model, which are listed in Appendix C.

The isentropic efficiency in Appendix C is obtained from the modelled inlet and outlet conditions of the compressor, compared to ideal isentropic compression as illustrated by Rogers and Mayhew (1992). A simple method of interpolation and extrapolation is employed within SIROGAS to obtain values between defined compressor performance points. The main discrepancies in compressor flow estimation occur during compressor start up when a recycle valve is used to manipulate flows until the compressor is exposed to full pipeline pressures and is

often referred to as "fully loaded". During these relatively short periods of time, the flow obtained from the compressor curves in Figure 3.5 is recycled back into the compressor inlet and is not actually introduced into the pipeline. The modelled compressor flow can also be under or over estimated if the compressor maximum power or fuel gas usage is calculated incorrectly.

Figure 3.5 GGT Ariel Compressor Performance Curves

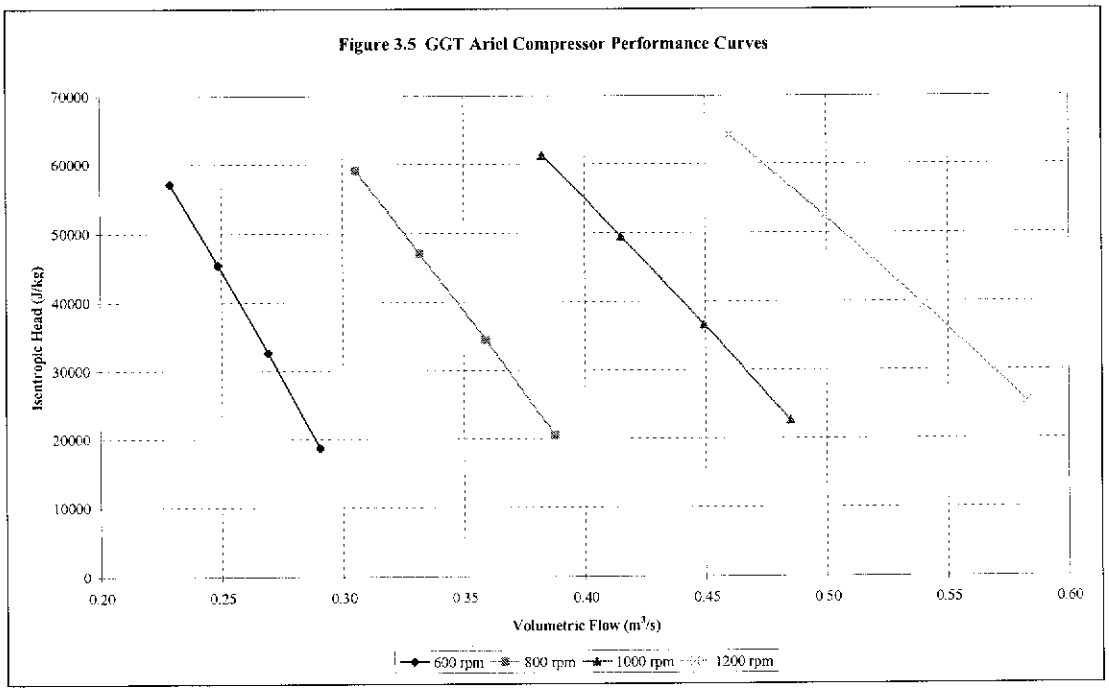

3.6 Pipeline Roughness

As mentioned in Section 1.1, the pipeline roughness is used to effectively remove any systematic errors from the model for a given set of input data. A physical measure of inner pipe wall roughness cannot be determined easily, therefore the quantity is adjusted to satisfy the known pressure and flow data being used in the model. Most of the other physical characteristics can be obtained readily with a known measure of uncertainty. This is why the pipeline roughness was calculated using actual operating data. Often this process is referred to as "tuning" the model, which in reality is using the pipeline roughness as a calibrating factor that compensates for all the cumulative errors in the model to produce results similar to the physically measured data.

The method used to calculate sectional roughness was iterative. An on-line model was constructed with an initial set of assumed sectional roughnesses. This was then run using real time pipeline data that produced calculated sectional flows. Actual sectional flows were obtained by using average measured input and output flows on the pipeline. The surface roughness was then adjusted using Equation 3.6 to make the calculated sectional flow equal the actual sectional flow. The on-line model was then executed with the revised sectional roughness. This process was repeated several times until convergence was obtained for sectional flows.

From the Darcy Equation we have the following equations that relate both the calculated flow $\dot{W}_1$, and the required flow $\dot{W}_2$.

$$\dot{W}_1 = \frac{k_1}{\sqrt{f_1}} \tag{3.2}$$

$$\dot{W}_2 = \frac{k_2}{\sqrt{f_2}} \tag{3.3}$$

Where k_1 and k_2 are constants of proportionality that incorporate pressure drop, average density of the gas, length and diameter of pipe section. The friction factor f_1 is calculated, whilst the required friction factor f_2 needs to be obtained in order to adjust the surface roughness to produce the desired flow. All these parameters do not change for the calculated and actual pipeline data, therefore k_1 equals k_2. Thus by taking the ratio of Equations 3.2 and 3.3, an expression can be obtained for f_2 in terms of $\dot{W}_1$, $\dot{W}_2$ and f_1.

$$f_2 = f_1\left(\frac{\dot{W}_1}{\dot{W}_2}\right)^2 \tag{3.4}$$

Once the new friction factor f_2 has been obtained using Equation 3.4, a new surface roughness can be calculated using Equation 3.5, which is a rearrangement of the Colebrook Equation listed by Munson *et al.* (1994) and Gudmundsson (1998).

$$\varepsilon = 3.7D\left[10^{-1/4\sqrt{f}} - \frac{1.255}{\mathrm{Re}\sqrt{f}}\right] \tag{3.5}$$

The new surface roughness ε, was then substituted back into the FlowTran model, which was executed against the same operational data. Due to Reynold's Number changing with the revised surface roughness and thus revised flow rates, this process was repeated until convergence of the sectional roughness value ε, was achieved.

The iterative algorithm converged within three iterations, providing sectional roughness values that in turn produced pressure values that matched the operating data. This process was repeated for each pipeline flow path between points where pressure data is measured in the pipeline. This was used to determine the sectional surface roughness values that were employed for the three pipeline sections chosen for investigation. These factors are listed in Table 3.4 on the following page.

The "tuning" process could be performed on-line, as this has been implemented by some operators an example of which is illustrated by Turner *et al.* (1992). However with this technique there is the risk that real systematic events such as the failure of a pressure transmitter, could be "tuned" out of the model by the continuous adjustment of the local pipeline section roughness parameters. This is not desirable, as these events should be highlighted as a false leak and be rectified. Periodic tuning of the model provides greater control over the model integrity.

It is evident from Table 3.4 there are considerable variations in the calculated roughness values between each pipeline section. Physically, there would not be such variance in roughness encountered along the length of a pipeline. This discrepancy is caused by anomalies between the model and on-line pipeline data such as inaccuracies in physical real time measurement, and assumptions made within the model. For example, if on a pipeline section the inlet pressure transmitter is indicating a lower pressure than in reality, and the outlet pressure transmitter is indicating a higher pressure than in reality, the modelled pipeline section flow will be lower than the actual section flow. This would also impact the adjacent pipeline

sections that share the same pressure transmitters. Therefore Equation 3.4 will compensate by reducing the refined friction factor, which in turn will impact the overall pipeline section roughness in Equation 3.5. This is acceptable due to the model being executed against the same two pressure transmitters that the pipeline roughness was calculated. Thus the friction factor has become a calibration factor for errors in the pressure transmitters and any other real time data used in the model. Without using the pipeline section roughness as a calibration factor, these systematic errors would produce an offset in modelled output data versus actual data. This is described in further detail in the following chapter.

Pipeline Section	Initial Roughness (mm)	Model Flow (TJ/day)	Measured Flow (TJ/day)	Flow Error	Final Roughness (mm)
Anaconda to Leonora	1.811357	35.639	35.639	0.00%	1.811357
Ned's Creek to Wiluna	0.007494	73.128	73.128	0.00%	0.007494
Jeedamya to Cawse	0.000146	35.639	35.639	0.00%	0.000146

Table 3.4 Determination of Sectional Pipeline Roughness

4.0 LEAK DETECTION

4.1 Mass Balance Technique

The term "leak" implies the presence of a system disturbance in addition to actual loss of gas from the pipeline. As mentioned earlier in Chapter 1, a method is required for calculating or detecting leaks, and this method must be insensitive to measurement noise. It was decided to employ a method of mass balance for each pipeline section as described by Turner and Mudford (1988) and Turner (1987).

An alternative method would be to examine the discrepancy in mass flow caused by forcing the measured pressure data into the Known Pressure Junction FlowTran device. This particular type of connection provides a FlowTran output, which is the flow required to maintain the measured pressure, which is essentially the leak flow at this point. Unfortunately, this method is extremely sensitive to measurement noise (particularly pressure) and rapid transients. By utilising the mass balance technique, this sensitivity is greatly reduced.

Most transmission pipelines utilise some form of mass balance technique to track any potential measurement errors relating to inlet and outlet meters on the pipeline. Figure 3.1 in the previous chapter illustrates the inlet and outlet meters on the entire GGT pipeline system. On a daily basis the total inlet flow, the total outlet flow and the net accumulation of gas within the pipeline is reconciled. This provides a reliable measure of the system metering accuracy, in addition to identifying any possible leaks within the system. This reconciliation process can be summarised by the following equation.

$$U = \sum W_{\text{in}} - \sum W_{\text{out}} - \Delta L \tag{4.1}$$

Where U is the unaccounted gas within the system, W_{in} and W_{out} are the total masses into and out of the system over the given period, and ΔL is the net accumulation of gas within the system during the same period. Equation 4.1 may estimate the magnitude of the unaccounted gas within the system satisfactorily, however it

provides no estimate of location along the entire pipeline. For a 1400 km long pipeline, the ability to estimate which pipeline section is likely to have a leak is extremely useful.

Figure 4.1 below illustrates a pipeline section at an initial time *t*. It contains an initial mass or inventory of gas L_t and has instantaneous flow rates upstream and downstream of the section $\dot{W}_U$ and $\dot{W}_D$ respectively. The flow rates $\dot{W}_U$ and $\dot{W}_D$ and instantaneous linepack L (gas contained within pipeline section) are provided at each measurement period by FlowTran.

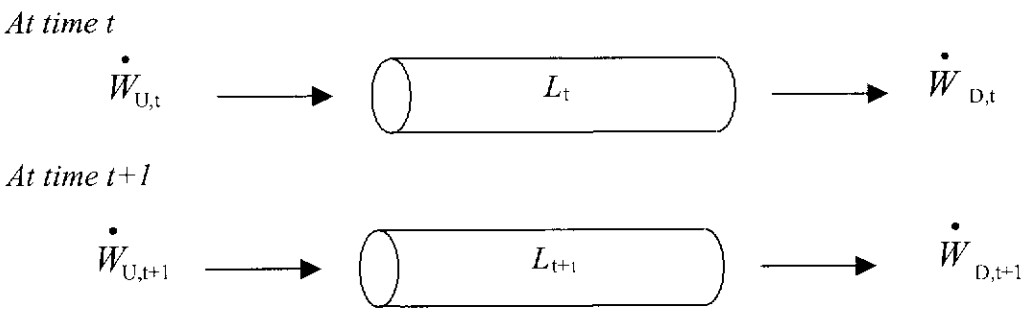

Figure 4.1 Pipeline Section Mass Balance

The strategy involves using all the measured pressures and temperatures to determine the mass of gas (linepack) L in the relevant pipeline section at the start of each measurement period.

The total average flow into and out of the pipeline section, is the linear average of the instantaneous flow rates at the start and end of each time step. This makes the assumption that the time step is small in comparison with the rate of change of flow, thus we have the first term of a Taylor series centred in time.

$$W_U = \frac{\left(\dot{W}_{U\,t} + \dot{W}_{U\,t+1}\right)\Delta t}{2} \tag{4.2}$$

$$W_D = \frac{\left(\dot{W}_{D\,t} + \dot{W}_{D\,t+1}\right)\Delta t}{2} \tag{4.3}$$

Therefore the total leak $\dot{B}$ is defined as follows, with the convention of an unaccounted loss of mass within the pipeline section being identified as a positive leak.

$$\dot{B} = \frac{W_U - W_D - \Delta L}{\Delta t} \tag{4.4}$$

4.2 Leak Location

The ability to estimate the location of a leak within a pipeline section may be useful for longer pipeline sections. Figure 4.2 demonstrates the effects of a leak on the pressure gradient and hence mass flow rate on a given pipeline section. It can be seen that that the mass flow rate is higher upstream of the leak compared with the downstream flow rate caused by the additional flow induced by the leak. It therefore follows that the pressure gradient is steeper on the upstream side of the leak compared with the downstream side.

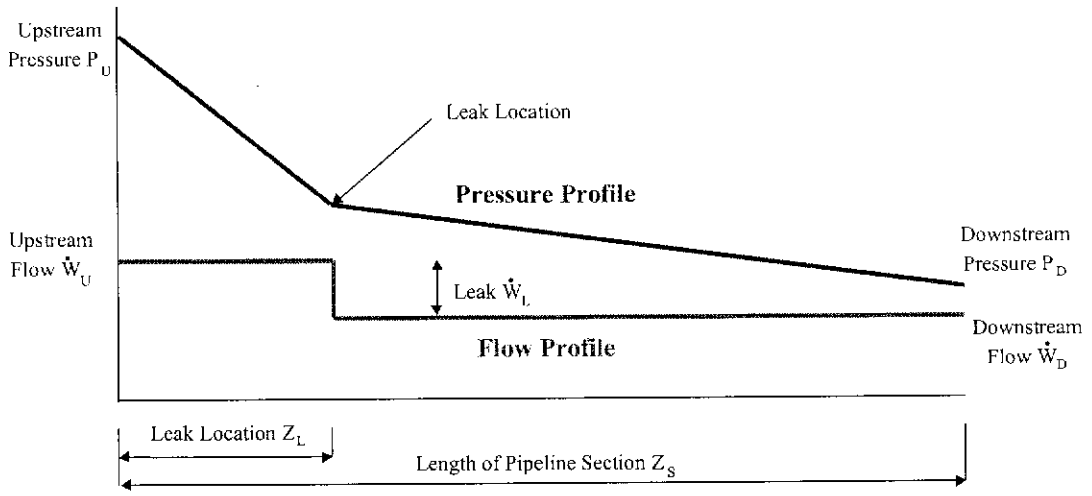

Figure 4.2 Effect of a Leak on Pipeline Section Pressure and Flow

If pressure and flow can be determined at each end of the pipeline section, an estimation of the leak location Z_L can be made. Using the Darcy equation to relate pressure and flow for both the sections upstream and downstream of the leak gives equations 4.5 and 4.6.

$$P_U - P_L = k_{UL} Z_L \dot{W}_U^2 \tag{4.5}$$

$$P_L - P_D = k_{LD}(Z_S - Z_L)\dot{W}_D^2 \tag{4.6}$$

Where k_{UL} and k_{LD} are factors that account for friction factor, density and diameter. Substituting equation 4.5 into 4.6 yields the following expression.

$$P_U - P_D = k_{UL} Z_L \dot{W}_U^2 + k_{LD} Z_S \dot{W}_D^2 - k_{LD} Z_L \dot{W}_D^2 \tag{4.7}$$

Substituting ΔP for $P_U - P_D$ and rearranging in terms of the leak location Z_L, we have the final equation 4.8 to determine the location of a leak on a pipeline section.

$$Z_L = \frac{\Delta P - k_{LD} Z_S \dot{W}_D^2}{k_{UL}\dot{W}_U^2 - k_{LD}\dot{W}_D^2} \tag{4.8}$$

If it is assumed that the differences between average friction factor and average fluid density upstream and downstream of the leak are small, then the following equations are obtained.

$$k = k_{UL} = k_{LD} \tag{4.9}$$

$$Z_L = \frac{\Delta P - k Z_S \dot{W}_D^2}{k(\dot{W}_U^2 - \dot{W}_D^2)} \tag{4.10}$$

To avoid calculating friction factor and density at each time step to determine k, the value of k can be obtained from data prior to the leak when Z_L equals zero. Assuming no leak flow, the following equation evaluates k at each time step.

$$k = \frac{\Delta P}{Z_S \dot{W}_D^2} \tag{4.11}$$

The procedure for determining the location of a leak would involve using the last value of k calculated prior to a leak being identified, over the period the leak is present with the current values of pressure and flow. This method is relatively simple and efficient, as it requires only the values of flow and pressure at the inlet and outlet of a section to be available to determine leak location.

Equation 4.10 was employed using the test pipeline section model shown in Figure 3.2a, outlined in Chapter 3. A leak of 10 TJ/day was simulated at three locations along the 100 km section, at 25 km, 50 km and 75 km. The leak was commenced at a simulation time of 100 minutes and held constant for the duration of the simulation. Figure 4.3 shows the value of Z_L versus simulation time for each of the simulated leak locations.

Figure 4.3 Calculated Leak Location

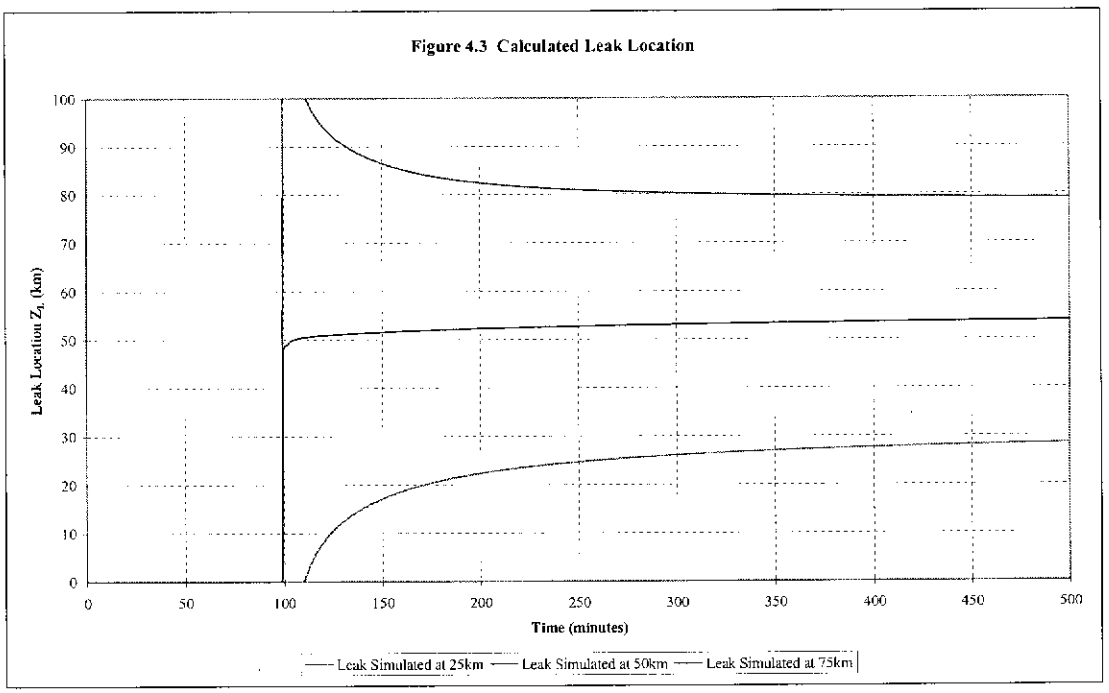

It can be seen from the graphs that equation 4.10 converges most rapidly for the leak situated at the mid point of the test pipeline section. For all three leaks, the algorithm for estimating leak location converged within five kilometres of the true leak location. This is a significant improvement in the operational response time in

locating a leak, over current estimates that would rely on the leak being sufficiently large enough to create local distortions in measured pressure.

The method described here is different to Turner and Mudford's algorithm, as an assumption is made that some form of flow measurement is available at each end of the pipeline section, in addition to pressure and temperature. Most pipelines may have check flow measurements along the pipeline at certain areas of interest, such as compressor stations. These flow values are sufficient to estimate the leak location once the mass balance technique has identified a leak.

4.3 Testing of Mass Balance Technique

For the case when model flows are used in place of measured flows, the mass balance technique was investigated by employing the two test pipeline section models illustrated in Figures 3.2(a) and 3.2(b). Initially the leak conditions for the pipeline section were obtained by using the model in Figure 3.2(a), where a constant 10 TJ/day leak was extracted at three locations along the pipeline section, 25 km, 50 km and 75 km. This represents a leak of approximately 10% of total throughput for the GGT pipeline. In this model, the pipeline section end point conditions of pressure and temperature were calculated by SIROGAS. When the leak detection model is employed in reality, the pressure, and temperature and possibly flow information is only available at the end points of each pipeline section for the model. Therefore this data was substituted as the input for the model in Figure 3.2(b), to simulate real data conditions.

This model is conservative in terms of transients experienced in a normal operating pipeline since the pressures further upstream and downstream of the test pipeline section are not being varied. However this provides an indication of the performance of leak estimation if modelled flow is used instead of measured flow if measured flow is not available. The effects of elevation (altitude) were not considered at this stage of the test model.

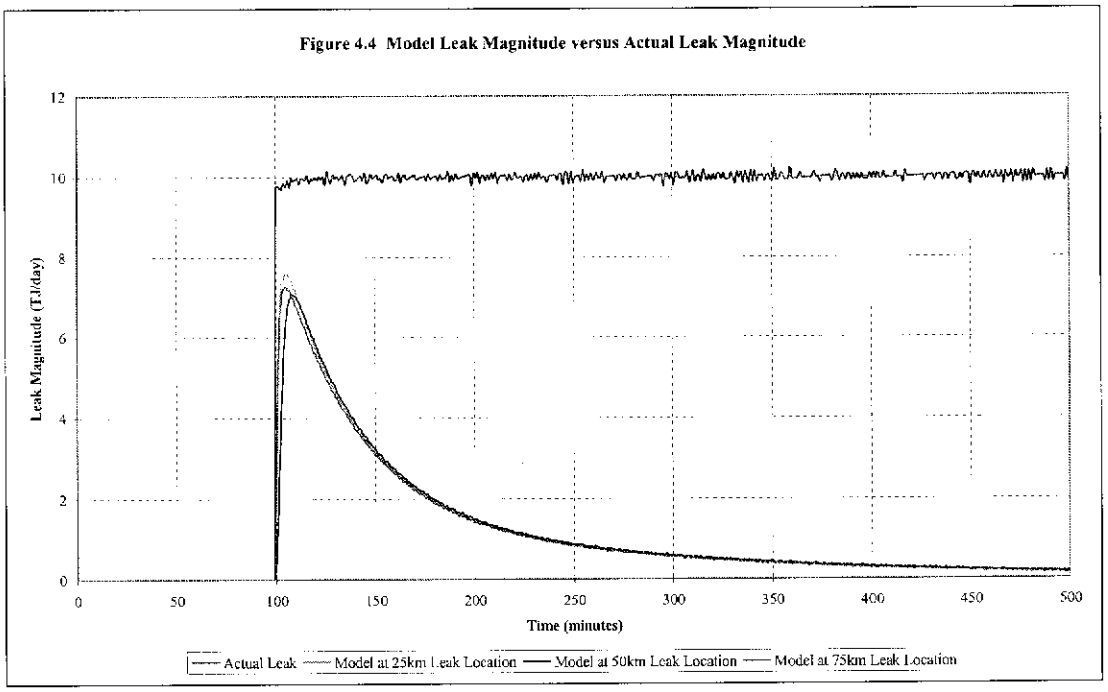

Figure 4.4 above shows the leak magnitude estimation based for each of three leak locations. The graph indicates that the mass balance technique underestimates leakage when only end point data is used in the model. This is due mainly to the upstream and downstream flow being calculated incorrectly by the model. It is also apparent from Figure 4.4, that the leak magnitude is largely independent of leak location. This indicates that modelled flow obtained from end point pressures and temperatures alone may not be suitable to estimate the correct leak magnitude.

Since there are only two pressure values available for input to the model, one at each end of the pipeline section, the model calculates a continuous pressure profile between the two pressures, and therefore does not compensate for the "kink" in the profile caused by the leak. This has the effect of underestimating the flow upstream of the leak and overestimating the flow downstream of the leak. Figure 4.5 illustrates the difference between the actual pressure and flow profiles compared to the modelled profiles, once steady state conditions have been restored after the leak has been present for a period of time. Figure 4.4 also illustrates that the leak flow decays over time even though the induced leak is at a constant flow rate. This is due to the pipeline section approaching steady state conditions by the upstream flow increasing to meet the demand of the leak flow. The overall effect is that the pipeline end point

pressures stabilise after a period of time, approaching the conditions represented in Figure 4.5.

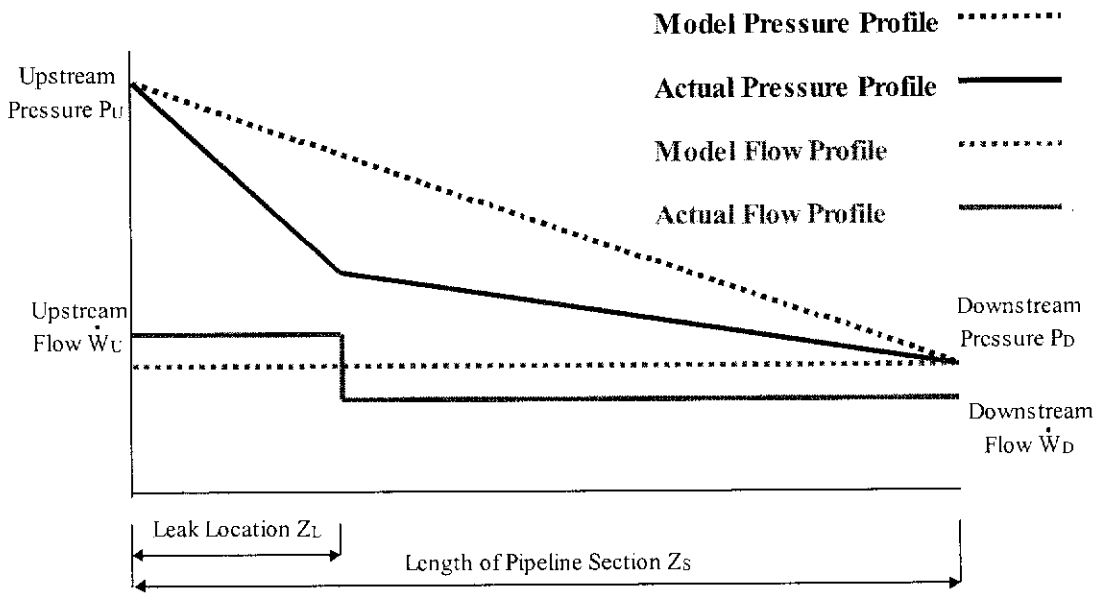

Figure 4.5 Comparison Between Model and Actual Profiles

The model cannot correctly calculate the increase in flow upstream of the leak, and the decrease in flow downstream of the leak from the pipeline section end point pressure alone. This is demonstrated by the flow errors from the misinterpretation of the pressure profile illustrated in Figures 4.6 and 4.7. Figure 4.6 compares the inlet flow for the pipeline section, which indicates the model using end point conditions underestimates the actual flow due to underestimating the actual pressure gradient towards the leak. Figure 4.7 illustrates that the model also overestimates the outlet flow due to overestimation of the actual pressure gradient away from the leak. These two errors combine in Equation 4.4 to underestimate the leak flow.

The flow error causes most of the underestimation in the overall leak magnitude for the pipeline section. This is apparent after the transient effects begin to diminish after leak initiation, and the pipeline section begins to establish steady state conditions after compensating for the additional leak flow.

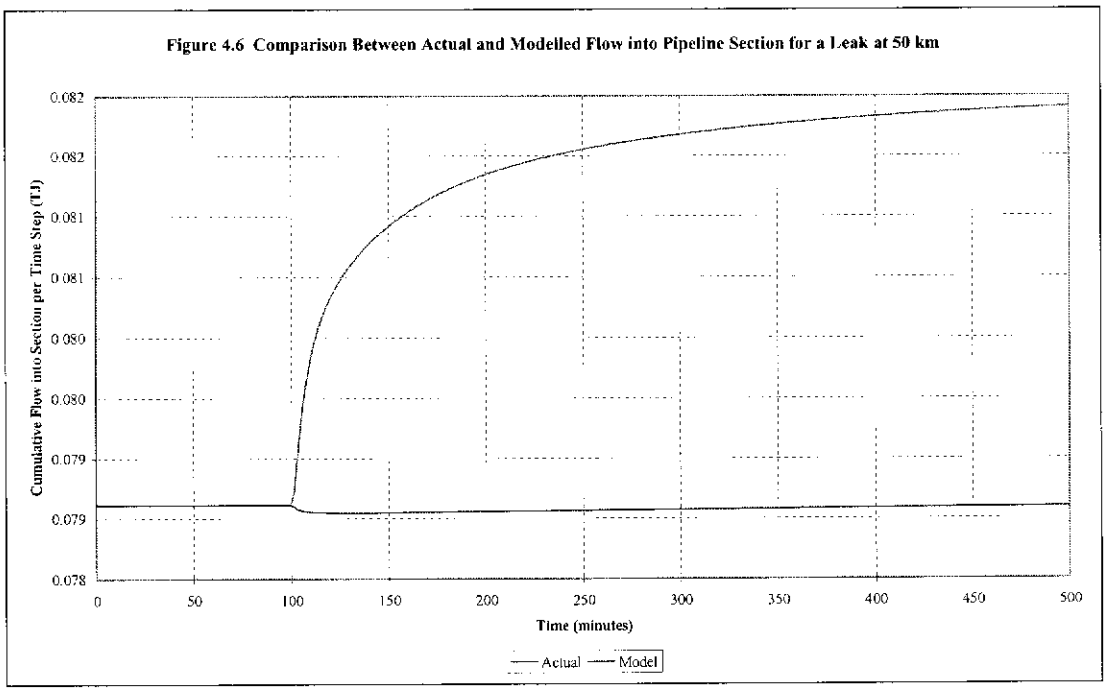

Figures 4.6 and 4.7 also show that the model initially indicates a reduction in pipeline section upstream flow and an increase in downstream flow, where in fact the opposite is true. This is solely due to not having pressure information, other than at the end points of the pipeline section. Interpretation of these pressures alone, causes erroneous flow estimation.

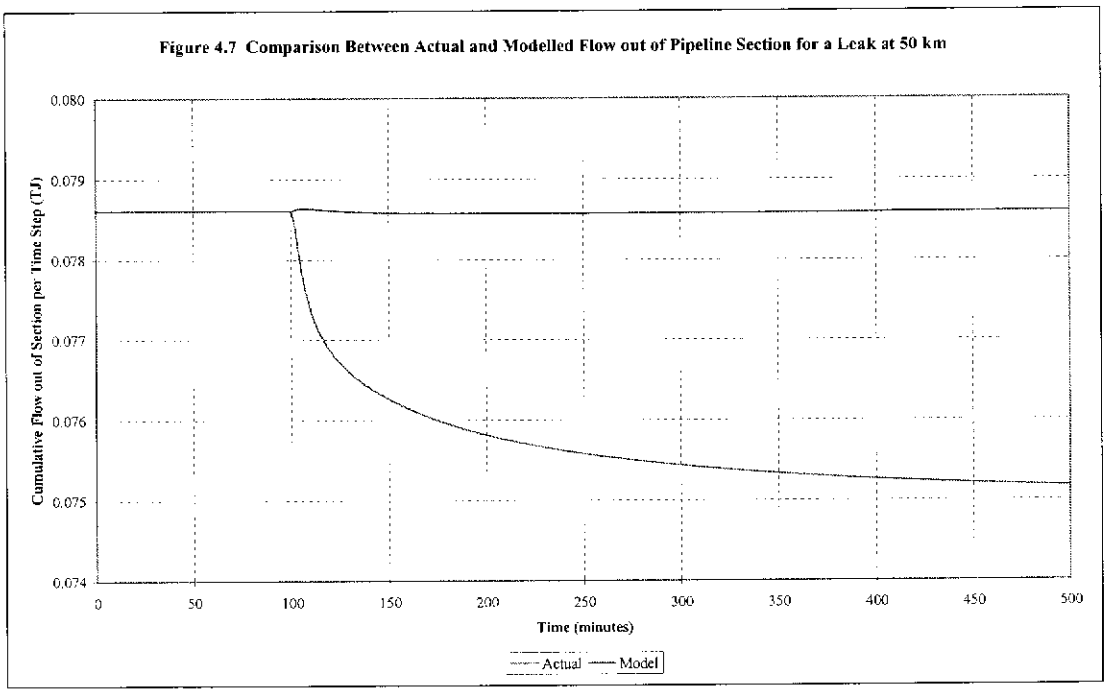

The magnitude of error in linepack estimation is much smaller than flow estimation between the model and actual data, as can be seen for Figure 4.8. This suggests that main sources of error in determining the leakage flow $\dot{B}$ from Equation 4.4, arise from $\dot{W}_U$ and $\dot{W}_D$ and not ΔL.

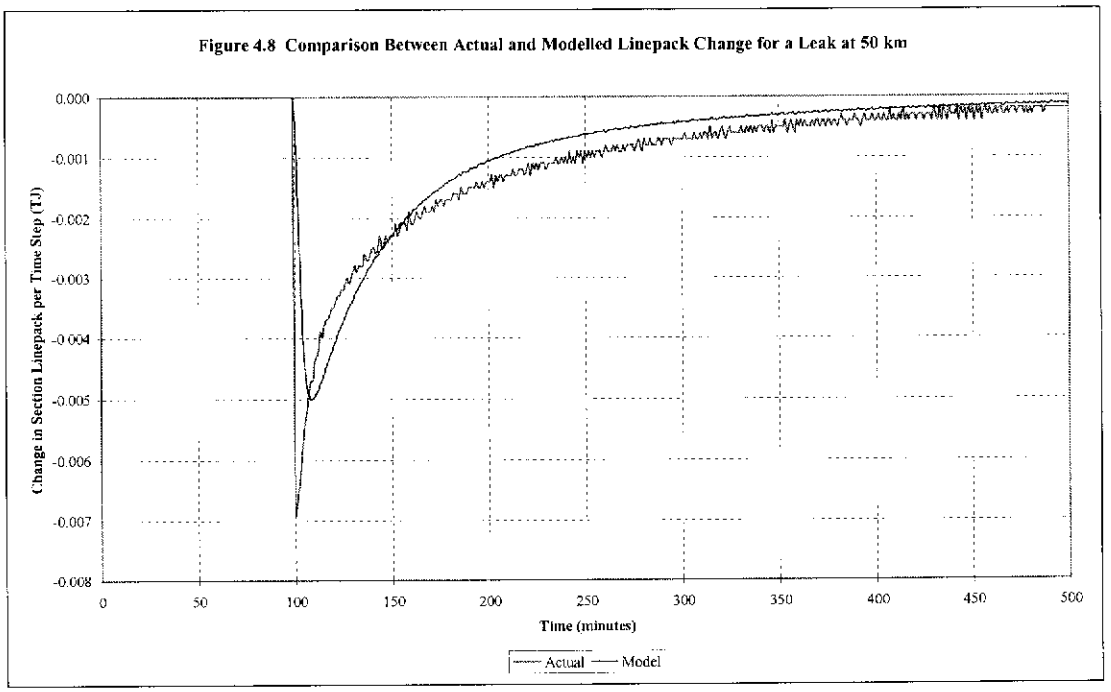

4.4 Effect of Measurement Uncertainty Using Modelled Flows

The concept of measurement uncertainty recognises that all measured values are subject to inherent error. Therefore no measured value can be stated with absolute confidence in the result. Since the model requires a range of measured inputs to calculate the leak magnitude on each pipeline section, the output of the model will be susceptible to all the individual uncertainties of these inputs. Each pipeline section requires pressure, temperature and gas composition as an input. For the purpose of this investigation, it will be assumed that the gas composition uncertainty has a small effect on the overall calculated leak uncertainty compared with pressure and temperature. Therefore when utilising calculated flow to estimate leak magnitude, only the effects of pressure and temperature on the overall calculated leak will be examined.

The term uncertainty that has been used to describe the difference between the actual value being measured (also known as the measurand), and the value produced by the measuring instrument. Uncertainty can also be related to the standard deviation of a set of measurements. For example, if a given quantity were measured a number of times by the same measuring instrument, the results would be normally distributed about a mean. The mean should be the true value only for an infinite number of averaged measurements compensating for non-systematic errors, and if the measuring instrument has no bias. An instrument could exhibit bias if it had not been calibrated properly or some other fault caused it to produce a systematic (non-random) offset or error. Figure 4.9 below illustrates the measurement uncertainty and systematic errors involved with measurement. The bias in field measurements was compensated by adjusting the pipeline section surface roughness, as outlined in Chapter 3.

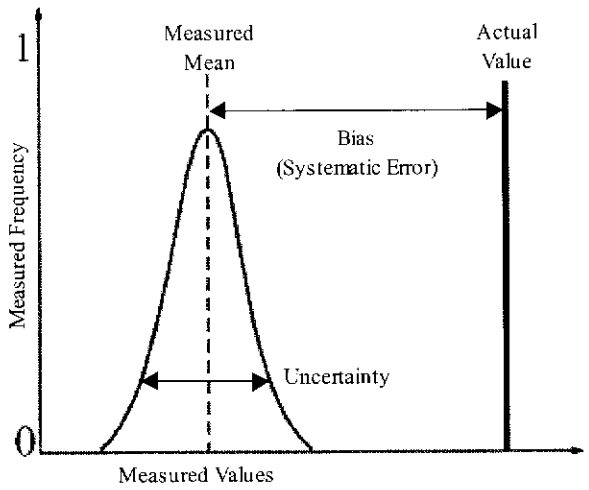

Figure 4.9 Measurement Uncertainty and Error

Turner investigated the effects of measurement uncertainty on the total calculated leak flow uncertainty. The total measurement uncertainty of a parameter that is calculated from variables each with their own uncertainty is given by the following equation from Keller *et al.* (1990).

$$\sigma_B = \sqrt{((\partial E/\partial x_1)\times\sigma_1)^2 + ... + ((\partial E/\partial x_n)\times\sigma_n)^2} \qquad (4.12)$$

Where E is the equation that defines the calculated parameter (in this case the leak $\dot{B}$), and σ_n is the uncertainty associated with the dependent variable x. By taking the partial derivatives of Equation 4.4 and substituting into Equation 4.12, the following equation is produced for total leak flow uncertainty $\sigma_{\dot{B}}$. It should be noted the effect of time stamp error has been ignored in Equation 4.13.

$$\sigma_{\dot{B}} = \sqrt{\sigma_{\dot{W}_U}^2 + \sigma_{\dot{W}_D}^2 + \sigma_{\Delta\dot{L}}^2} \tag{4.13}$$

Where $\sigma_{\dot{W}_U}$ is the uncertainty of flow into the pipeline section, $\sigma_{\dot{W}_D}$ is the uncertainty of flow out of the pipeline section, and $\sigma_{\Delta\dot{L}}$ is the uncertainty of the gas accumulation rate within the pipeline section. In this case, the flow is obtained by calculation within the model from the input pressures and temperatures. If the flow were measured, the uncertainty would be the inherent accuracy of the measuring instrument. Since the case where the modelled flow is used for leak estimation is being examined, a relationship between pressure, temperature and flow needs to be developed. The uncertainty in the calculated leak will also be referred to as the leak detection threshold, since if a leak is not greater than this value, it cannot be detected. An examination of the leak detection threshold for different forms of filter is conducted in the following Chapter.

It is useful to be able to estimate the effect of pressure and temperature uncertainty on $\sigma_{\dot{W}_U}$, $\sigma_{\dot{W}_D}$ and $\sigma_{\Delta\dot{L}}$ since it is assumed that these will be functions primarily of pressure and temperature uncertainty. Firstly the model flow can be approximated by the following simplification of Darcy's equation.

$$P_U - P_D = k_W \frac{\dot{W}^2}{\rho} \tag{4.14}$$

Where k_W is a constant of proportionality that contains calorific value, friction factor, pipeline section length and diameter. Assumptions made here are that there is no uncertainty in the measurement of length and diameter, the friction factor remains

basically constant for small changes in pressure, and finally, there is no uncertainty in time measurement to obtain the flow and linepack rates. It is unlikely that there can be any reduction in the uncertainty of diameter, length and time measurements. However, pressure and temperature measurements can be improved by either reducing the measuring instrument span, or by filtering the input data.

An approximation for density ρ is made in the following equation of state, where $\overline{T}$ is the pipeline section average gas temperature, and R is the gas constant.

$$\rho = \frac{\overline{P}}{R\overline{T}} = \frac{(P_U + P_D)}{2R\overline{T}} \tag{4.15}$$

Substituting Equation 4.15 into 4.14 and rearranging in terms of flow, Equation 4.16 is obtained which provides a simplified equation for flow in terms of pressure and temperature only.

$$\dot{W} = \dot{W}_U = \dot{W}_D = \sqrt{\frac{(P_U^{\,2} - P_D^{\,2})}{2R\overline{T}k_W}} = k_{\overline{W}}\sqrt{\frac{(P_U^{\,2} - P_D^{\,2})}{\overline{T}}} \tag{4.16}$$

Equation 4.16 is only valid if the constant $k_{\overline{W}}$ is independent of changes in upstream pressure, downstream pressure and average pipeline section temperature. The only quantity contained within $k_{\overline{W}}$ that will vary with these conditions is the pipeline section friction factor since upstream and downstream pressure will affect flow, which in turn will result in a change in friction factor. However, for the range of flow conditions that are being examined, this change is relatively small, therefore the assumption of the constant is sufficient to examine the behaviour of pressure and temperature uncertainty, on flow uncertainty.

Similarly for linepack, the following expression in terms of pressure and temperature arises. Again k_{CV} is used to convert from mass to energy. The rate of linepack change is determined by the difference in linepack between the beginning and end of a measurement period, divided by the interval of the measurement period. Therefore the Δt term is the interval between measurements, and it is assumed if this is small

the absolute values for pressure and temperature do not change significantly between measurement periods.

$$\Delta\dot{L} = \frac{k_{CV}}{\Delta t}\frac{\overline{P}V}{R\overline{T}} = \frac{k_{CV}}{\Delta t}\frac{(P_U + P_D)V}{2R\overline{T}} = k_{\overline{L}}\frac{(P_U + P_D)}{\overline{T}} \tag{4.17}$$

Taking the partial derivatives of Equations 4.16 and substituting into Equation 4.12 we have the following equation assuming that the uncertainty of both pressure measurements, P_U and P_D are the same.

$$\sigma_{\dot{W}_U} = \sigma_{\dot{W}_D} = k_{\overline{W}}\sqrt{\frac{(P_U^2 + P_D^2)}{\overline{T}}}\sqrt{\frac{\sigma_P^2}{(P_U^2 - P_D^2)} + \frac{\sigma_{\overline{T}}^2}{4\overline{T}^2}} \tag{4.18}$$

Applying the same process for the linepack relationship in Equation 4.17, and again assuming the uncertainty of both pressure measurements are the same, Equation 4.19 is obtained.

$$\sigma_{\Delta\dot{L}} = \frac{k_{\overline{L}}(P_U + P_D)}{\overline{T}}\sqrt{\frac{2\sigma_P^2}{(P_U + P_D)^2} + \frac{\sigma_{\overline{T}}^2}{\overline{T}^2}} \tag{4.19}$$

Using Equations 4.18 and 4.19 the effect of pressure or temperature measurement uncertainty can be examined separately by letting σ_P or $\sigma_{\overline{T}}$ equal zero. The equations for flow and linepack uncertainty then become linear with increasing values of uncertainty for pressure or temperature as illustrated in Figures 4.12 to 4.14. By evaluating the constants in equations 4.18 and 4.19, the results can also be substituted into Equation 4.13 to provide an expression for total leak flow uncertainty in terms of pressure and temperature uncertainty directly.

This relationship can be verified by again using the test pipeline section in Figure 3.2(b). The same inlet and outlet conditions for the model were used as previously, however this time they were held constant to simulate a no leak, steady state situation. As expected, the calculated leak flow was zero throughout the simulation period. The next step was to add uncertainty or noise to the pressure and temperature measurements that are used in the simulation. This was done by using the random

number function in Microsoft Excel ™, which uses a Gaussian (normal) distribution. Typical values of uncertainty for pressure are 0.025 MPa and 0.3 K for temperature. The nominal values or measurand for inlet pressure, outlet pressure and temperature were 9.387 MPa, 8.725 MPa and 298.15 K respectively. Therefore all input values were normally distributed about the measurand as the mean, plus or minus the stated total uncertainty. It should be noted here that all uncertainty amounts relate to the absolute value measured. Figure 4.10 shows the pressure and temperature inputs including measurement noise.

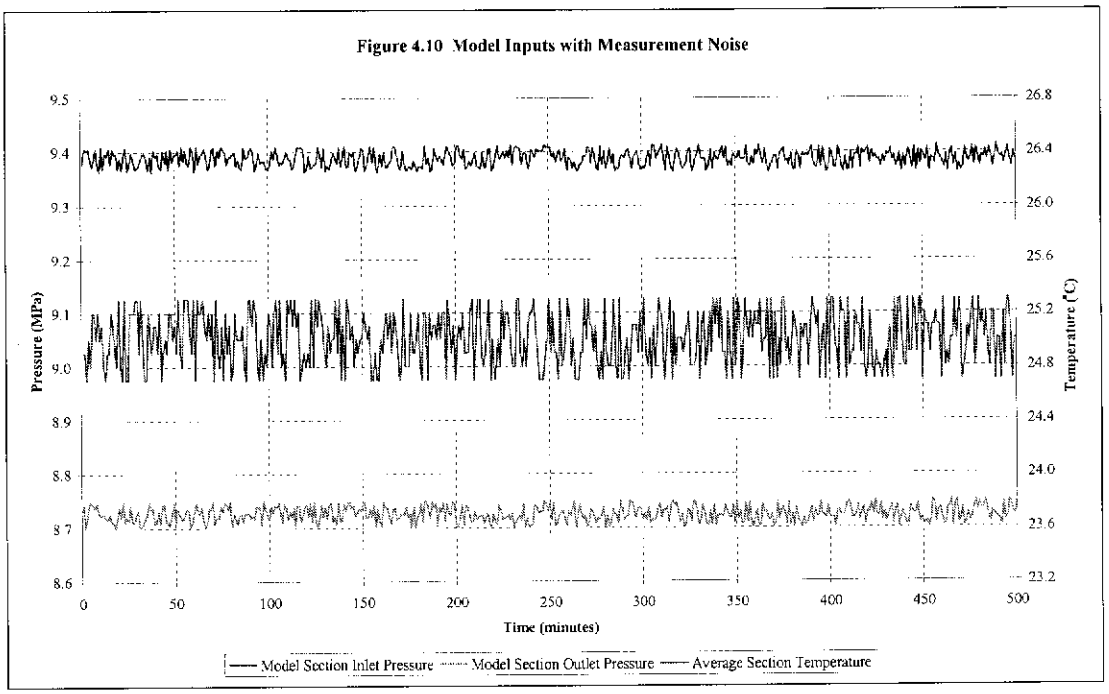

The calculated leak flows from the SIROGAS model using the data in Figure 4.10 were extremely noisy as can be seen from Figure 4.11, with a total leak flow uncertainty of 85.629 TJ/day. By solving for the constants $k_{\bar{W}}$ and $k_{\bar{L}}$, and substituting into Equations 4.18 and 4.19, the expected uncertainty for leak flow can be obtained via Equation 4.13. This produced a calculated leak flow uncertainty of 86.145 TJ/day that demonstrates good agreement with the actual leak flow uncertainty obtained from the model output and shown in Figure 4.11.

Figure 4.11 Leak Flow Uncertainty Caused by Measurement Noise

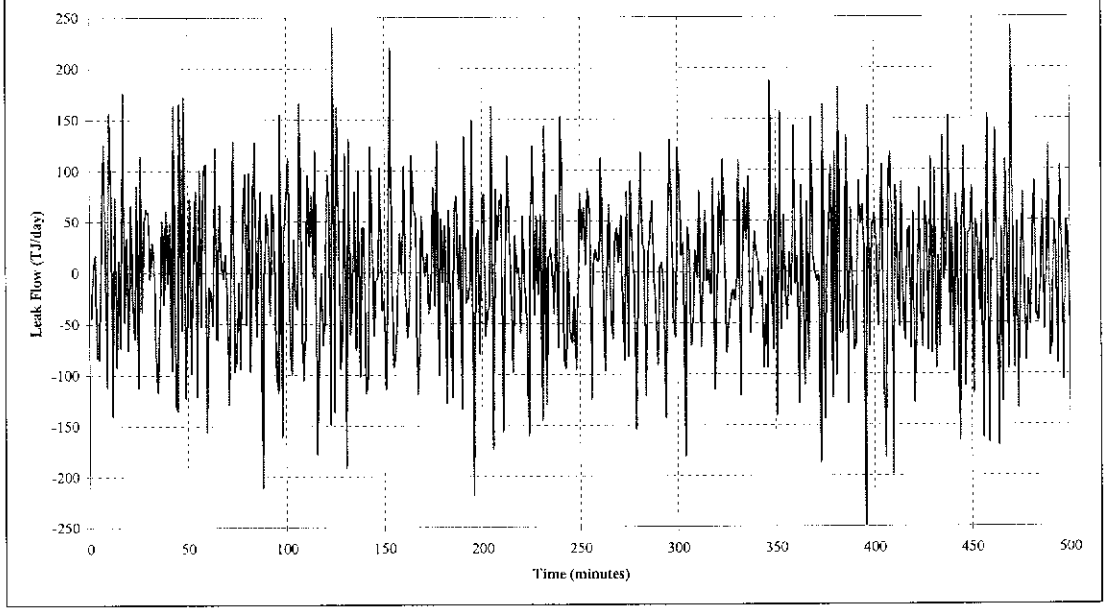

4.5 Effect of Measurement Uncertainty Using Measured Flows

The focus of the investigation thus far, has been the use of modelled flows in the mass balance technique. This is due to the lack of pipeline section flow measurement available on the GGT Pipeline, which is representative of most gas transmission pipelines. However, if the use of modelled flows calculated from pipeline section pressures and temperatures proves to be unsuccessful with the mass balance technique for detecting leaks reliably, it will be useful to know the minimum flow measurement required to achieve a satisfactory level of leak detection. This flow measurement can then be installed at predefined locations.

Again using the equation state, a relationship for the rate of change of section linepack can be determined.

$$\dot{L} = \frac{\overline{P}AZ}{R\overline{T}\Delta t} C_V \tag{4.20}$$

The term A represents the pipeline section cross sectional area, and the constant C_V is the calorific heating value of the gas to convert linepack units from mass to heating

energy units of gas. This is still basically a mass measurement, but as mentioned earlier, gas flow measurement and linepack are typically measured in terms of the gas heating value, which is represented in terms of energy. By substituting Equation 4.20 into Equation 4.4, an expression for leak flow can be obtained when measured pipeline section flow is available.

$$\dot{B} = \dot{W} - \frac{\overline{P}AZ}{R\overline{T}\Delta t} C_V \tag{4.21}$$

The term $\dot{W}$ is the measured flow rate difference (accumulation) into and out of the pipeline section. Taking partial derivatives of Equation 4.21 and substituting into Equation 4.12, an equation for the uncertainty in leak estimation in terms of flow and pressure measurement can be obtained.

$$\sigma_{\dot{B}} = \frac{1}{\sqrt{n}} \sqrt{\sigma_{\dot{W}}^2 + \left(\frac{AZC_V}{R\overline{T}\Delta t} \right)^2 \sigma_{\overline{P}}^2} \tag{4.22}$$

It should be noted that the contribution of pipeline section temperature uncertainty to linepack uncertainty and hence leak uncertainty was omitted in Equation 4.22, as this is demonstrated to be small compared to pressure measurement uncertainty in the following section.

In the design and construction of a new gas pipeline, or when considering the implementation of a leak detection system, it may be useful to understand the maximum distance between pipeline flow measurements to obtain reliable leak detection. The uncertainties for pressure and flow measurement are readily available from manufacturer's data for the respective instruments. The pipeline operator will define the uncertainty for calculated leak flow from the smallest leak to be detected, and the number of samples averaged n by how quickly the leak needs to be detected. Once these parameters are obtained the maximum allowable distance between flow measurements can be calculated from Equation 4.23.

$$Z = \frac{R\bar{T}\Delta t}{AC_V}\sqrt{\frac{n\sigma_{\dot{B}}^2 - \sigma_{\dot{W}}^2}{\sigma_{\bar{P}}^2}} \tag{4.23}$$

Equation 4.23 will be used later when the implementation of flow measurement for the GGT Pipeline is investigated.

4.6 Leak Detection Threshold

It is important at this point to define the minimum leak size the model is able to detect. In the previous section the uncertainty of measured inputs was defined, which is the standard deviation of a set of measurements assuming they are normally distributed about the mean. In a similar manner, the uncertainty of the calculated leak or leak detection threshold can be defined as the standard deviation of a set of calculated leak values from the model. Therefore if an actual leak is not larger that the uncertainty of the leak detection model, the leak will be deemed to be undetectable. It is apparent from Equation 4.13 the leak detection threshold of the model can be reduced in the following ways;

1. by reducing the uncertainty in the inputs to the model or;
2. by reducing the uncertainty of the calculated leak flow from the model.

Figure 4.11 demonstrates that without some means of noise reduction, the output from the leak detection model will be meaningless. Therefore in the following chapter methods of reducing the measurement and hence leak noise will be investigated.

To verify Equations 4.18 and 4.19 are in fact linear, the uncertainty associated with the pressure inputs to the model was varied whilst the uncertainty associated with temperature measurements was held at zero. The converse was repeated for temperature. The uncertainty values were expressed as relative uncertainty, which is a percentage of the average pressure and temperature so that comparisons can be made. Figure 4.12 shows the results of this investigation.

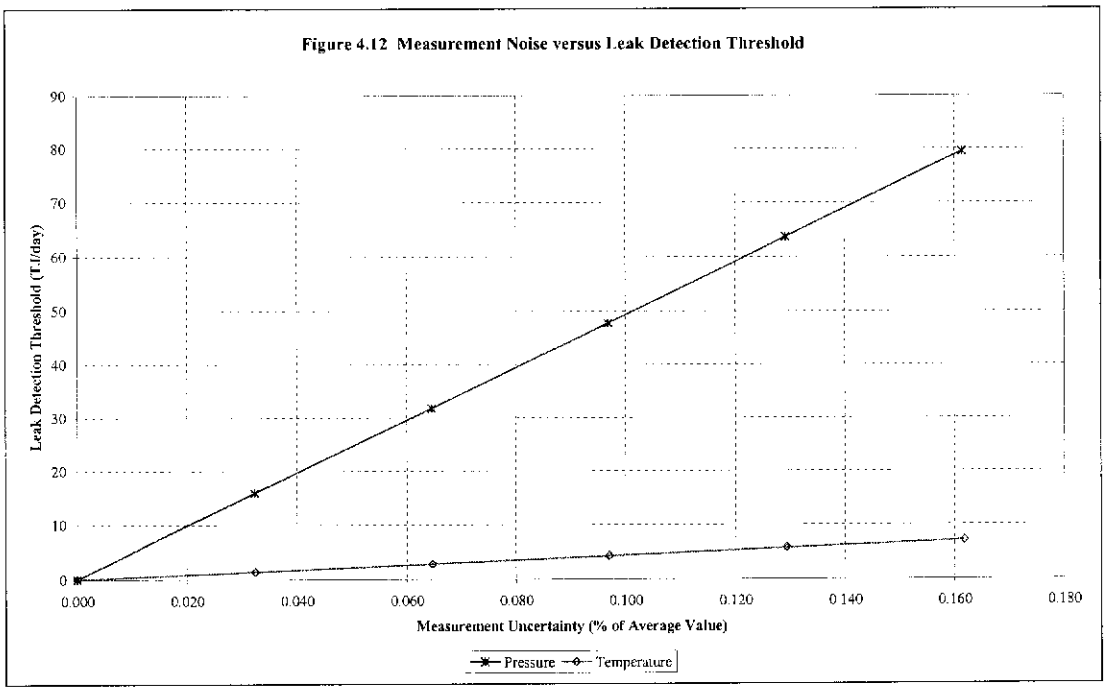

From the graph it is evident that relatively small uncertainties in pressure and temperature measurement can result in a large leak detection threshold. More importantly, pressure dominates the contribution to calculated leak uncertainty for equivalent magnitudes of measurement uncertainty. The ratio of leak detection threshold for pressure compared to that for temperature is approximately 11. It should be noted that in practice, the relative uncertainty in pressure is typically of the order of three times the relative temperature uncertainty. Therefore reducing the uncertainty in pressure measurement either by filtering the data or physically changing the configuration of the pressure transmitter will be more beneficial for reducing the overall leak detection threshold than reducing the temperature measurement uncertainty.

In addition to identifying which model input measurement contributes the most to calculated leak flow uncertainty, it is also useful to note whether the calculated flow or linepack is influenced the most by the measurement uncertainty. Figure 4.13 below shows the relationship between flow and linepack uncertainty for varying pressure uncertainty.

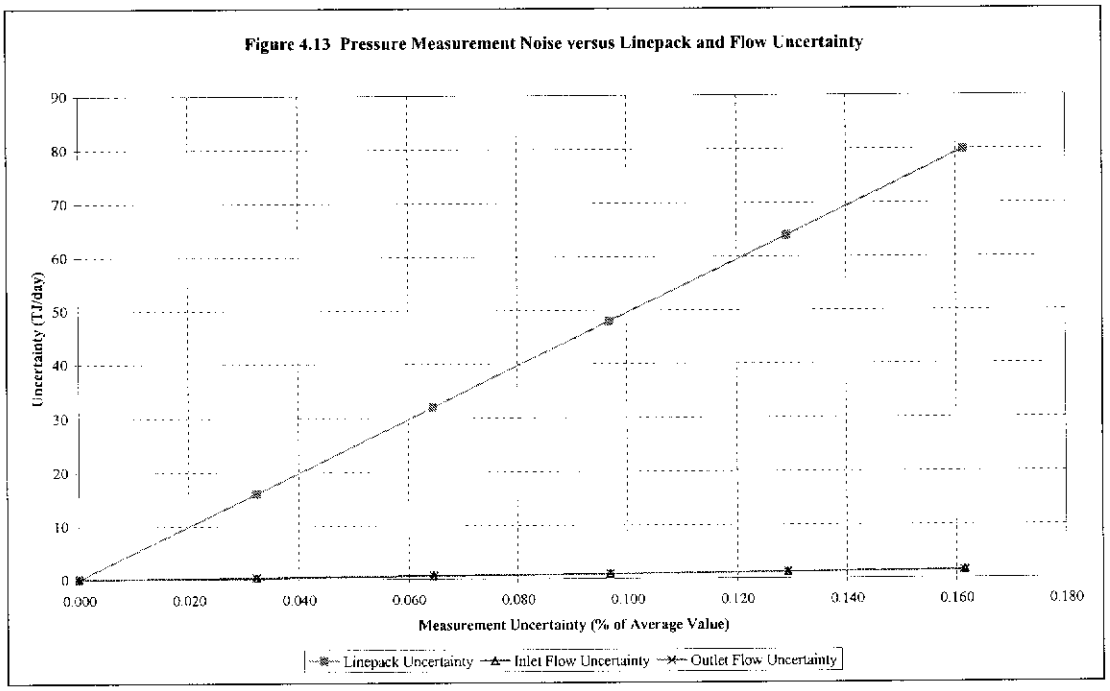

It is evident from the graph that increasing the pressure measurement uncertainty has a much greater effect on the linepack calculation rather than the flow. The ratio of linepack uncertainty to flow is approximately 54 throughout the range of data. This indicates the linepack uncertainty is clearly the main contributor to leak flow uncertainty and thus the leak detection threshold. The only way to reduce the linepack uncertainty is to reduce the size of the pipeline sections, which means less distance between pressure and temperature measurements, since they determine the size of a pipeline section.

Figure 4.14 shows a similar analysis, this time based on temperature uncertainty. The ratio of linepack uncertainty to flow uncertainty is much higher than that for pressure at approximately 195 throughout the range of values. Again it is the linepack that is affected most by measurement uncertainty.

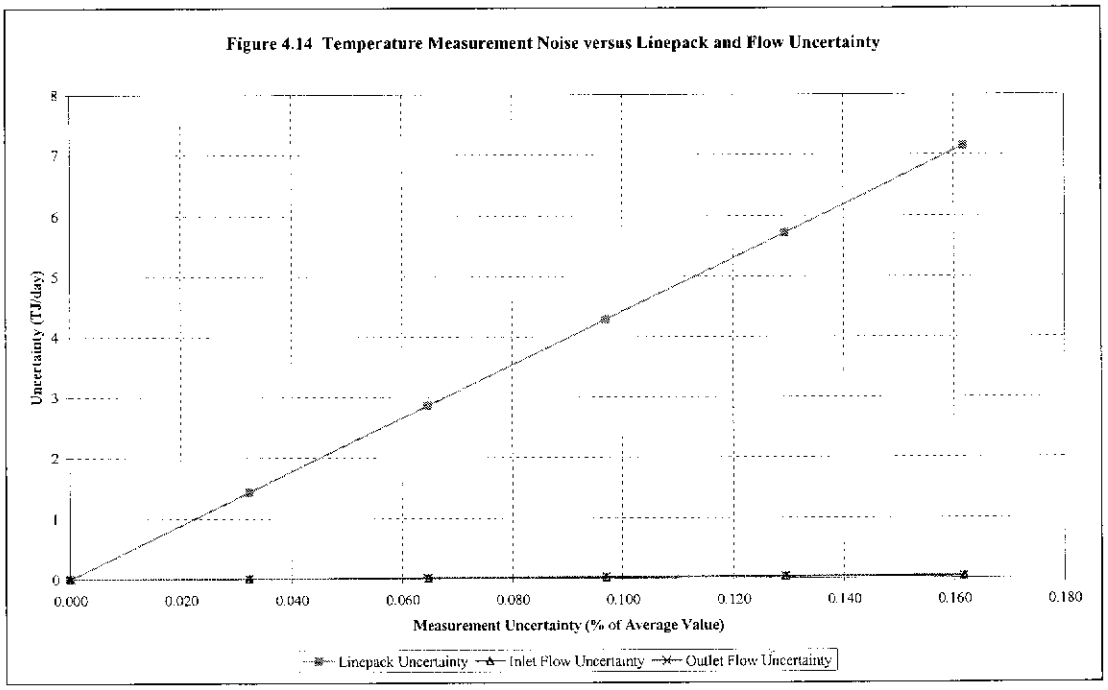

Lastly, it is interesting to note that typical values of uncertainty were used in generating the leak flows of Figure 4.11. The leak flow uncertainty of 86 TJ/day would make most leaks undetectable. Recall that previously a 10 TJ/day leak was simulated in Section 4.3. Clearly a strategy for reducing the leak flow uncertainty is required and this will be investigated in the following chapter.

5.0 REDUCTION OF LEAK UNCERTAINTY

5.1 Selection of Filters

Due to the effects of measurement uncertainty on the calculated leak flow, a method needs to be derived to reduce these effects so that the leak flow data is able to indicate actual leaks reliably. The measurement uncertainty causes values to be input to the model to be randomly distributed about a mean. This behaviour resembles random noise, which is sometimes referred to Gaussian noise. To reduce the noise on the output of the model, and hence have accurate and reliable leak flow data, it is apparent that some form of on-line filtering is required on the input data, output data, or both. There are many excellent texts available that provide guidance in the use of filters. Gabel (1973), Hamming (1977) and Lahti (1992) are examples of some publications. Three filters were chosen for investigation that are commonly used, and are well suited for removing random noise. These filters are as follows:

- Moving Average
- Weighted Moving Average
- Low Pass

The first two filters are time domain based, whereas the low pass filter is a frequency domain filter. Each filter was assessed against the following criteria:

- Ability to reduce the leak detection threshold
- Response to a step input simulating a leak i.e. the ability to keep the time constant to a minimum

To assess each filter, the randomly generated noise of the previous chapter was super-imposed on the input data to the simulation of the test section that was described in Chapter 3. The use of actual pipeline data is not introduced until Chapter 6 after an optimum filter has been selected.

The response of the filter and estimation of leak magnitude was tested using a simulated leak size of 10 TJ/day. This step change in leak value for 0 TJ/day to 10 TJ/day commences at a simulation time of 100 minutes, as shown in Figure 5.1 with no noise present.

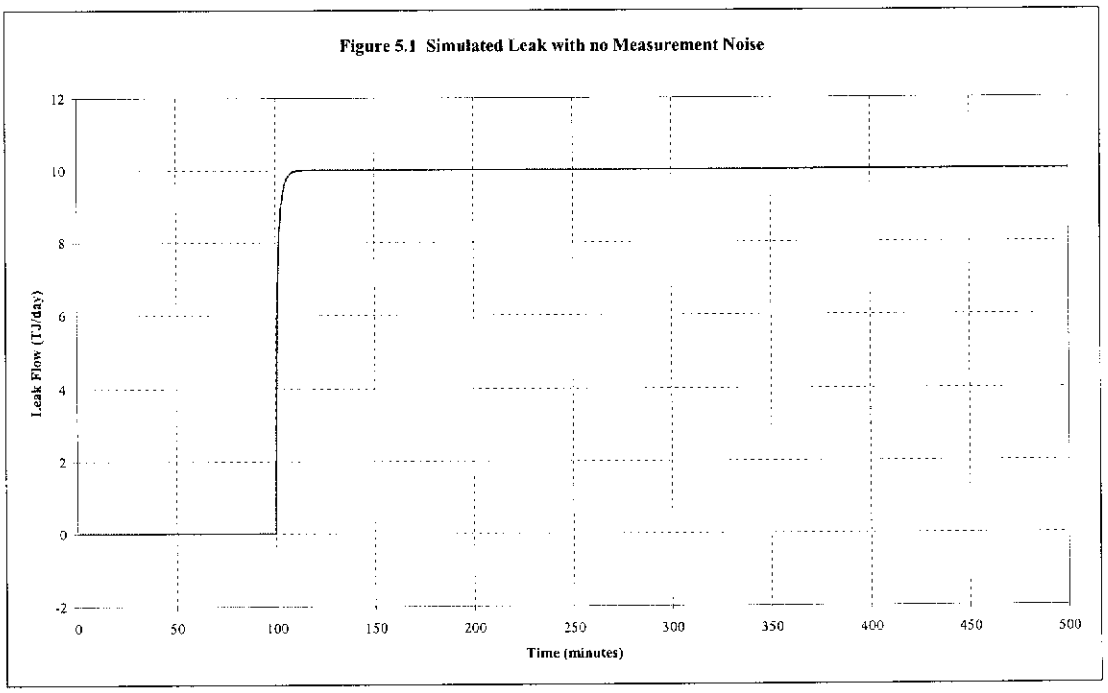

Now the same level of measurement uncertainty was added to the pressure and temperature inputs as was used in Chapter 4 to produce the output shown in Figure 5.2.

The induced measurement noise consisted of a maximum uncertainty of 0.025 MPa for pressure, and 0.3 K for temperature from the measurand. The effects of the measurement noise completely concealed the leak as can be seen in Figure 5.2. Each of the filters were then compared using the data shown in Figures 4.11 and 5.2 to find the filter or combination of filters which have the highest noise reducing capability without substantially delaying the detection of a leak from the actual time of inception.

Figure 5.2 Simulated Leak with Measurement Noise

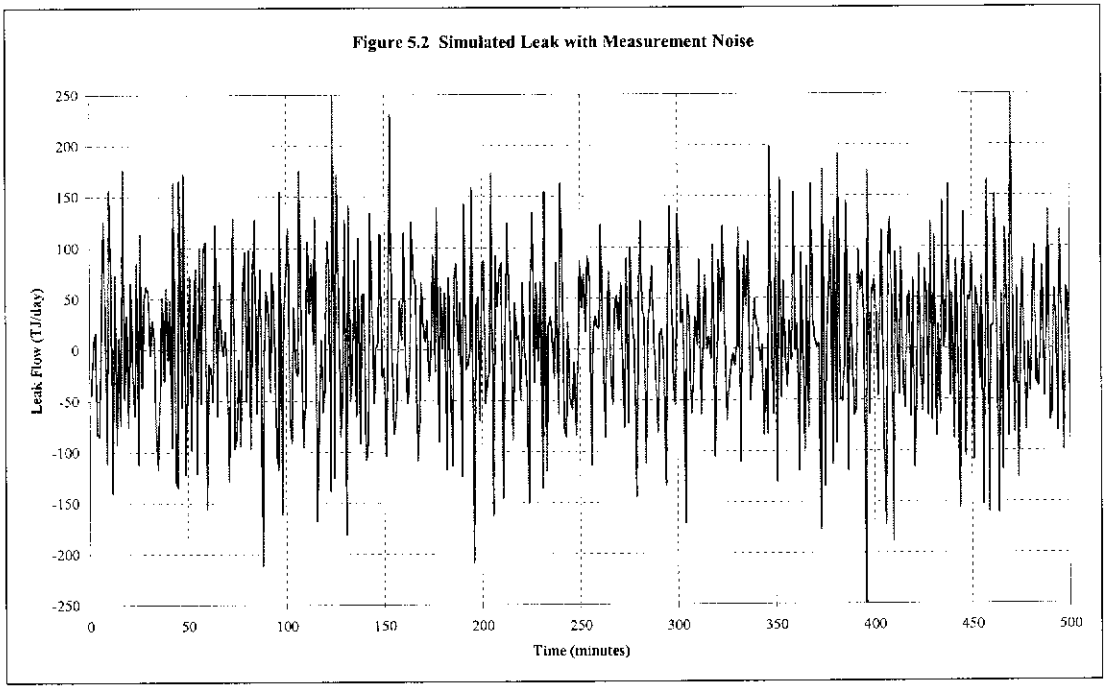

5.2 Moving Average Filter

The moving average is the most common filter in discrete signal processing, mainly because it is the easiest digital filter to understand and use. In spite of its simplicity, the moving average filter is optimal for many common tasks, which require a reduction in random noise whilst retaining a sharp step response. This makes it one of the best filters for time domain encoded signals, which would be expected from the measurement noise generated from non-systematic errors. However, the moving average is the worst filter for frequency domain encoded signals, with little ability to separate one band of frequencies from another. However, due to the nature of filtering being performed in this application, there is no requirement to separate or eliminate one set of frequency characteristics from another. The main objective is to reduce random noise, therefore the moving average filter is more than adequate to perform this function. There is a range of filters related to the moving average that have similar characteristics including the Gaussian, Blackman, and multiple-pass moving average. Since the moving average is the simplest, it is efficient computationally and relatively straightforward to implement.

As the name implies, the moving average filter operates by averaging a number of neighbouring points from the input signal to produce each point in the output signal. To reduce the calculated leak flows caused by measurement noise, Turner and Mudford (1988) averaged the output leak flow results over several consecutive measurement periods to produce a more stable and less sensitive leak flow rate. This is a basic form of data filtration and is in effect a type of low pass filter. The general algorithm employed to produce an average leak flow is shown below.

$$\dot{B}_n = \frac{1}{n}\sum_{i=1}^{n}\dot{B}_i \tag{5.1}$$

Since the calculated leak flow noise is generated from the measurement noise on the model inputs, the effects of removing the noise from the source data were also investigated. Therefore a comparison was made between input data filtering only (pressure and temperature), output filtering only (leak flows), and a combination of both input and output data filtering. The number of consecutive measurements n has to be determined to provide optimum leak detection sensitivity. By increasing n, the noise reduction is improved, but as a compromise resolution of a step change is reduced which effectively creates a time delay in leak detection.

Figure 5.3 Leak Detection Threshold for Increasing Samples Averaged
MOVING AVERAGE FILTER

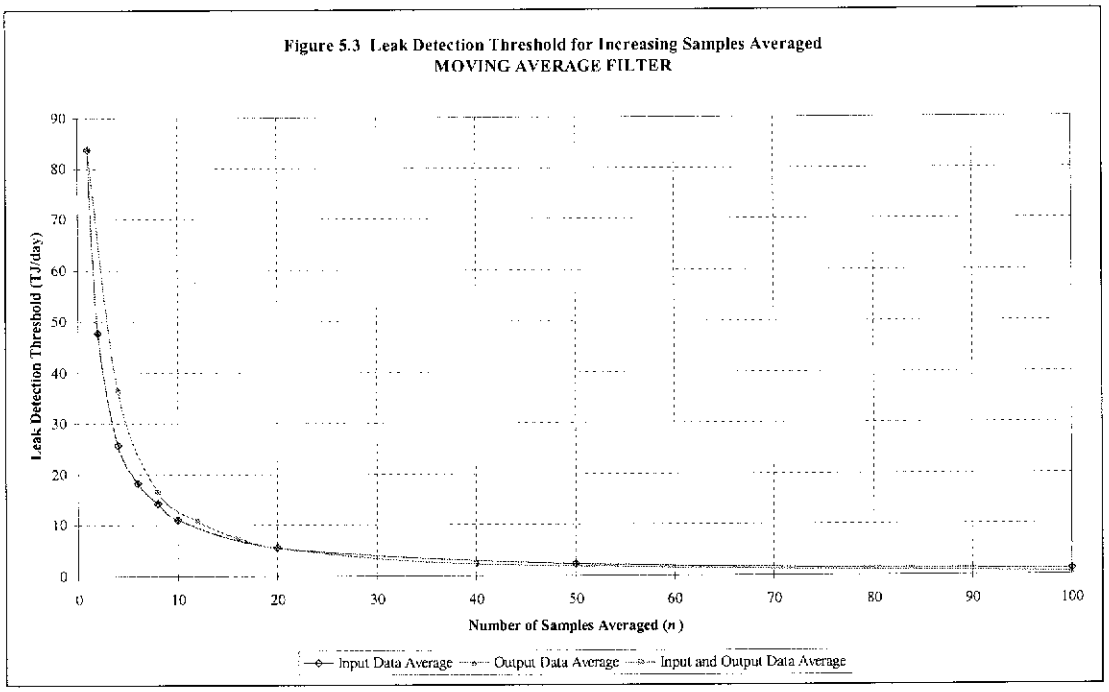

Figure 5.3 shows the noise reduction by increasing n for each set of data that was filtered. The moving average filter was applied in three different ways. Firstly the filter was only applied to the input data for the model, namely the pipeline section inlet and outlet pressure, and temperature. The second method investigated was to apply the moving average only to the leak flow output of the model. Finally, the moving average filter was applied to the input data and leak flow output.

It is evident from Figure 5.3 that the greatest rate of improvement for noise reduction was obtained from between n equal to 1 and 20 measurement periods for all three cases. Increasing n to 20 measurement periods reduced the leak detection threshold by approximately 92% for all three cases, but increasing n from 20 to 100 only provided an additional reduction in the leak detection threshold.

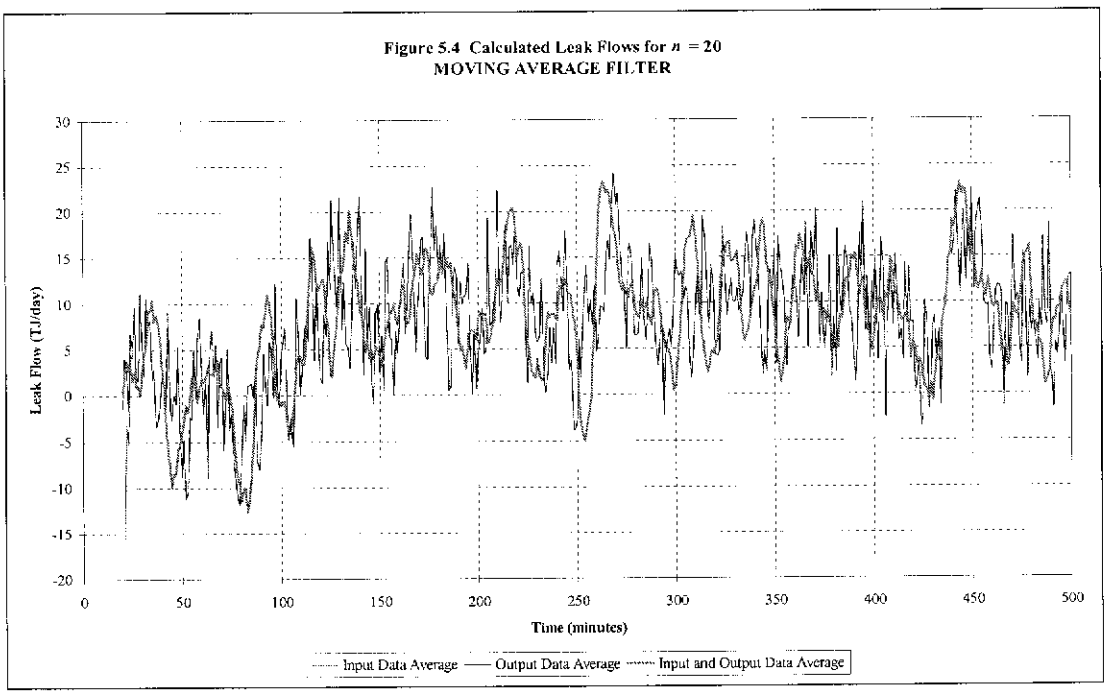

The combined input and output data filter was compared to the single filters by matching the delay or offset produced by the filter. For example, averaging 10 input measurement periods and then averaging the corresponding 10 output measurements, produces an overall offset of 20 measurement periods. Therefore this case was then examined against both the input only and output only filter for n equal to 20 to produce a fair comparison. The results of the corresponding filtered output of the model can be seen in Figure 5.4.

Figure 5.5 illustrates the further improvement for n equal to 100 measurement periods. The noise has been reduced substantially compared to the unfiltered data in Figure 5.2, however it is still difficult to ascertain the leak magnitude from Figure 5.4. Figure 5.5 clearly illustrates the magnitude of the leak to be approximately 10 TJ/day and the offset of 100 minutes from leak inception can also be seen. It is interesting to note that input only, and output only filters produced nearly identical results, whereas the combined filter had a greater smoothing effect.

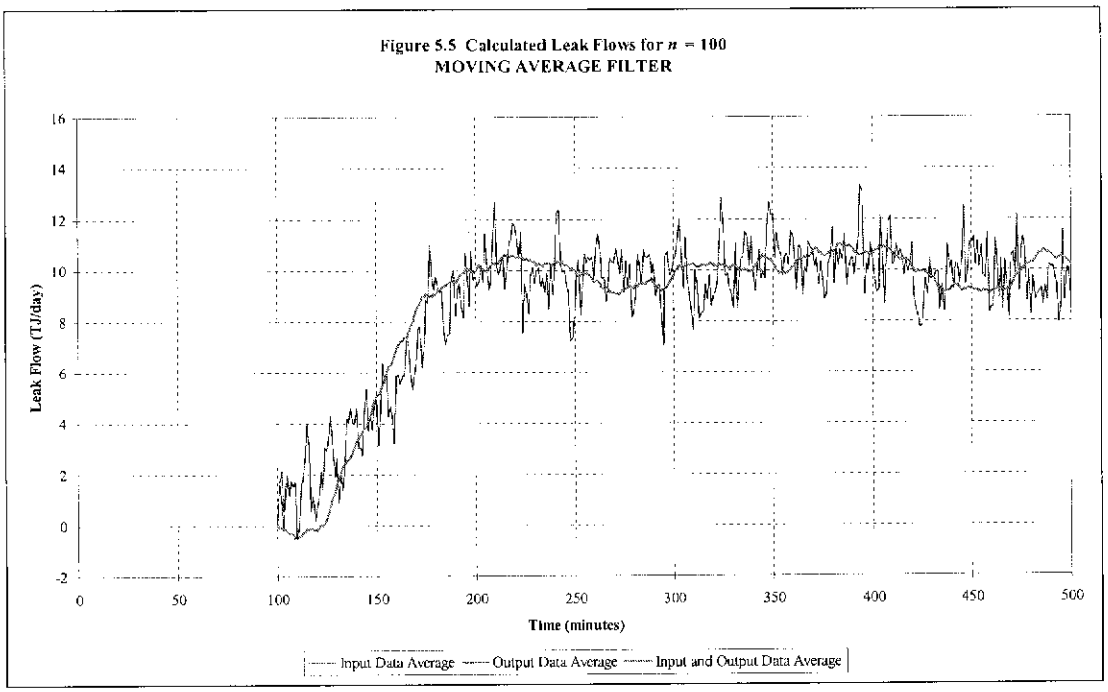

5.3 Weighted Moving Average Filter

The weighted moving average filter is similar to the moving average filter except for the use of a kernel that applies weights to each of the values in the range. Turner (1987) derived weights by optimising the equations for leak flow uncertainty, and demonstrated that the weights were far from optimum if the ratio of measured flow to linepack uncertainty is small. For this reason, a Gaussian kernel was selected for this application that is often referred to as Gaussian smoothing. In the previous

section, the weighting for each of the values in the average was simply $1/n$. Equation 5.1 can be written in terms of individual weights.

$$\dot{B}_n = \sum_{i=1}^{n} a_i \dot{B}_i \tag{5.2}$$

Where the sum of the weights in the sample equals unity as shown in Equation 5.3.

$$\sum_{i=1}^{n} a_i = 1 \tag{5.3}$$

In this case the weighting will follow the relationship of the Gaussian distribution given by Equation 5.4 below.

$$G(x) = \frac{1}{\sqrt{2\pi}\sigma} e^{-\frac{x^2}{2\sigma^2}} \tag{5.4}$$

Since the average will be performed on-line in real time, the most recent value will have the largest weighting. The weights will follow the shape of half a normal distribution curve, where x is a value that ranges from 1-n to 0, and σ is the standard deviation of the distribution.

The standard deviation of the weighting values affects the degree of influence the most recent values has over the entire averaged value. Therefore as σ approaches infinity, the values of each of the weights in the distribution approaches $1/n$, which is simply the uniformly weighted moving average filter demonstrated in the previous section. This is illustrated clearly in Figure 5.6, where various values of σ were examined for a 20 sample weighted average.

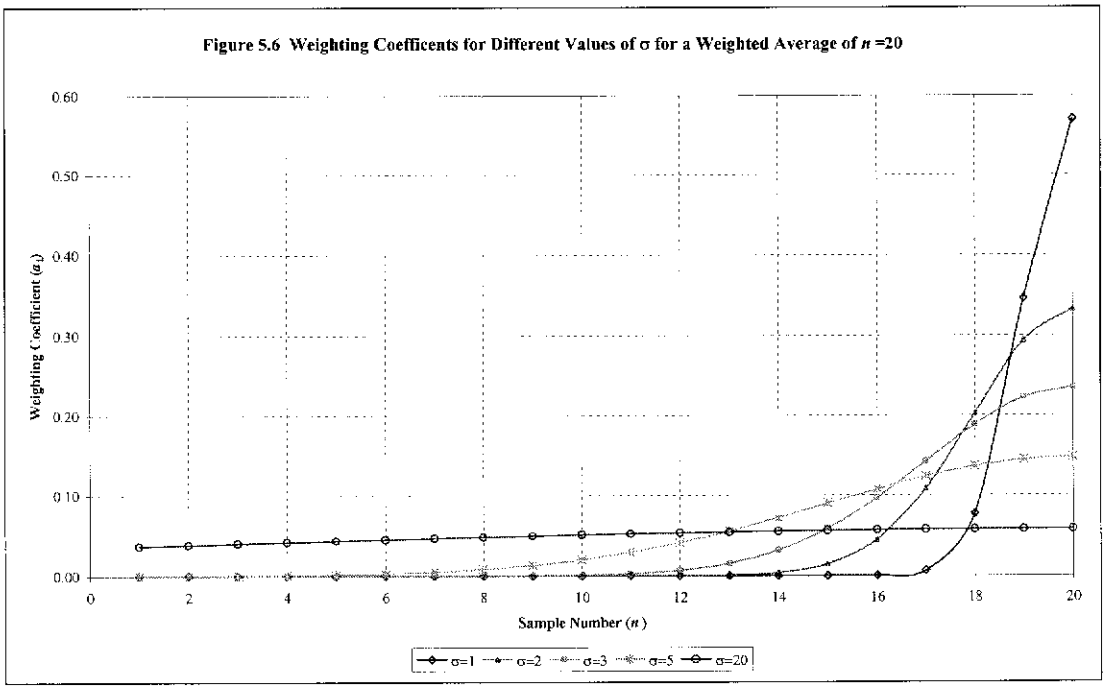

The value of σ was optimised to minimise the standard deviation of the sample being filtered, whether that be input or output data for the model.

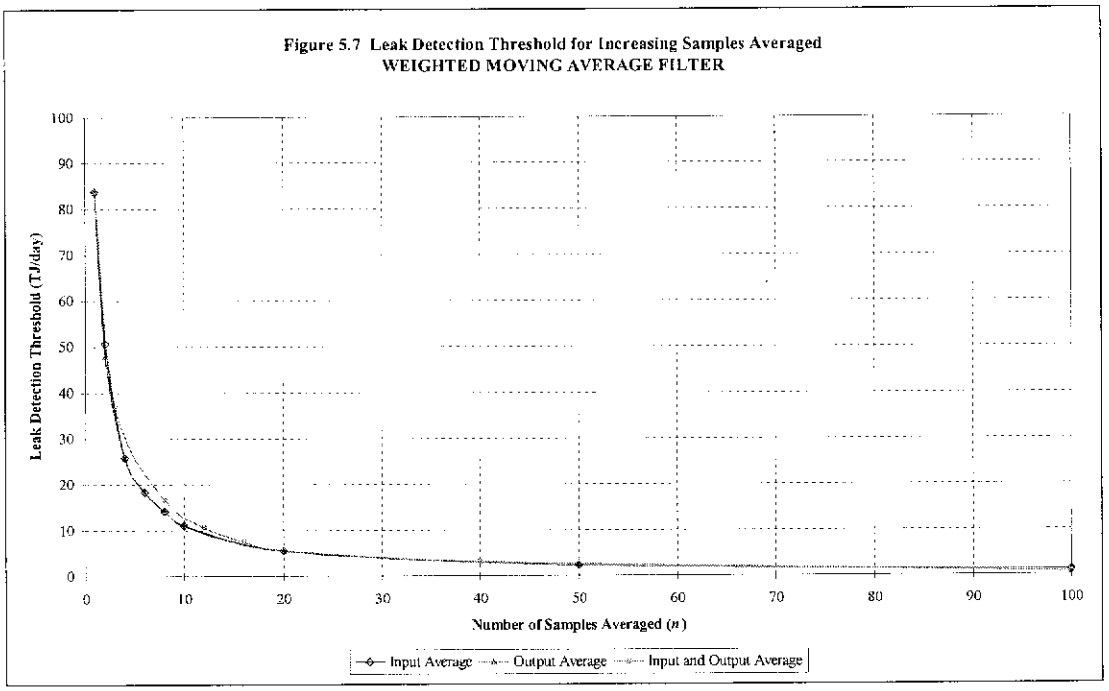

Figure 5.7 shows that there was a small improvement when Gaussian smoothing was applied to the output of the model directly for optimised values of σ . However the optimised value of σ for filtering input or combined input and output data was large,

thus there was little improvement from the moving average filter. This is due to the optimum noise reduction produced by uniform weights, whereas lower values of σ possess better response to a step input, at the sacrifice of noise reduction.

Figure 5.8 illustrates the improvement when Gaussian smoothing is applied directly to the output of the model for a 100 sample moving average.

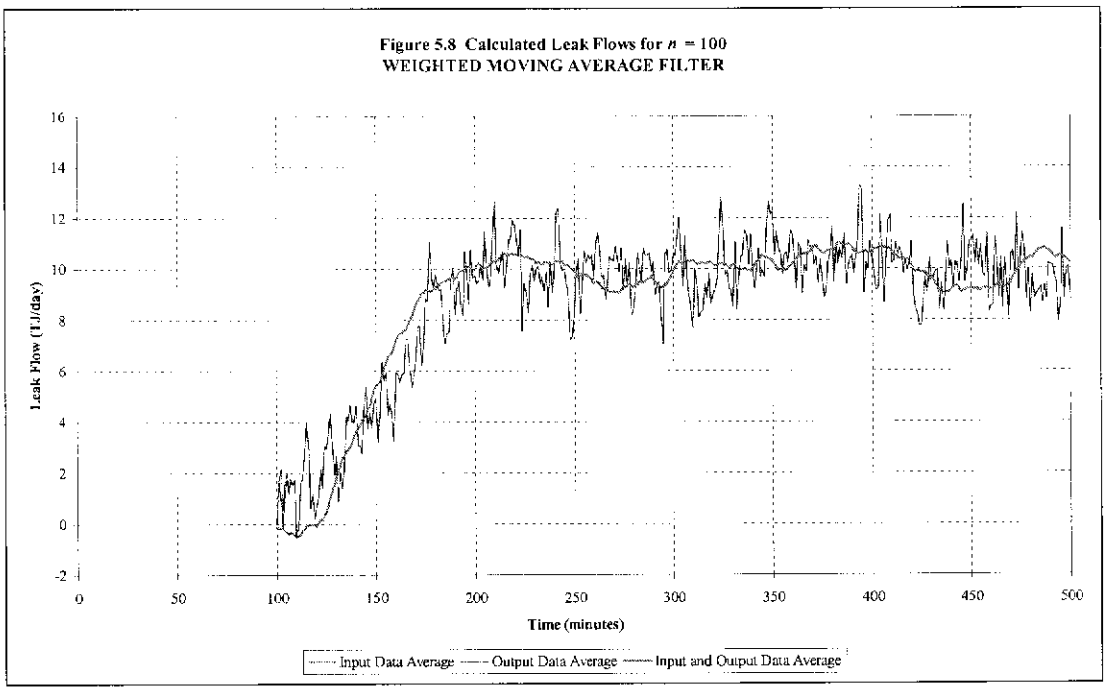

The level of noise reduction from the weighted moving average filter is similar to the moving average filter. This is due to the Gaussian weights being optimised to provide the best noise reduction.

5.4 Low Pass Filter

Typically, when it is desirable to remove one set of frequencies from another, some form of low pass filter is employed. This is a common technique covered in detail by nearly all signal processing publications and is quite a robust filter for removing random background noise. The process involves examining the power spectrum to verify which frequencies dominate the signal in the time domain. This is outlined in many signal processing texts including Astola (1997), Cappellini (1978), Hamming

(1977) and Ifeachor (1993). Once this is verified, all frequencies above this region are eliminated and the signal is transformed from the frequency domain back into the time domain by way of Fourier transformation, which is covered in detail by Nussbamer (1981), Phillips (1995), Terrell (1988), Tolimieri (1989) and Vaseghi (1996). This frequency above which, other frequencies are blocked is often referred to as the cut off frequency f_c. In this case, only the lowest frequency was allowed to pass, to provide the best noise reduction. Therefore the cut off frequency varied, depending on the number of samples used.

The number of samples used in this case is required to follow the relationship 2^n as demonstrated by Brigham (1988), therefore sample numbers of 4, 8, 16, 32, 64 and 128 were chosen for investigation. Noise reduction as a function of sample size is shown in Figure 5.9, since the leak was commenced at a simulation time of 100 minutes, the 128 sample filter would not have produced an output until the leak had been present for 28 minutes.

It is evident from Figure 5.9 where the input, output and combined data filters converge to the same level of noise reduction for sample numbers greater than 64. For sample numbers less than this, the output and combined low pass filters had superior performance compared to the input low pass filter alone. This is most likely due to the higher proportion of values in the frequency spectrum that were allowed to pass for high values of n compared to low values of n. For sample numbers greater than 64 a higher proportion of frequencies were passed for the same cut off frequency, resulting in less noise reduction but greater response.

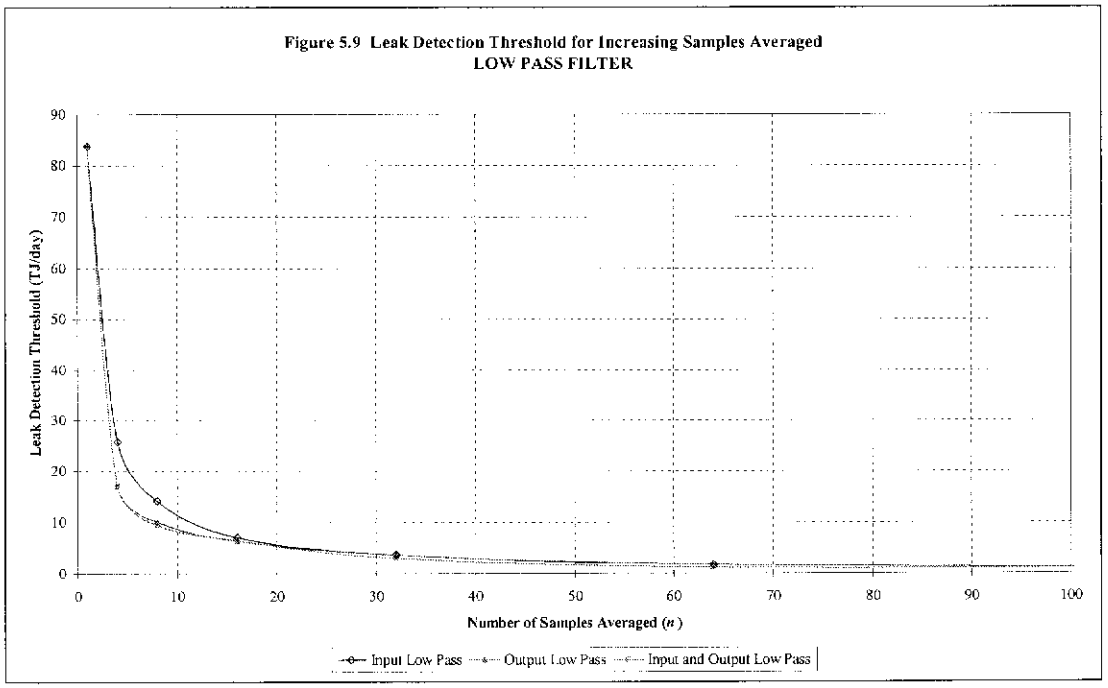

Figure 5.10 shows the performance of the low pass filter when a moving sample of 128 values is applied. It is interesting to note that all three variations of the application of the low pass filter produce exactly the same level of noise reduce in the time domain for 128 samples.

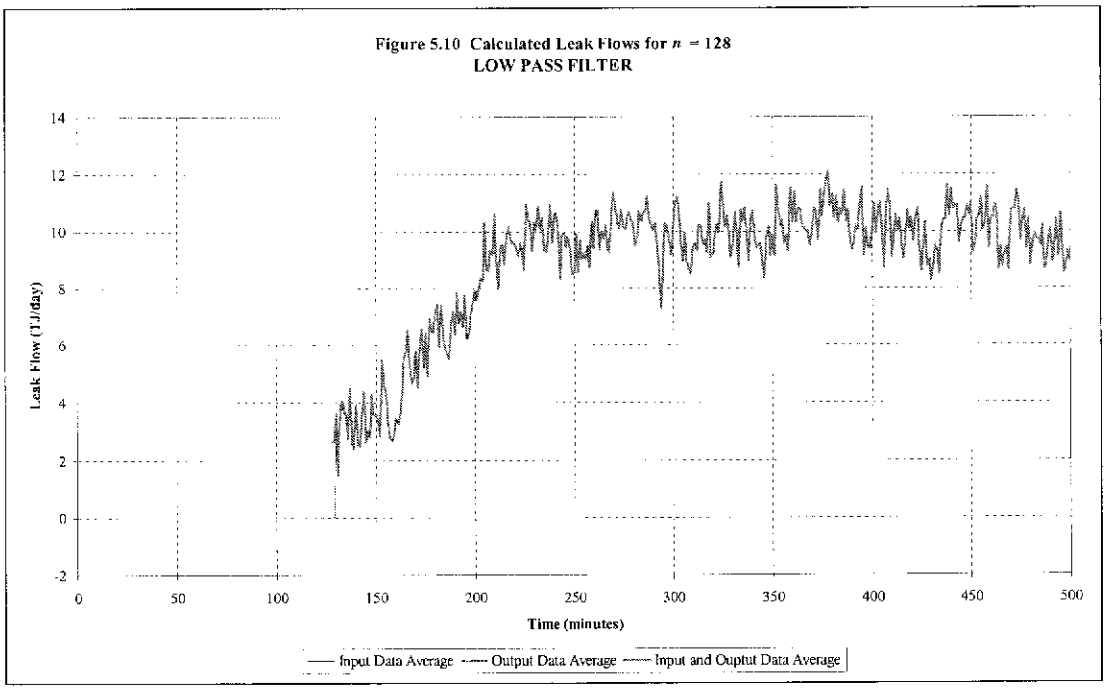

5.5 Comparison of Filters

Each of the filters tested had similar noise reduction properties when applied to both input and output data for the model. To determine the most suitable filter to apply using actual pipeline data in the following chapter, each filter was assessed for the ability to reduce the leak detection threshold, provide good response to a step input or leak, and to overall smooth random fluctuations in leak flow.

Figure 5.11 illustrates there was virtually no difference in performance between both of the time based moving average filters when applied to the input data only. The low pass filter however, did not perform as well for larger values of n. Therefore since the moving average filter is the simplest for implementation and was equal to the weighted moving average in noise reduction, this was chosen for the optimum input filter.

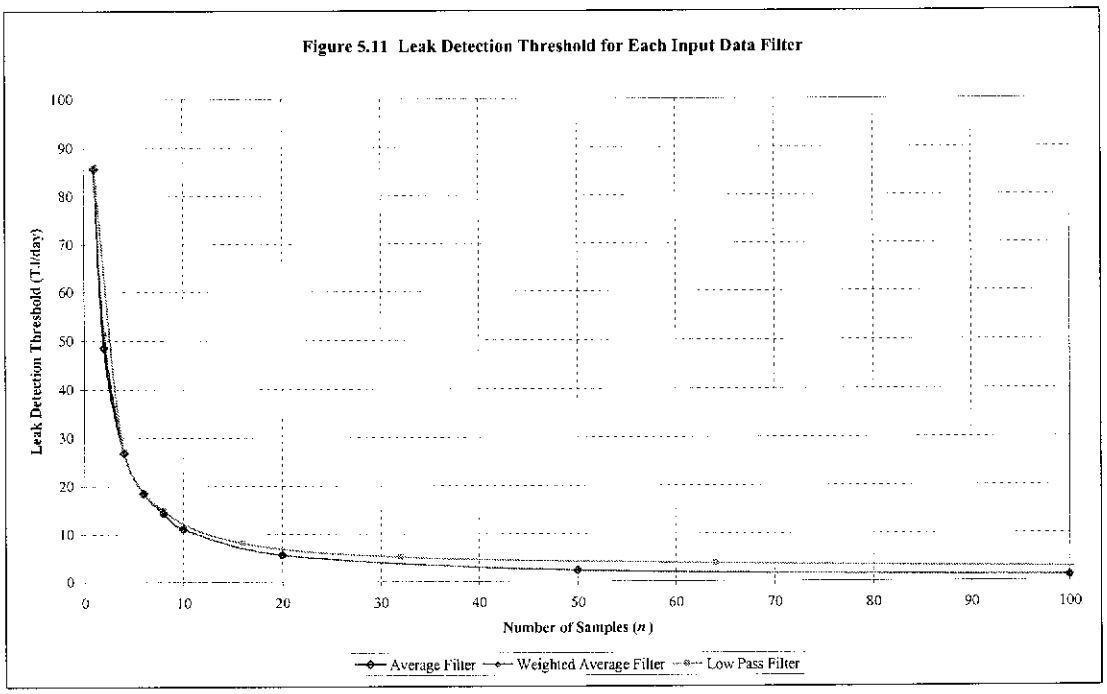

Due to the relatively small amount of measurement noise on each of the inputs resulting in a large amount of leak flow noise on the output, even small improvements in reducing measurement noise resulted in large improvements in leak flow noise reduction. However, a corresponding delay was introduced proportional

to the number of measurements n that was filtered. Therefore a compromise has to be made between leak flow noise reduction, and delay of response to leak initiation.

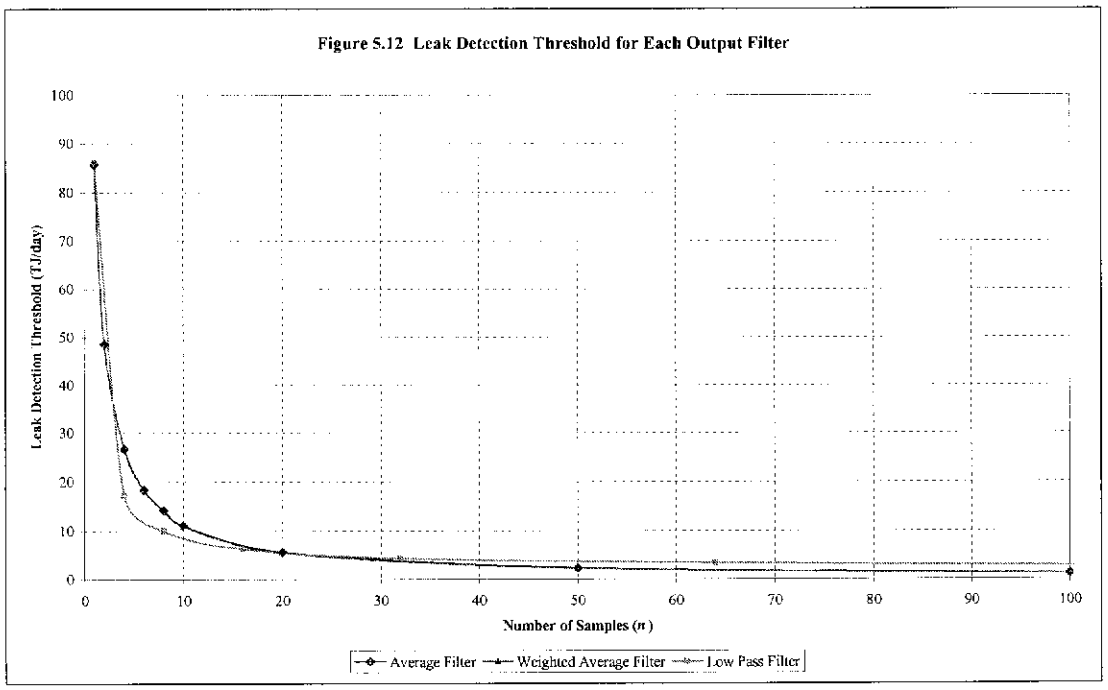

Figure 5.12 shows the performance of each of the filters when applied directly to the model output. The low pass filter when applied directly to the output leak flows of the model has superior performance than both moving average filters for low values of n. For values of n greater than 16 the low pass filter provides a slightly inferior level of noise reduction as both the moving average filters.

Figure 5.13 shows that for the combined filters, the moving average filter provides superior noise reduction compared to the other filters for sample numbers greater than 20. For sample numbers less than 20, again the low pass filter provided the highest noise reduction.

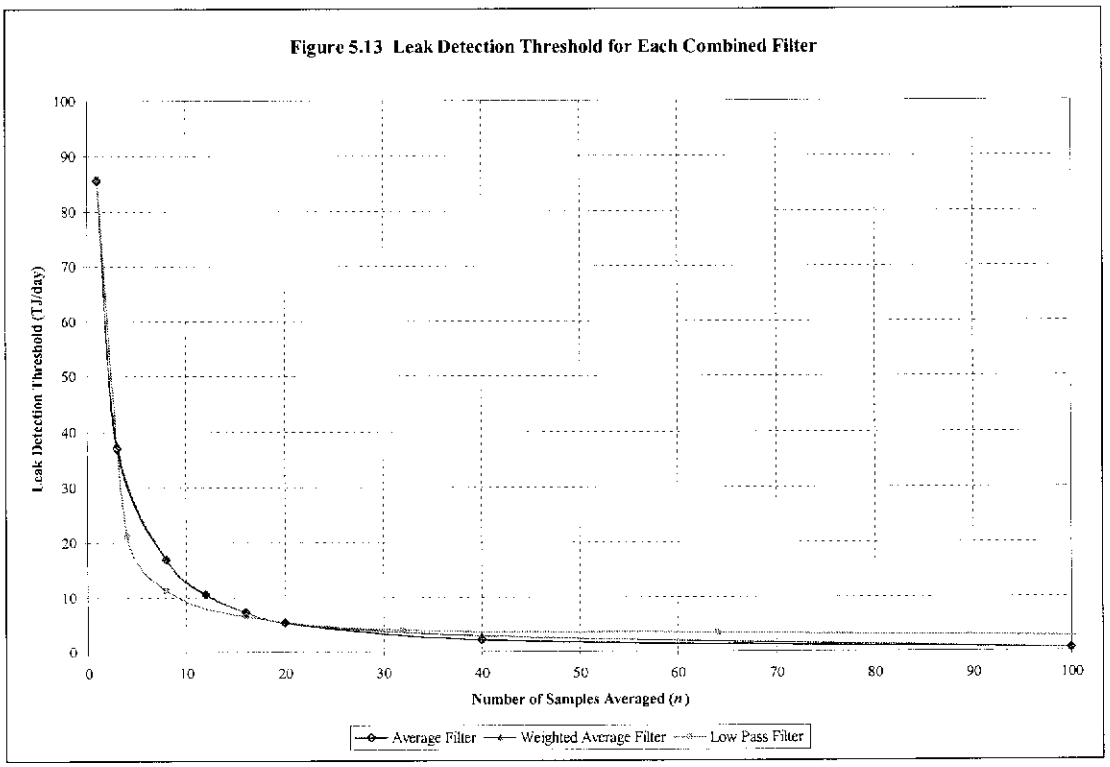

5.6 Selection of Optimum Filter

The results in this chapter assisted in deciding which filter or combination of filters would be suitable for testing against real pipeline data for the pipeline sections chosen in Chapter 3. Due to the similar performance of each of the filters, it was decided to proceed with the simplest, the moving average filter. The moving average filter performed surprisingly well, especially when applied to the input and output data of the model. The choice of the number of samples to average n, is a compromise between noise reduction and the response delay to a step leak input. Therefore an initial estimate of 30 input samples and 30 output samples was investigated against the real time pipeline measurements. This should provide a stable estimate of leak magnitude within 60 minutes of leak onset.

6.0 TESTING OF OPTIMUM FILTER

6.1 Introduction

In Chapter 5, the moving average filter was selected as the most favourable. In this chapter, the moving average filter is applied to the real time data from the GGT pipeline for the selected pipeline sections outlined in Chapter 3. The ability for the selected filter to reduce noise compared to the unfiltered data is examined. In addition to noise reduction, the filter response to an induced leak step input is investigated against the real pipeline data. The simulated leak was created by reducing the inlet and outlet pressure of each selected pipeline section by a constant amount at each time step. A uniform decrease in inlet and outlet pressure at each time step will produce a calculated leak of constant magnitude. The relationship is linear, therefore the required pressure change for a given leak flow can be determined through trial and error relatively quickly. This pressure behaviour is not likely to occur in practice, as was previously discussed in Chapter 4, the upstream pipeline section flow will increase to compensate for the leak. However, this method is sufficient to provide a constant step change to examine the filter performance.

The simulated leak was commenced at a simulation time of 5000 minutes, and lasted for a duration of 200 minutes for each pipeline section. This duration was chosen as the inlet and outlet pressures could not be reduced for an extended period of time, without the pressures dropping to abnormally low levels. The simulated leak was held constant at a magnitude of 10 TJ/day for each of the three selected pipeline sections. This corresponded to approximately 28% of the typical flow for the pipeline sections Anaconda to Leonora and Jeedamya to Cawse, and approximately 14% of the typical flow for Ned's Creek to Wiluna. The three pipeline sections are to be examined before confirming the final configuration of the model and filter. If the configuration examined is acceptable for all three sections, which represent the range of pipeline sections that will be encountered on the GGT pipeline, this will be used in the final on line implementation.

For the presentation of results, the y-axis scales, which represent leak flow magnitude on each of the graphs, were kept at the same limits. This provides the ability to compare the calculated leak flow results for each of the pipeline sections examined. There is extensive graphical data presented in this chapter, as it is necessary to present the filter performance for the large amounts of actual pipeline data collected.

6.2 Anaconda to Leonora

The first section examined was Anaconda to Leonora that also has the lowest retention time as outlined in Chapter 3. It was expected that this pipeline section would have the lowest overall calculated leak flow noise, as this is dominated by the calculated linepack noise and Anaconda to Leonora has the lowest linepack to flow ratio.

The data used was eight days or 11520 one minute samples of pressure and temperature from each of the pipeline section end points. Figure 6.1 shows the input data for the model over the eight day period. Initially the model was run without filtering the data to determine the extent of the unfiltered leak detection threshold for the pipeline section.

The diurnal temperature variations can be clearly seen from the model input data shown in Figure 6.1. The gas temperature measurements are taken at above ground stations on the pipeline. Therefore this indicated that the temperature transmitters are affected of ambient diurnal temperature variations on the above ground station. In reality, since the majority of the pipeline is buried, the gas temperature for the section should be immune to ambient temperature effects and only show seasonal variations.

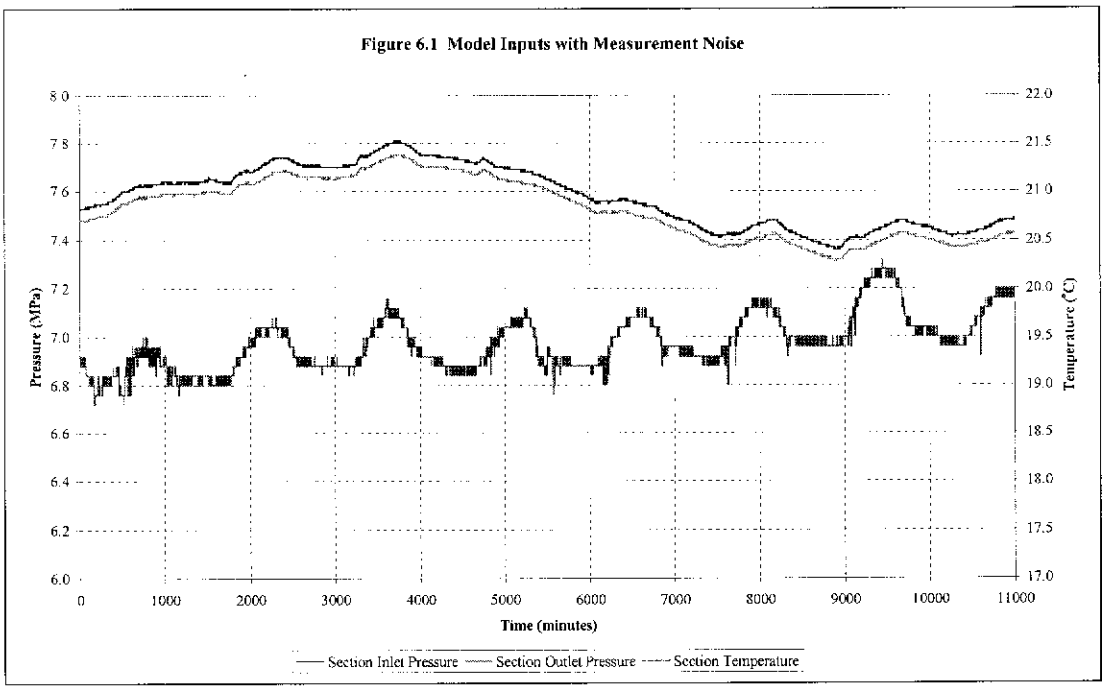

Figure 6.2 shows the uncertainty in leak flow estimation when the data used in the model is unfiltered. The leak uncertainty is much lower than that simulated for the larger test pipeline section. The unfiltered leak detection threshold for Anaconda to Leonora was approximately 2.98 TJ/day compared with 85.63 TJ/day for the test pipeline section. Therefore a lower leak detection threshold is attainable for the equivalent filter applied to the larger test section. It becomes evident that due to the diversity in pipeline section sizes on the GGT pipeline, the performance of the leak detection model will vary from section to section.

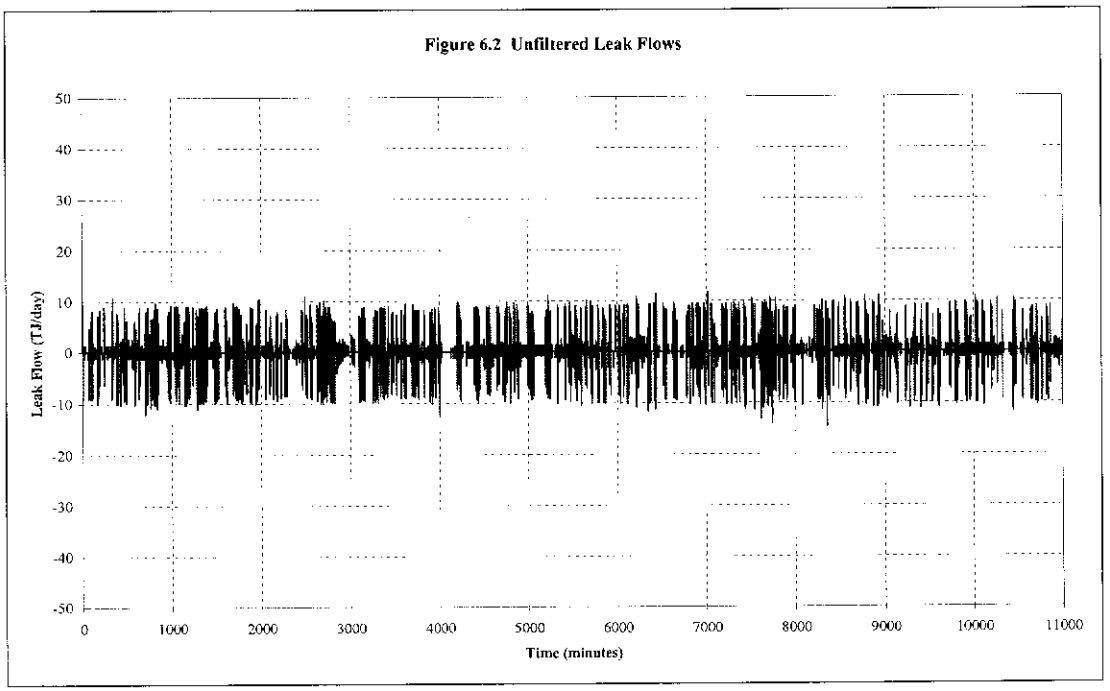

The combined input and output moving average filter was then applied to the model data. The pressure and temperature input data was averaged over 30 measurement periods to reduce the measurement noise. The corresponding calculated leak flow data produced from the model was also averaged over 30 measurement periods. Therefore the maximum anticipated delay between detecting the correct magnitude of the leak and the actual leak onset should be less than 60 measurement periods. Since measurements are taken at one minute intervals the maximum delay in detecting a leak should be less than 60 minutes.

The filtered input measurements are shown in Figure 6.3, where it can be seen that the random measurement variations caused by the uncertainty of each measurement have been reduced.

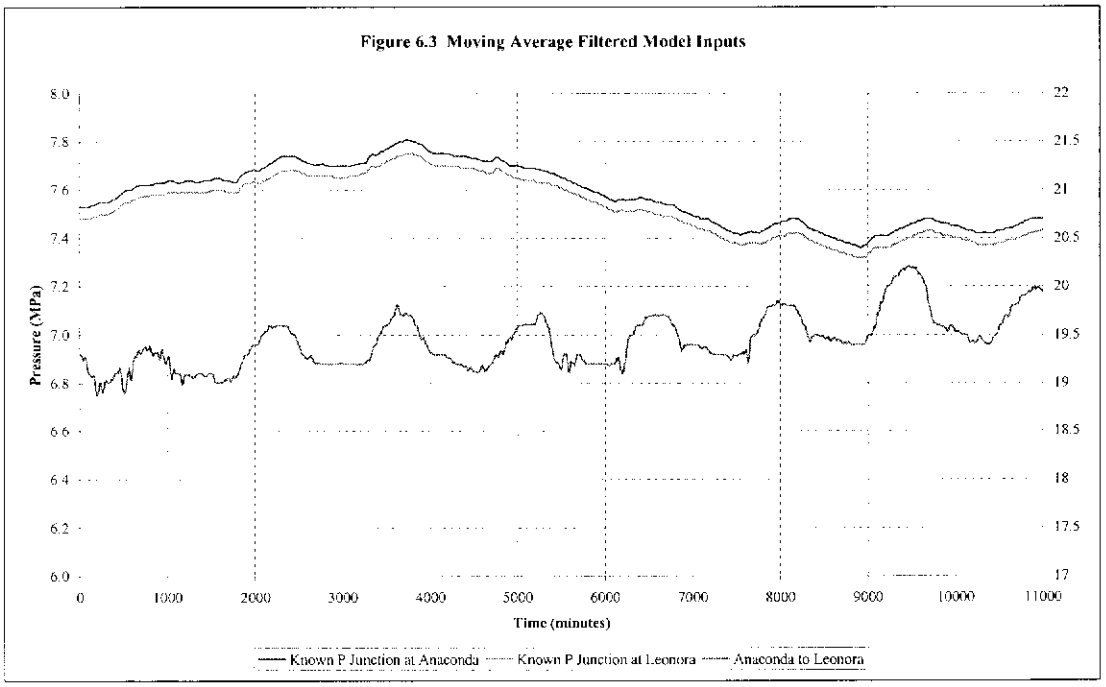

Figure 6.4 illustrates the effectiveness of the moving average filter in removing the calculated leak flow noise. The leak flow uncertainty has been reduced from 2.98 TJ/day for the unfiltered data, to 0.24 TJ/day for the filtered data.

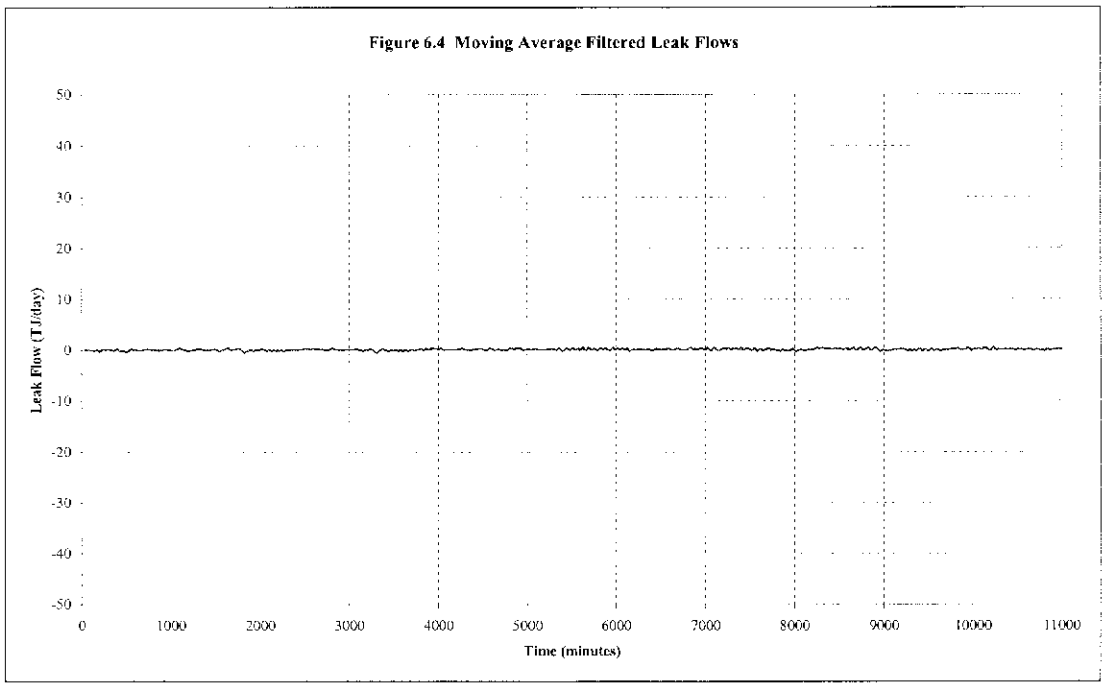

The number of input measurements that are averaged can be increased for further noise reduction, however the possibility of under estimating the magnitude of a

transient leak that has a duration less than the averaged samples becomes greater. Since it has already been confirmed that the mass balance technique already under estimates leak magnitude, it is advisable to keep the number of input samples averaged to a minimum once overall leak uncertainty has been reduced to acceptable levels.

The final test of the filter was to verify the ability to respond to a step input caused by a leak. Reducing the measured inlet and outlet pressures of the pipeline section by approximately 7.35 kPag each measurement period simulated a 10TJ/day leak of constant magnitude. The corresponding filtered input data is shown in Figure 6.5. It can be seen for the calculated flows to detect this leak, an extremely large drop in pressure is required for simulation in the smaller pipeline section. This is an unrealistic scenario, as this would not occur in reality for a leak of this magnitude, indicating that using the modelled flows in this situation would not be ideal.

Figure 6.5 Moving Average Filtered Model Inputs for a Simulated Leak

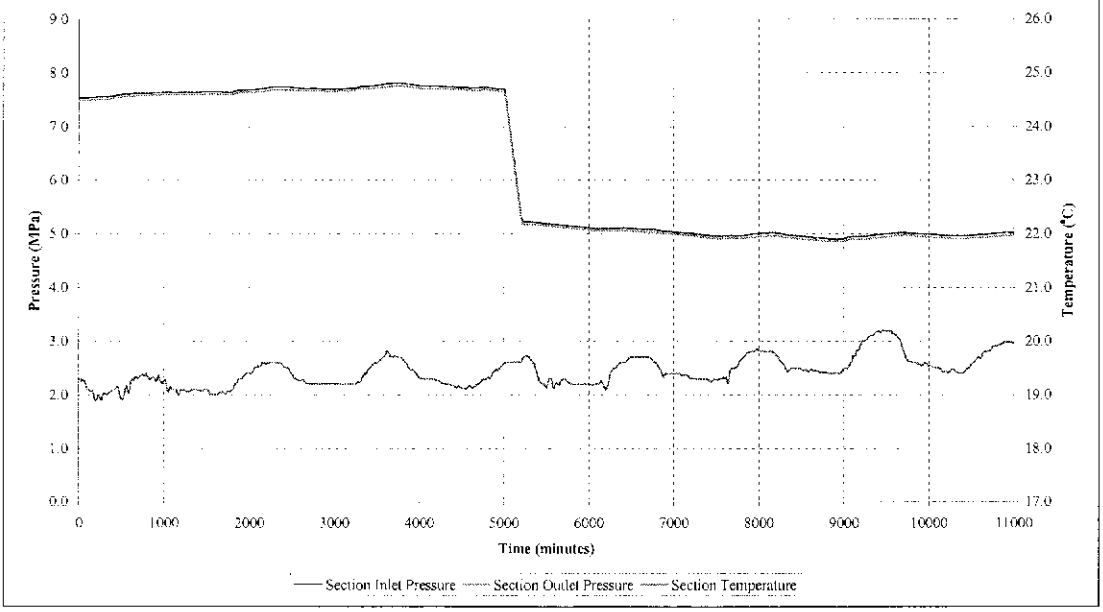

When analysing the results in Figure 6.6 it is evident that there is a delay of 60 minutes between the simulated leak onset at a simulation time of 5000 minutes, and the time at which a stable leak magnitude is determined. This confirms the presumption of maximum delay in estimating the leak magnitude when selecting the optimum filter. Figure 6.6 illustrates that the leak onset time and magnitude is

clearly visible. Therefore it is deemed that the level of filtering is suitable for this pipeline section. If more rapid response times are required, the number of samples averaged can be reduced, but the ability to estimate the magnitude accurately may be compromised in addition to increasing the risk of false alarms.

Figure 6.6 Moving Average Filtered Leak Flows for a Simulated Leak

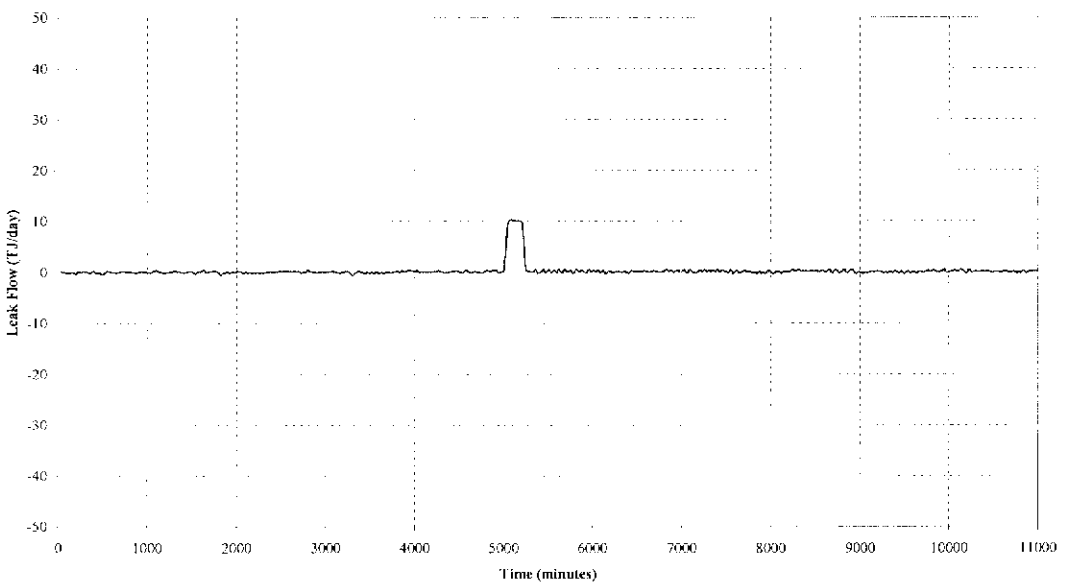

6.3 Ned's Creek to Wiluna

The next section examined was Ned's Creek to Wiluna which has a mid range retention time when compared to other pipeline sections on the GGT pipeline. It was expected that this pipeline section would have more calculated leak flow noise than the Anaconda to Leonora pipeline section, since it has a higher linepack to flow ratio.

Again, the data used was eight days or 11520 one minute samples of pressure and temperature from each of the pipeline section end points. Figure 6.7 shows the input data for the model over the eight day period. Initially the model was run without filtering the data to determine the extent of the unfiltered leak detection threshold for the pipeline section.

The diurnal temperature variations can again be clearly seen from the model input data shown in Figure 6.7. The gas temperatures are higher for this pipeline section compared to Anaconda to Leonora due to Ned's Creek to Wiluna being located approximately 300 km north of Anaconda to Leonora in a warmer region of Western Australia. A transient disturbance in pressure can be seen between the simulation time of 0 and 1000 minutes. These rapid changes were caused by the Ilgarari Compressor, upstream of the pipeline section being examined.

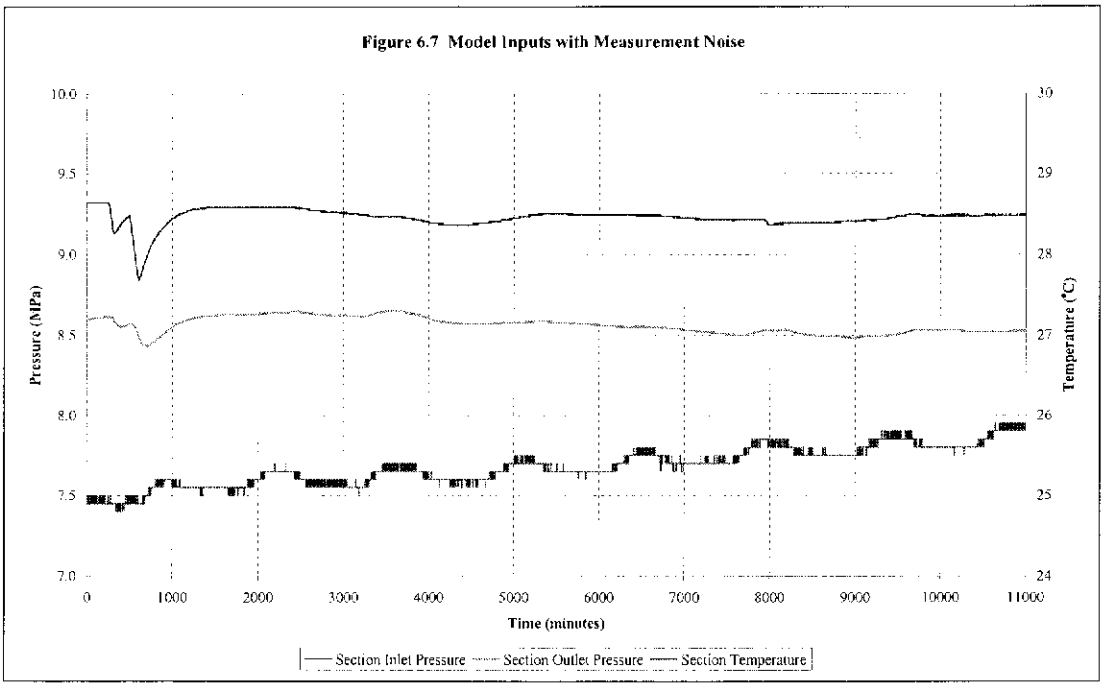

Figure 6.8 shows the uncertainty in leak flow estimation when the data used in the model is unfiltered. Again, the calculated leak uncertainty is much lower than that simulated for the larger test pipeline section. The unfiltered leak detection threshold for Ned's Creek to Wiluna was approximately 11.78 TJ/day compared with 85.63 TJ/day for the test pipeline section. However, as predicted the uncertainty in calculated leak flows for Ned's Creek to Wiluna is higher than Anaconda to Leonora, due to the larger linepack to flow ration of the Ned's Creek to Wiluna section. Once again, a lower leak detection threshold is attainable for the equivalent filter applied to the larger test section. The pipeline section from Ned's Creek to Wiluna is actually longer than the test pipeline section, however the diameter of the test section is larger, causing the overall linepack to be higher. Therefore it is expected the leak

detection threshold will not be able to be reduced to the same levels as the pipeline section from Anaconda to Leonora by applying the same filter.

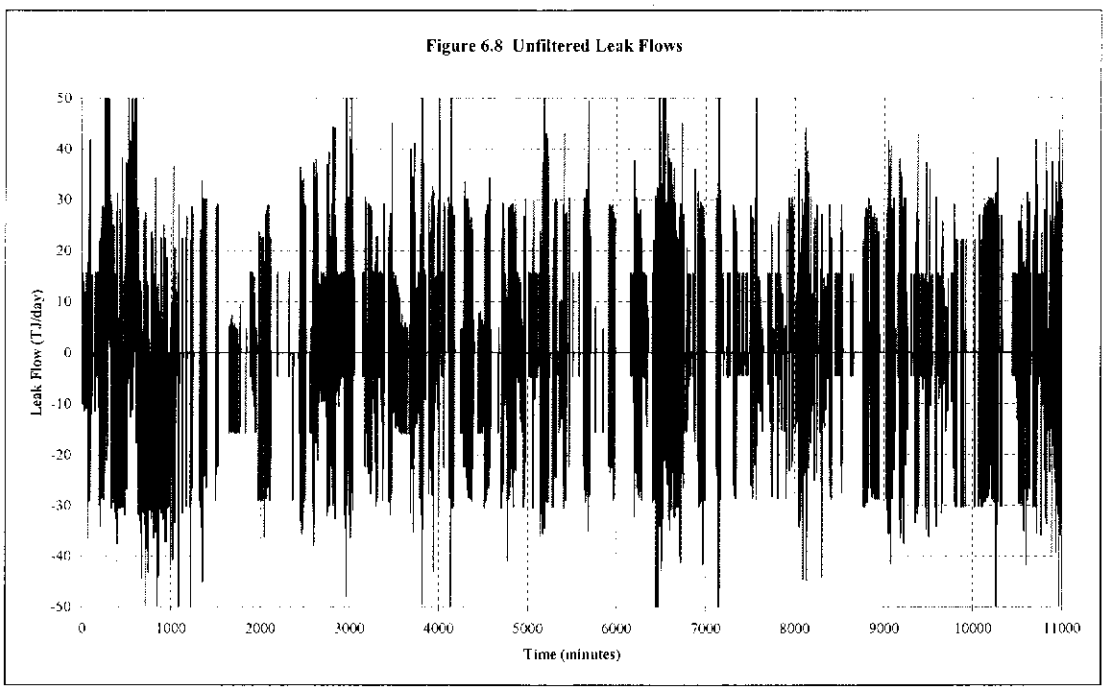

The same combined input and output moving average filter was again applied to the model data. The filtered input measurements are shown in Figure 6.9, where it can be seen that the random measurement variations caused by the uncertainty of each measurement have again been reduced.

The transient pressure effect caused by the upstream compressor is still large after filtering. This was the cause of the false leak estimation during the transient period shown in Figure 6.10.

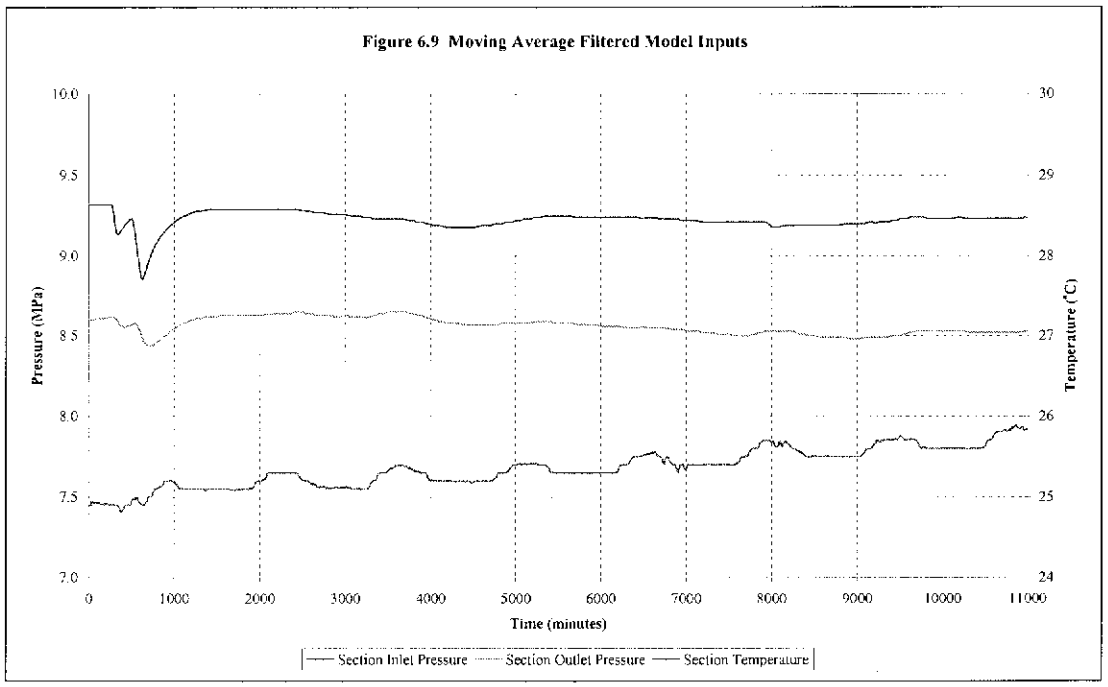

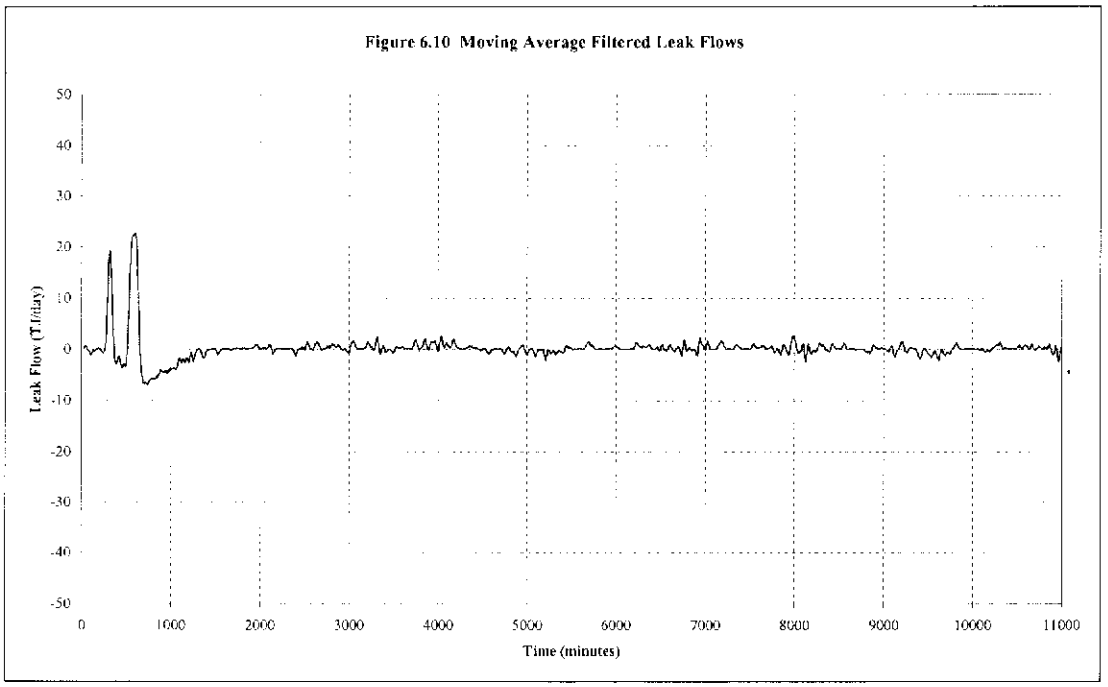

Figure 6.10 also illustrates the effectiveness of the moving average filter in removing the calculated leak flow noise. The leak flow uncertainty has been reduced from 11.78 TJ/day for the unfiltered data, to 2.51 TJ/day for the filtered data. The threshold is higher than the pipeline section Anaconda to Leonora. This was expected since the pipeline section Ned's Creek to Wiluna is approximately 11 times

the size of Anaconda to Leonora, which is proportional to the ratio of leak thresholds for the two pipeline sections.

As previously highlighted, there are two disturbances in calculated leak flow, one at a simulation time of approximately 320 minutes and the other at 610 minutes. On further investigation of other pipeline data, it appears that the disturbance corresponds with two compressor shut downs and restarts approximately three hours apart at the Ilgarari compressor station that is approximately 200 km upstream of Wiluna. This raises the issue that the model has not estimated the flow correctly into the pipeline section during the period of rapid pressure transients. Each time the inlet pressure of the section has increased rapidly, the model has over estimated the inlet flow to the section over that short period. Since the mass (linepack) within the section has not changed substantially during the same period, a leak is falsely indicated. This indicates the inability to prevent false leak indication when pressure is used to estimate flow.

The next investigation was again to examine the filter with an artificially created leak. A 10TJ/day leak of constant magnitude at the midpoint of the pipeline section was simulated by reducing the measured inlet outlet pressures of the pipeline section by approximately 3.87 kPag each measurement period. The corresponding filtered input data is shown in Figure 6.11.

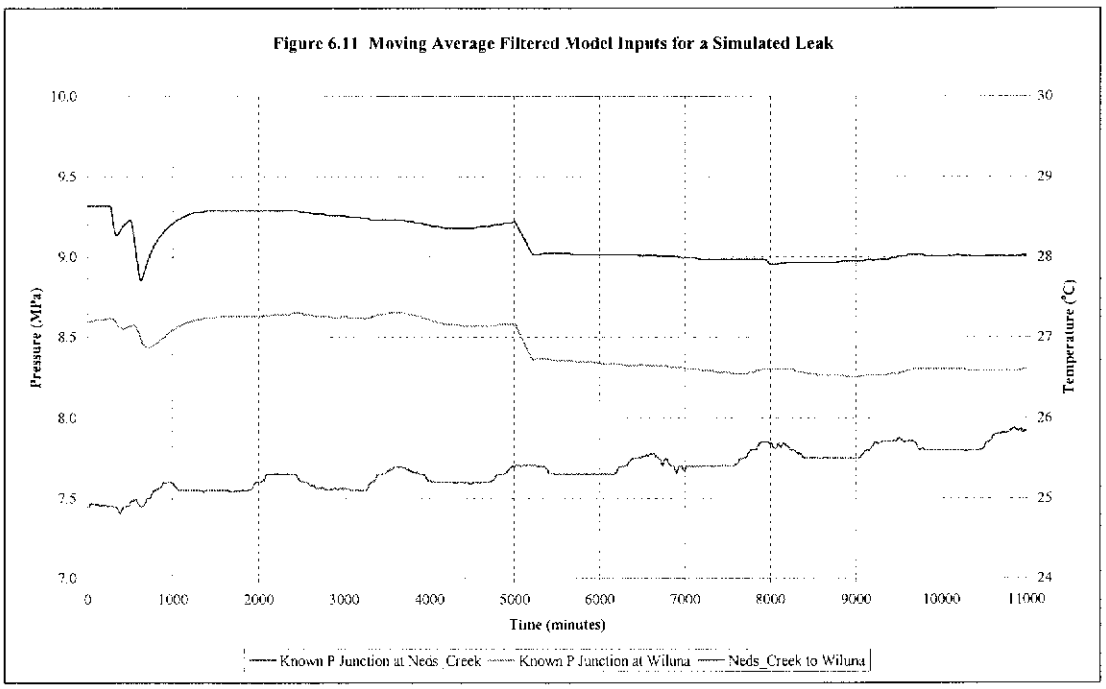

Figure 6.12 shows the induced leak was clearly identified at the correct magnitude. Apart from the compressor transient effects at the start of the simulation, the calculated leak flows were reduced to low levels prior to and after the induced leak at the simulation time of 5000 minutes.

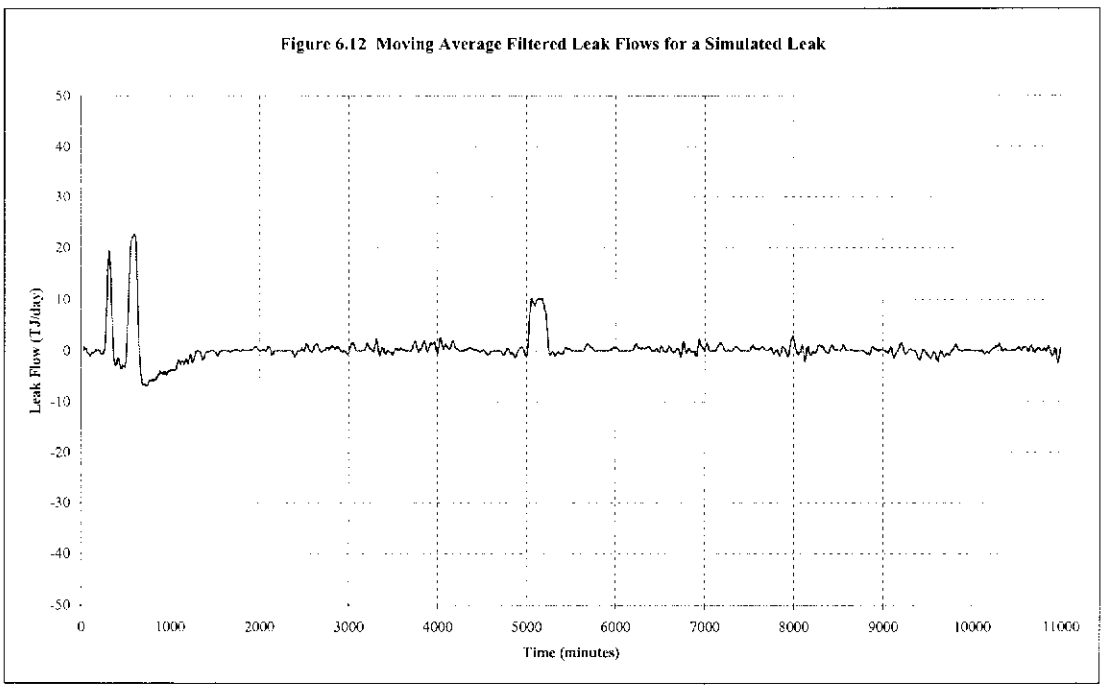

6.4 Jeedamya to Cawse

The final section examined was Jeedamya to Cawse, which has the highest retention time of all pipeline sections on the GGT pipeline. It was expected that this pipeline section would have more calculated leak flow noise than both the Anaconda to Leonora and Ned's Creek to Wiluna pipeline sections, since it has the highest linepack to flow ratio.

Again, the data used was eight days or 11520 one minute samples of pressure and temperature from each of the pipeline section end points. Figure 6.13 shows the input data for the model over the eight day period. Initially the model was run without filtering the data to determine the extent of the unfiltered leak detection threshold for the pipeline section. The measured inlet and outlet pressures show little evidence of transient disturbances, as this pipeline section is sufficiently far away from any compressors or pressure controlling devices to remain unaffected.

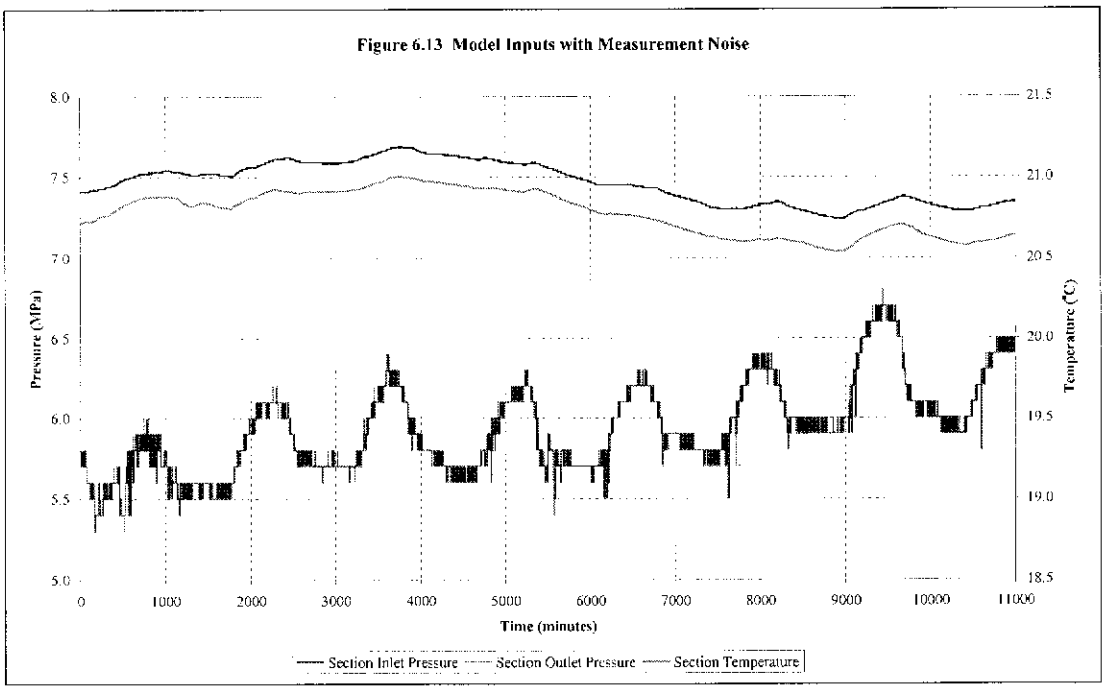

Figure 6.14 shows the uncertainty in leak flow estimation when the data used in the model is unfiltered. Again, the calculated leak uncertainty is much lower than that simulated for the larger test pipeline section.

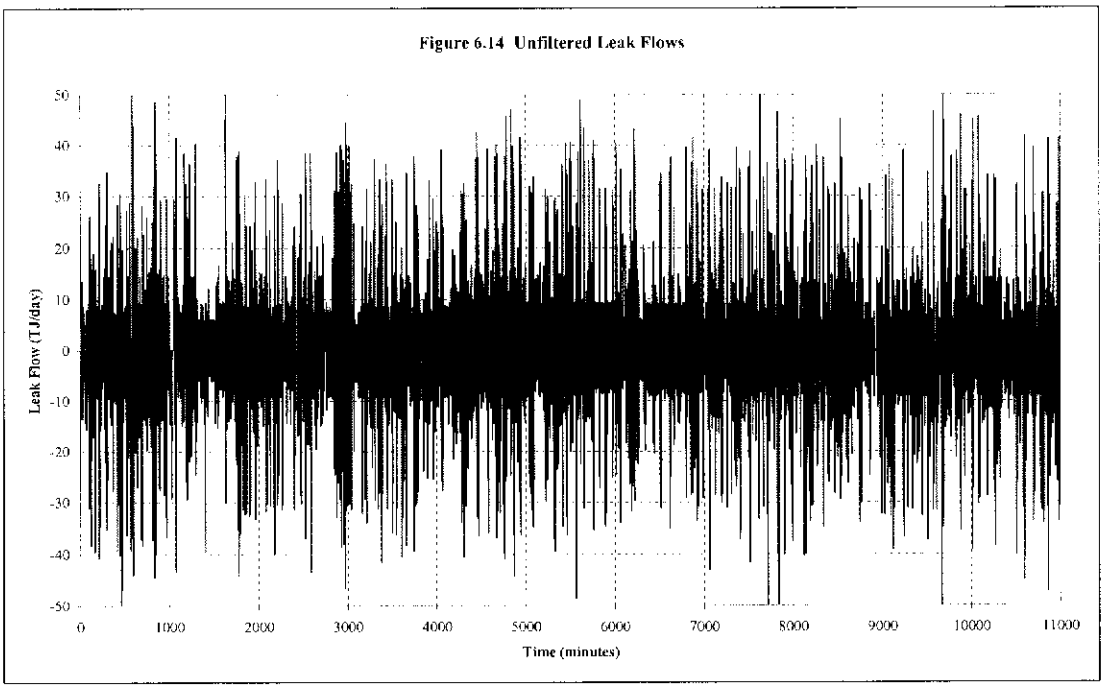

The unfiltered leak detection threshold for Jeedamya to Cawse was approximately 11.05 TJ/day compared with 85.63 TJ/day for the test pipeline section. However, the uncertainty in calculated leak flows for Jeedamya to Cawse is lower than Ned's Creek to Wiluna, due to the overall size of Ned's Creek to Wiluna section. Therefore as predicted in Chapter 5, pipeline section flow has little influence over the leak flow uncertainty and is purely dictated by pipeline section size. Once again, a lower leak detection threshold is attainable for the equivalent filter applied to the test pipeline section.

The same combined input and output moving average filter was again applied to the model data. The filtered input measurements are shown in Figure 6.15, where it can be seen that the random measurement variations caused by the uncertainty of each measurement have been reduced. There were no noticeable transient pressure effects as was evident in the previous section.

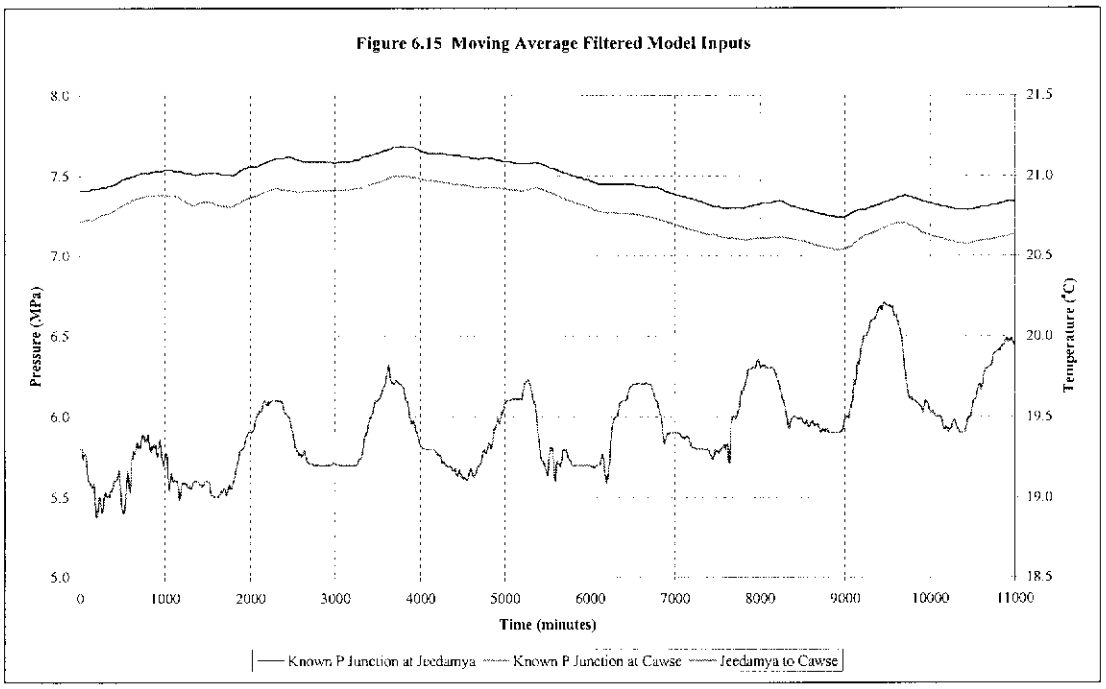

Figure 6.16 illustrates the effectiveness of the moving average filter in removing the calculated leak flow noise. The leak flow uncertainty has been reduced from 11.05 TJ/day for the unfiltered data, to 1.22 TJ/day for the filtered data.

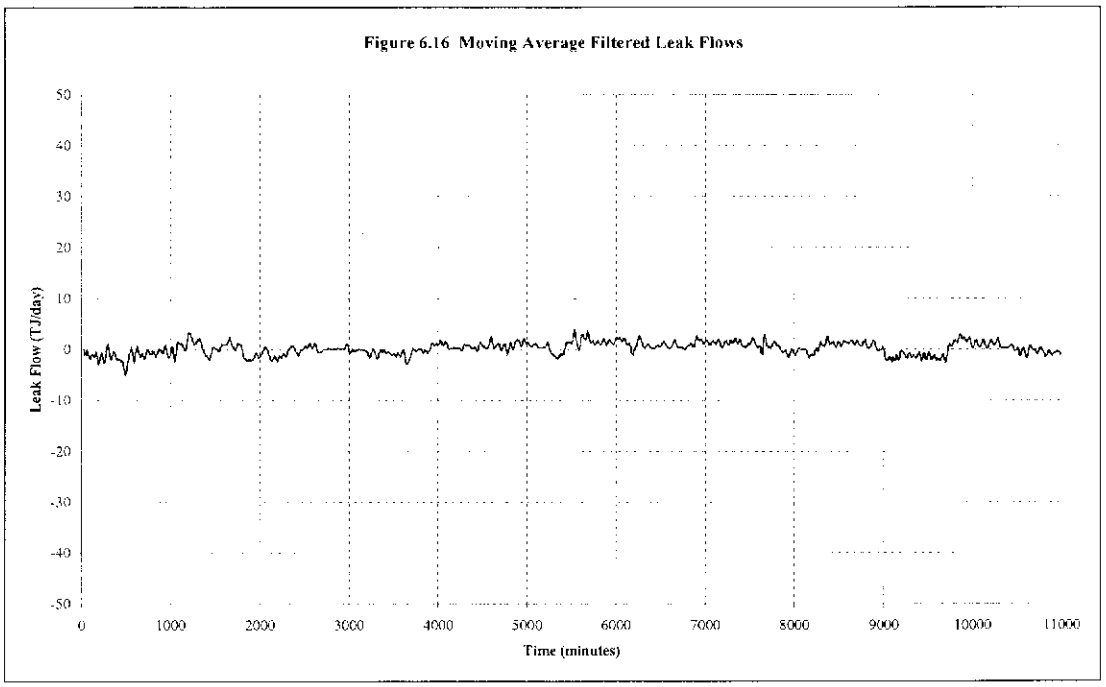

The next investigation was again to examine the filter with an artificially created leak. A 10 TJ/day leak of constant magnitude at the midpoint of the pipeline section

was simulated by reducing the measured inlet outlet pressures of the pipeline section by approximately 3.82 kPag each measurement period. The corresponding filtered input data is shown in Figure 6.17.

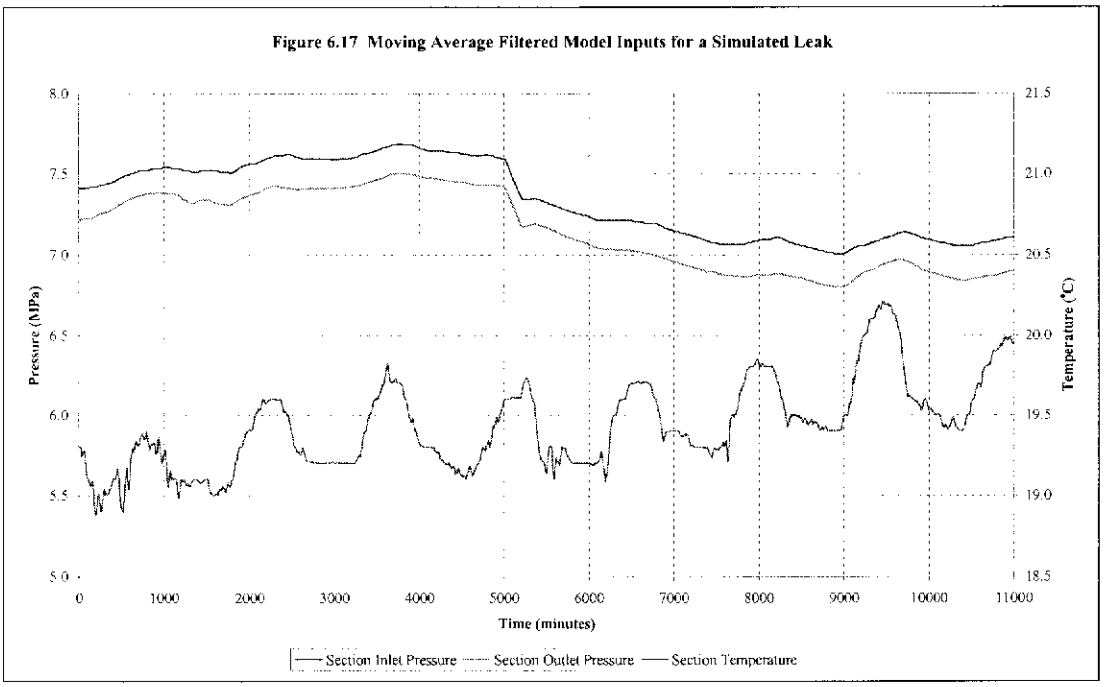

Figure 6.18 illustrates that the leak onset time and magnitude is clearly visible from the typical calculated leak flow rates when no leak is present. Therefore it is deemed that the level of filtering is suitable for this pipeline section.

Figure 6.18 Moving Average Filtered Leak Flows for a Simulated Leak

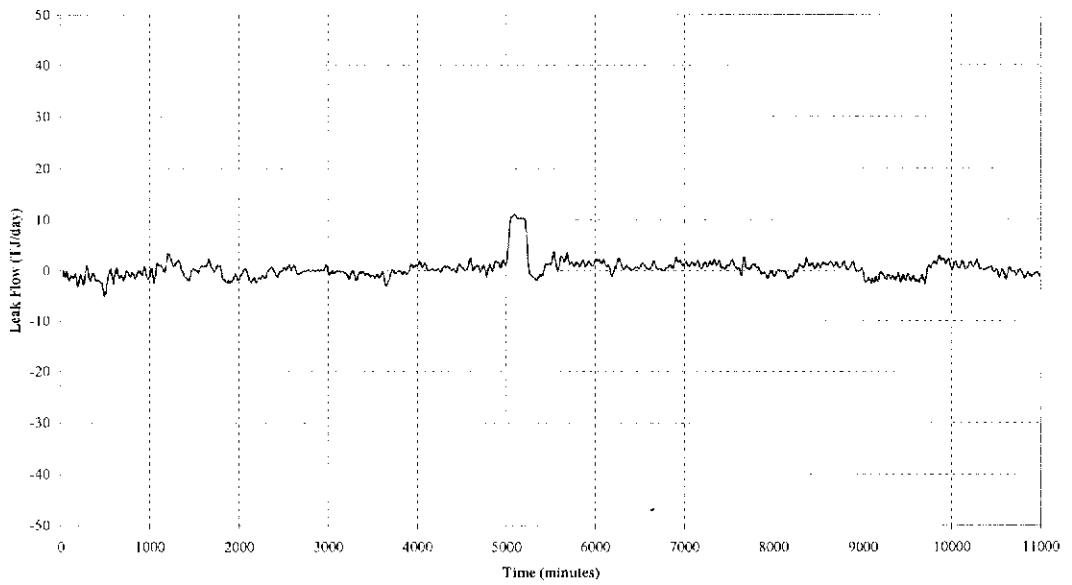

6.5 Summary of Results

The results in this chapter have confirmed the filter configuration was acceptable for all three sections, which represent the range of pipeline sections that will be encountered on the GGT pipeline, therefore this will be used in the final on line implementation.

Pipeline Section	Unfiltered Leak Detection Threshold	Filtered Leak Detection Threshold	Percentage of Section Typical Flow	Section Typical Linepack
Anaconda to Leonora	2.98 TJ/day	0.24 TJ/day	0.71%	4.0 TJ
Ned's Creek to Wiluna	11.78 TJ/day	2.51 TJ/day	3.51%	51.0 TJ
Jeedamya to Cawse	11.05 TJ/day	1.22 TJ/day	3.56%	37.5 TJ

Table 6.1 Summary of Leak Detection Thresholds

Table 6.1 illustrates that the for the representative pipeline sections examined in this chapter, the achievable leak detection threshold was as low as 0.71% of section flow for the smaller pipeline section and as high as 3.56% for the larger pipeline section.

The percentage is higher for Jeedamya to Cawse since the typical flow for that section is less than half of the typical section flow for Ned's Creek to Wiluna.

7.0 DISCUSSION

7.1 Validity of Model

The pipeline sections tested against real data confirmed that the selected configuration and filter would be suitable for implementation into the final on-line model as it provided a robust and stable platform to execute against the real pipeline data. The initial tuning of the model by adjusting the sectional surface roughness values was successful in reducing the amount of "offset" in leak flow values. The model performed satisfactorily when rapid transients were encountered such as the start up and shut down of compressor stations, and the rapid change in delivery flow at an outlet. The input data from the SCADA system was not altered in any way to provide an artificial environment for the model apart from the simulation of leaks. Even though the model produced reliable results throughout the investigation, these transient events were detected as false leaks as was evident from the pipeline section Ned's Creek to Wiluna. In reality if a known event was occurring, it is relatively simple to disregard the leak flow on that pipeline section for a period after the event. The length of this period would be determined from operational experience with the model being on-line.

The main issue with using leak detection systems on gas pipelines that employ a mass balance on each section is that the model has to deal with the transient conditions observed with compressible flow. This compressibility effect allows large changes in the mass within each pipeline section and therefore large differences between mass flow into and out of a section under transient conditions, even without the presence of a leak. That is why leak detection is commonplace on liquid pipelines with incompressible flow, but reliability is still illusive on gas pipelines. Obviously, as the distance between pressure, temperature and flow measurements increase, i.e. the pipeline sections become longer, the problem with compressibility becomes worse. In addition to this, the larger pipeline sections only require small changes in pressure and temperature measurements at the end points, to produce large changes in total section mass (linepack). Thus for the same level of measurement uncertainty, a smaller pipeline section will have lower linepack

uncertainty and hence a lower leak detection threshold. This was highlighted in the results, when the shorter pipeline sections exhibited more stable leak flow results than the longer pipeline sections, irrespective of the flow through the pipeline section. It was demonstrated in Chapter 5 that linepack which is a function of the pipeline section size, dominated the leak flow uncertainty. Therefore, the solution is to have more frequent pressure and temperature measurements along the pipeline. The main disadvantage with this is the large increase of construction cost of the pipeline that could threaten the feasibility of some pipelines. Currently on the GGT pipeline, there are 17 pressure measurement points on a pipeline nearly 1380 km long. This averages to a pressure measurement approximately every 80 km.

If increasing the number of measurement points on the pipeline is not an option, the best way to reduce these effects is to have a very accurate transient model, with adequate filtering. The main area that generated false leaks during this study was in the vicinity of the compressor stations. Even though the manufacturer's compressor curves were input into the FlowTran model, and these proved to be reliable for steady state operating data, this was not the case for start up and shut down of the compressor units. Figure 6.10 clearly shows the transient effects of a compressor shut down in the adjacent pipeline sections, when the model indicated leaks of up to 20 TJ/day during a shut down and subsequent restart. However, in each instance the false leak decayed relatively quickly as the corresponding transient disappeared. This problem may be reduced by comparing the leak flows generated in each pipeline section to the unaccounted gas in the entire pipeline network from Equation 4.1. The entire pipeline system will not be affected to the same extent from rapid transients as the pipeline sections adjacent to the source of the transient. Therefore if Equation 4.1 does not indicate a leak of similar magnitude as that of any pipeline section indicating a leak, it can generally be regarded as false.

It should be highlighted that the leaks were created by manipulating the inlet and outlet pressures of each pipeline section to replicate the effects of a leak. In reality, this would not occur. If a real rupture were to occur on a pipeline section, the upstream flows would increase to compensate for the additional flow. After a period of time the system would approach steady state conditions and the rapid changes in

pressure at each end of the pipeline section seen at the leak onset would diminish. This was apparent in Figure 4.4 when the calculated leak flow rate quickly decreased as the pipeline section approached steady state, even though the leak was still present. Another issue to consider with the modelling of each of the leaks was the assumption that a leak flow rate would remain constant. Turner (1987) noted that the flow rate in the vicinity of a leak might be quite "noisy" and change rapidly at the rupture site as the local pressures change. In this case the leak flow may not converge to a single value, as was the case in this model. The deviation nevertheless, will still be present, but will be rapidly changing.

7.2 Selection of Filter

The three different filters used in the leak flow data analysis all produced similar levels of noise reduction. The unfiltered results from the model were unintelligible thus being no use in their current form. This was mainly due to the random noise generated by measurement uncertainty from real time data used as input to the model. It was demonstrated in Chapter 5 that the pressure data contributed the most to leak flow noise, due to the uncertainty it created in the calculated pipeline section linepack. The filter selected needed to eliminate this random noise whilst still retaining a sharp response to a step function, namely a leak.

The moving average performed this function most adequately out of all the filters examined, due to its noise reduction capabilities in addition to its computational simplicity. Smith (1999) identifies the moving average filter as the optimum for this task. Turner (1987) investigated the use of average and weighted average filters on the output of the leak detection model. Turner demonstrated that the relative increase in noise reduction by averaging more than 20 measurement periods begins to decline. This was also demonstrated in Chapter 5 for the test pipeline section. Thus the noise reduction compared to the delay of detecting the leak onset becomes less attractive after average 20 samples. Not withstanding this, some judgement must be exercised taking into account the type of pipeline system being modelled. For the GGT pipeline, it is deemed that a delay of 60 minutes is an acceptable offset. It was

illustrated in Chapter 6 that for a 30 sample input and 30 sample output average the delay in detecting the correct leak magnitude was approximately 60 minutes for each of the pipeline sections examined. However the noise reduction and hence smoothing of the leak flow output by averaging both input and output data was better than simply averaging 60 samples of output data that causes a similar delay.

The other two filters that were investigated but not employed in the final on-line model implementation were the weighted moving average and the low pass filter. Both these filters demonstrated similar properties to that of the moving average filter. The weighted moving average filter performed well when there were high levels of linepack noise present. When these levels were reduced by filtering the input data, the weights approached $1/n$ which provided the same level of noise reduction as the moving average filter.

The low pass filter possessed superior noise reduction capabilities for values of n below 20, however for higher values of n, the filter produced similar results to that of the moving average and weighted moving average filters. This may raise the possibility of using multiple, or all types of filters on both input and output. These filters would theoretically have the same response time to a leak and may have superior noise reduction properties, however three separate filtering processes are involved which adds computational complexity. The practicalities of constructing an on-line model have to be considered in the decision of which filter to use. The computational processes employed in the on-line model are required to be robust and reliable, having to run every minute for 24 hours a day, therefore the most efficient processes should be employed. Thus the gain of additional processes has to be justified against the possible loss of reliability.

7.3 Use of Measured Flow

The results indicated that in many cases flow measurement is required to estimate leak flow reliably and accurately. Using pressure and temperature measurements at each end of a pipeline section are not sufficient for leak detection in a variety of

circumstances. The purpose of this section is to define the minimum flow measurement required on the GGT Pipeline to obtain leak detection to a standard acceptable to the pipeline operator.

The effects of using measured flow on leak detection were examined using a pipeline section of the same dimensions as the test pipeline section, which is representative of the GGT Pipeline. Using Equation 4.23, different parameters were varied to examine the effect on the maximum distance allowable between flow measurements. Table 7.1 shows the values used in Equation 4.23 for investigating the effect of increasing the number of leak flow results averaged.

Parameter	Value	Units
R	4.30E+02	J/kgK
$\overline{T}$	3.00E+02	K
D	3.94E+02	mm
A	1.22E-01	m^2
C_V	4.98E+07	J/kg
Δt	6.94E-04	Day
$\sigma_{\dot{B}}$	2.00E+00	TJ/day
$\sigma_{\dot{W}}$	2.00E+00	TJ/day
$\sigma_{\overline{P}}$	2.50E+03	Pa

Table 7.1. Parameters Used in Flow Measurement Investigation

The uncertainty chosen for leak flow was 2 TJ/day, which is the minimum range of leak flow required to be detected. The uncertainty for flow measurement of 2 TJ/day corresponds to an assumed 2% accuracy for the anticipated flow pipeline section flow rate of 100 TJ/day. This is a common level of accuracy in many flow meters manufactured today. The pressure uncertainty of 2.5 kPa was derived from the 30 measurement input average used in Chapter 6. Figure 7.1 illustrates the effect of increasing the amount of leak flow values averaged has on the distance required between flow measurements.

Figure 7.1 Number of Samples Averaged vs Section Length

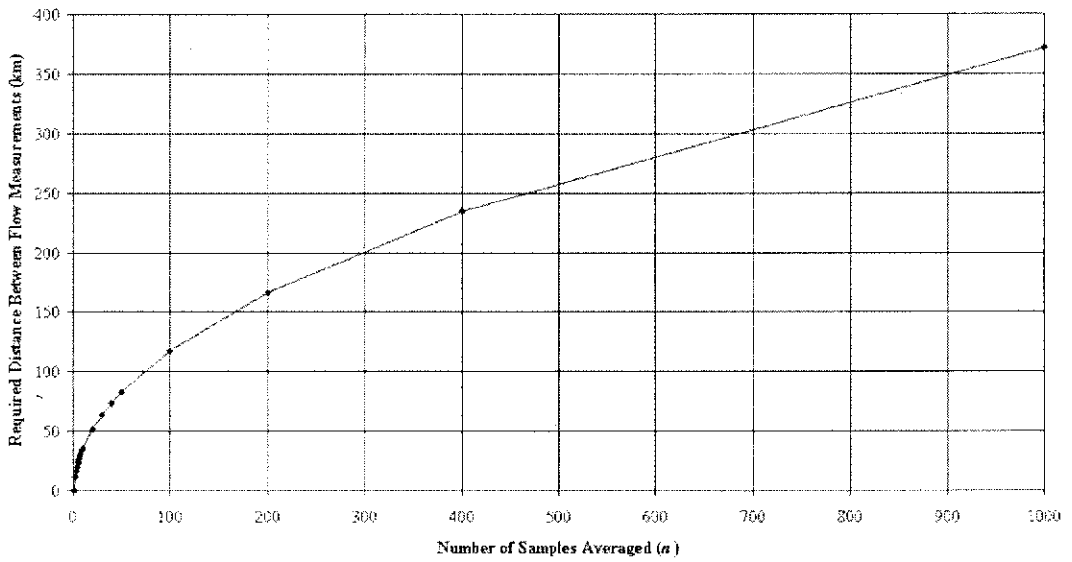

It can be seen from Figure 7.1 that even if flow measurement were installed at every location where pressure and temperature is measured, which is on average more than 100 km apart, the time delay to detect the actual leak magnitude would be more than two hours.

The next stage to examine was the relationship between leak flow uncertainty and maximum distance required between flow measurements. The values in Table 7.1 were used again with the number of leak flow measurements averaged n, being held constant at 30. This corresponds to the 30 input, 30 output average filter used in Chapter 6.

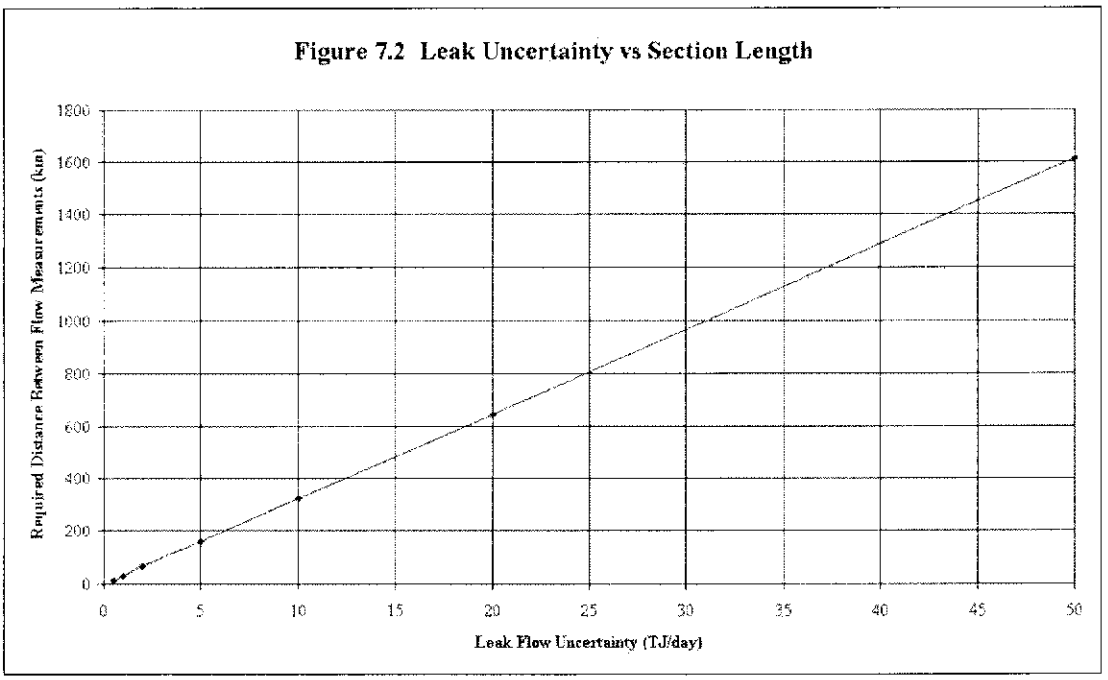

Figure 7.2 illustrates the linear relationship between leak flow uncertainty and distance between flow measurements. Therefore if a pipeline operator deemed it acceptable to double the acceptable leak magnitude detection limit, the required distance between flow measurements would also be doubled.

The final parameter that was investigated was the effect of pressure measurement uncertainty on leak detection uncertainty. Again the values in Table 7.1 were used with the number of output values averaged, n held constant at 30 and the pressure uncertainty was varied.

Figure 7.3 shows that the required distance between flow measurements reduces rapidly as pressure uncertainty increases between 0 and 2 kPa. Therefore if pressure uncertainty can be minimised, the distance required between flow measurements could be greatly increased. In theory this can be achieved without substantially increasing the time to detect the leak if the main source of pressure uncertainty is non-systematic.

Figure 7.3 Pressure Uncertainty vs Section Length

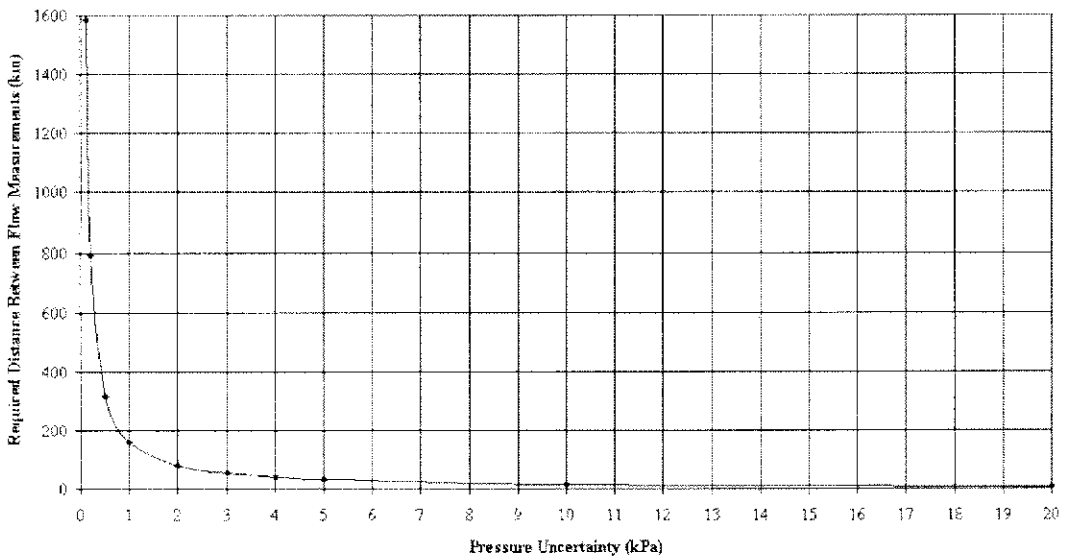

The way in which pressure measurement non-systematic error could be greatly reduced is by performing averaging at the source of the measurement. As discussed earlier, the central SCADA system only receives updated pressure values once a minute. Therefore each addition sample averaged to remove random error increases leak detection time by one minute. However, as illustrated in Figure 2.4, the field RTU is receiving much more frequent updates at approximately each 100 milliseconds. An averaging process could be simply implemented within the RTU to provide an already filtered pressure to the SCADA system each minute. Even if the RTU performed an average once per second, the reduction in pressure uncertainty is significant. Using this in addition to the 30 value input average outlined in Chapter 6, the pressure uncertainty is reduced to less than 0.3 kPa. This produces a required distance between flow measurements from Figure 7.3 of more than 520 km. This would mean that flow metering would only need to be installed at three or four locations on the GGT Pipeline.

8.0 CONCLUSION

8.1 Summary

Reliable leak detection can be achieved by using a combination of an accurate transient model and common signal processing techniques. Important factors that required addressing during the implementation of the leak detection model were accuracy and spacing of field measurements, accurate compressor performance models and successful "tuning" of the model to operating data. The main significance of this work lies in the demonstration of the theory presented by utilising real world data from a large gas transmission pipeline, which is representative of many other pipelines throughout the world. Furthermore, there had been no previous investigation of into the effects of averaging the input data for model to reduce measurement uncertainty. This proved to be successful in reducing overall leak flow uncertainty, and hence lowering the leak detection threshold of the model. The techniques employed in this investigation are supported by the publication of actual pipeline operating data in Chapter 6 substantiating the effectiveness of each of the methods investigated. Using the calculated pipeline section flows obtained from recorded pressure and temperature data demonstrated several limitations in detecting leaks adequately. These included the decay of leak magnitude for a leak of constant value, the ability to adapt to rapid pressure transients, and the large pressure changes required for small pipeline sections to detect a leak. Even acknowledging the limitations of the proposed leak detection system, it has been demonstrated that a range of leak flows can now be reliably detected if the correct pipeline infrastructure is in place.

The main deficiency in the model was the requirement to use calculated pipeline section flows instead of measured pipeline flows. The results demonstrated that by using the calculated section flows the leak detection magnitude would always be conservative and also decay with time as the model reaches steady state after initial leak propagation. Chapter 7 demonstrated that reliable leak detection could be achieved to a minimum of 2% of total pipeline throughput with only minor metering additions. This means that the useful limits of the model range from the smallest

leaks able to be detected by conventional means on most pipelines, down to the leak detection threshold of the model. To detect all leaks smaller than 2% within a pipeline system, substantial infrastructure would need to be implemented on the GGT Pipeline. The threshold varies depending on the size of the pipeline section, as was demonstrated in Chapter 6 when actual operating data from the GGT pipeline was utilised. Thus for small pipeline sections, the leak detection threshold will be much lower than that for larger pipeline sections for the same level of filtering. For example if flow metering were to be installed at every location where pressure and temperature are measured, the leak detection uncertainty could be reduced to 0.60% of pipeline throughput for the larger pipeline sections, and as little as 0.37% for the smallest pipeline sections. This retrospective implementation would cost over AUS$3,500,000 for the already operating GGT Pipeline, and probably would not be justified for the small increase in leak detection resolution. However, this cost is not prohibitive for a large pipeline being constructed, as this amount is only a small percentage of the overall construction cost.

Using calculated pipeline flow, the ability of the model to reduce leak flow uncertainty and yet respond to an induced step input simulating a leak was verified using actual measured data from the GGT pipeline. The performance of the model was not ideal, and most results indicated that additional pipeline flow metering would need to be installed to achieve reliable leak detection. Taking this into account, the leak detection system tested would still provide useful data and would be better than having no system at all. For example, it is estimated that a leak of more 20 TJ/day (approximately 25% of pipeline throughput) or more would be required to create a noticeable pressure distortion, depending on the location on the pipeline section. The distortion in the pressure gradient of the pipeline would even then, only be noticeable if someone were already looking for a problem in the vicinity. Alarm limits on the SCADA system could not be reliably set to detect this on rate of change or absolute value of pressure, since these values are within normal operating conditions. Therefore even though a pressure gradient distortion begins to commence at a leak of 20 TJ/day, it is more likely that the leak would have to be much larger to be detected by conventional techniques. The filtered leak detection thresholds for each of the pipeline sections summarised in Table 6.1 were 0.24

TJ/day for Anaconda to Leonora, 2.51 TJ/day for Ned's Creek to Wiluna, and 1.22 TJ/day for Jeedamya to Cawse. Therefore a range of leaks from approximately 2.5 to 20 TJ/day that were currently undetectable, are now readily detectable. This is even more important when it is highlighted that leaks from ruptures are likely to fall within this range.

The mass balance technique for leak detection produces similar results independent of leak location. This is advantageous since results are consistent irrespective of the leak location along a pipeline section. It was also demonstrated in Chapter 4 that the mass balance method was conservative due to the model not estimating the pipeline section inlet and outlet flow correctly. Therefore to be able to estimate the amount of gas inventory lost in the event of a leak, it is more reliable to use the entire pipeline network mass balance outlined in Equation 4.1. Thus a total pipeline mass balance should be used in conjunction with leak flow information from each pipeline section to both estimate the true magnitude of the leak, and to eliminate false leaks. The total pipeline mass balance calculation should be performed at the same frequency as each of the pipeline section mass balance calculations, so that a comparison can be made. Therefore once the initial leak initiation time and magnitude is identified by the total pipeline mass balance, a comparison can be made to each of the calculated leak flows on each pipeline section. The pipeline section that exhibits similar imbalance properties to that of the total pipeline mass balance is likely to be the section that contains the leak. If none of the pipeline sections indicate a similar imbalance, the problem is probably due to a systematic error with the total pipeline mass balance caused by an error in boundary flow measurement. Once the pipeline section on which a leak exists is identified, the location can be accurately defined if flow measurement at each end of the pipeline section is present, as was demonstrated in Chapter 4.

8.2 Further Work and Recommendations

By utilising the combination of total pipeline mass balance, and pipeline section mass balance, the likelihood of false leak alarms is greatly reduced. This methodology,

along with the 30 sample moving average filter applied to the input and output of the model was implemented for an extended on-line test period on the SCADA system. The system has been on-line for extended periods of time and has proved to be stable and reliable, with no generation of false alarms. The platform on which the model was implemented, allows the engineer the flexibility to modify the system to meet the requirements of different pipelines. Other long term benefits of the on-line model have included the ability to track gas composition along the pipeline, and the use of prediction models for real time capacity management.

From the results in Chapter 6 and the finding regarding the utilisation of flow measurement in Chapter 7, it is recommended that flow measurement be installed at a minimum of four locations along the GGT Pipeline. This would reduce the distance between measured flow data to a maximum of 300 km and theoretically reduce leak detection uncertainty to less than 2 TJ/day. Flow metering is already installed at the inlet of the pipeline and all outlets (delivery points). It is proposed to install the additional metering at the following locations:

- Paraburdoo Compressor Station;
- Ilgarari Compressor Station;
- Wiluna Compressor Station;
- Jeedamya Scraper Station.

Compressor stations were chosen based on the even spacing along the pipeline and the ability to use the measured flow data for compressor performance monitoring in addition to leak detection. Once flow measurement is installed, further testing to could be conducted to verify its success. Additional metering could be installed at later stages if the need or the funds becomes apparent.

Further work could involve the verification and investigation of the on-line model behaviour when a leak occurs. This could be either from an actual leak or induced conditions, for example by venting a substantial quantity of gas from the pipeline. Routine public awareness demonstrations are held where gas quantities are vented which would provide an opportune forum to test the effectiveness of the leak

detection model. Data will be collected from such events, analysed and published in the future.

REFERENCES

ASTOLA, J. (1997) Fundamentals of Nonlinear Digital Filtering

CRC Press

BOWLES, E.B., MORROW, C.R. (1996) Automatic and Remote Valves for Pipeline Break Detection

AGA Operations Conference, Montreal, Canada.

BOWLES, E.B., MORROW, C.R. (1996) Gas Pipeline Rupture Detection and Control

ASME International Pipeline Conference, Calgary, Canada.

BRIGHAM, E.O. (1988) The Fast Fourier Transform and Its Applications

Prentice Hall Inc, 448pp.

BRYANT, M. (1997) Complex Compressor Station Modelling

Pipeline Simulators Interest Group Conference, Tuscon, Arizona

BUTLER, N.C. (1982) Pipeline Leak Detection Techniques

Pipes and Pipelines Int. pp. 31, 33, 35

CAPPELLINI, V. (1978) Digital Filters and their Applications

Academic Press

Del REY, F. (1996) Real Time Modelling of a Gas Transmission Pipeline

Pipeline Simulators Interest Group Conference, San Francisco, California

FLETCHER, C.A.J. (1991) Computational Techniques for Fluid Dynamics Vol I

Springer-Verlag, Berlin

GABEL, R.A. (1973) Signals and Linear Systems

John Wiley and Sons, 415pp.

GRAHAM, J.T., WUKOVITS, V.J., YURCHEVICH, J.D. (1989) On-Line Modelling "A Diamond in the Rough"

Pipeline Simulators Interest Group Conference, El Paso, Texas

GUDMUNDSSON, J. (1998) Flow Experiments with High Pressure Natural Gas in Coated and Plain Pipes

Pipeline Simulators Interest Group Conference, Denver, Colorado

HAMMING, R.W. (1977) Digital Filters

Englewood Cliffs, N.J. Prentice Hall

HARDY, R.M. (1978) Evaluation of the Hydrocarbon Leak Detection Device Leak "x"
Environmental Impact Control Directorate, USA
HOEVEN, T. van der (1985) Gas Network State Estimation with Equal Error Fraction Method
Proceedings of the 11th IMACS World Congress on System Simulation and Scientific Computation
IFEACHOR, E.C. (1993) Digital Signal Processing: a Practical Approach
Addison-Wesley
KELLER, G., WARRACK, B. and BARTEL, H. (1990) Statistics for Management and Economics
Wadsworth Publishing Company, New York
LAHTI, B.P. (1992) Linear Systems and Signals
Berkeley-Cambridge Press, 656pp.
MARIANI, O. (1997) Design of a Gas Pipeline: Optimal Configuration
Pipeline Simulators Interest Group Conference, Tuscon, Arizona
MODISETTE, J.L., WHALEY, R.S. and STERBA, V. (1989) Commercial Applications of Gas Pipeline Simulatons
Pipeline Simulators Interest Group Conference, El Paso, Texas
MUNSON, B.R., YOUNG, D.K., OKIISHI, T.H. (1994) Fundamentals of Fluid Mechanics
John Wiley and Sons
NUSSBAUMER, H.J. (1981) Fast Fourier Transform and Convolution Algorithms
Berlin: Springer-Verlag
OPPENHEIM, A.V. (1978) Applications of Digital Signal Processing
1st Edition - Prentice Hall
OSIADACZ, Dr A.J. (1998) Comparison of Isothermal and Non-Isothermal Transient Models
Pipeline Simulators Interest Group Conference, Denver, Colorado
OSIADACZ, Dr A.J. (1996) Different Transient Flow Models – Limitations, Advantages and Disadvantages
Pipeline Simulators Interest Group Conference, San Francisco, California

PEREIRA dos SANTOS, S. (1997) Transient Analysis – A Must in Gas Pipeline Design

Pipeline Simulators Interest Group Conference, Tucson, Arizona

PHILLIPS, C.L. (1995) Signals, Systems, and Transforms

Prentice Hall

POSTVOLL, W. (1996) Experience with Computational Analysis of the Norwegian Gas Transport Network

Pipeline Simulators Interest Group Conference, San Francisco, California

RAKESH, V. (1997) Visual Basic: Pipeline SCADA & Enterprise Wide Management

Pipeline & Gas Journal p64-65

RASINS, R. (1997) Electronic Mapping to System Flow Model

Pipeline Simulators Interest Group Conference, Tuscon, Arizona

REITH, K., SCHMIDT-WEMHOFF, W., SCHEERER, H. and ZAWORKA, J. (1990) Online Installation and Application of a Transient Simulation Model to Support Dispatching Activities at Ruhrgas AG

Pipeline Simulators Interest Group Conference, Baltimore, Maryland

ROGERS, G.F., MAYHEW, Y.R. (1992) Engineering Thermodynamics Work and Heat Transfer

4th Edition – Basil Blackwell Ltd.

SCHWENDEMAN, T.G. (1987) Underground Storage Systems : Leak Detection and Monitoring

Lewis Publishers

SMITH, S.W. (1999) The Scientist and Engineer's Guide to Signal Processing

California Technical Publishing. San Diego, California

STANLEY, W. (1975) Digital Signal Processing

Reston Publishing Co.

TERRELL, T.J. (1988) Introduction to Digital Filters

2nd ed. Basingstoke: Macmillan Education

THELEN, J.C. (1995) Tracking Gas Quality

AGA Conference Las Vegas, USA.

TISDALE, E. (1997) Testing Real-Time Modeling of a Gas Transmission Pipeline

Pipeline & Gas Journal p44-47

TOLIMIERI, R. (1989) Algorithms for Discrete Fourier Transform and Convolution
New York: Springer-Verlag

TOLLEFSON, E.L. (1972) Sources of Air Pollutants and Future Trends in Air Quality Standards
University of Calgary, Alberta

TURNER, W.J., MAGUIRE P.A. (1993) SIROGAS - Software for the Simulation of Flow of Fluid in Pipeline Networks
CSIRO Report 747

TURNER, W.J., MAGUIRE P.A., SMITH, C. and McCONNEL, P. (1992) Tracking and Prediction Models of the Moomba-Sydney-Newcastle Natural Gas Pipeline
Pipeline Simulators Interest Group Conference, Corpus Christi, Texas

TURNER, W.J., MUDFORD N.R. (1988) Leak Detection, Timing, Location and Sizing in Gas Pipelines
Mathl. Comput. Modelling Vol. 10 No 8 pp. 609-627

TURNER, W.J (1987) Better Leak Detection in Gas Pipelines
Comput. Math. Applic. Vol. 15 No 1 pp. 69-75

Van der HOEVEN, T. (1998) Gas Quality Control in Simulation
Pipeline Simulators Interest Group Conference, Denver, Colorado

VASEGHI, S.V. (1996) Advanced Signal Processing and Digital Noise Reduction
John Wiley

WIKE, A. (1993) SCADA Data for Real Time Modelling
AGA Conference Orlando, USA.

WIKE, A. (1991) The Changing Significance of SCADA Information
AGA Conference, Houston, USA

WOODHOUSE, J. (1998) Developing a Real Time Pipeline Simulation System
Pipeline Simulators Interest Group Conference, Denver, Colorado

WRIGHT, S. (1998) Compressor Station Optimization
Pipeline Simulators Interest Group Conference, Denver, Colorado

ZHANG, Dr J. (1996) Designing a Cost Effective and Reliable Pipeline Leak Detection System
Pipeline Reliability Conference, Houston, Nov 19 1996

ZHOU, Dr J. (1995) Simulation of Transient Flow in Natural Gas Pipelines
Pipeline Simulators Interest Group Conference, Albuquerque, New Mexico

APPENDIX A – VISUAL BASIC CODE

```
'   ON-LINE LEAK DETECTION SIMULATION
'   WRITTEN BY  : W. TURNER AND M. SULLIVAN
'   VERSION     : 5.0
'   DATE        : 12/10/2000
'   WRITTEN FOR : GOLDFIELDS GAS TRANSMISSION
'
'   PROGRAM DESCRIPTION
'    This program utilises the SIROGAS.DLL function to pass pipeline measurement
values
'   within this spreadsheet to a pipeline model created on FlowTran.  The values are
'   transferred into the model via FTP to the SCADA system controlled
'   via this program.  The FlowTran model outputs values back into this spreadsheet
'   where signal processing techniques are used to generate reliable leak detection
'   values.  This values are then written back to the SCADA system via a FTP process
'   also controlled via this program.
'
Option Explicit
'SIROGAS DLL Subroutines. This dll is installed in the windows system directory
'Once a function is called and the SIROGAS input and output files opened, the dll can
only be released by closing the workbook.
Private Declare Sub SGNAME Lib "SiroGas" (versnm As Double, ByRef iflag As Long,
ByVal stub As String, ByVal wsgs As String, ByVal comp As String, ByVal prof As
String, ByVal eqns As String, ByVal rstr As String, ByVal i As Long, ByVal j As Long,
ByVal k As Long, ByVal l As Long, ByVal m As Long, ByVal n As Long)
Private Declare Sub SGSTRT Lib "SiroGas" (iagin As Long, iagout As Long, ichapt As
Long, nouendd As Long)
Private Declare Sub SGRUN Lib "SiroGas" (iflag As Long, sgtime As Double, argind As
Double, iagin As Long, outtime As Double, ichapt As Long, argoutd As Double, iagout
As Long)
Private Declare Sub SGDESC Lib "SiroGas" (io As Long, iaposn As Long, ByVal arrkey As
String, ByVal ayaxl As String, ByVal aun As String, ipos As Long, ByVal descrp As
String, ByVal iarr As Long, ByVal iay As Long, ByVal iaun As Long, ByVal ides As
Long)
Global InpFileFound As Integer 'Can only check for inp once as SIROGAS does not
release once started.
Global Tnext As Double 'time to simulation to
Global sgtime As Double 'time in seconds passed to and from SIROGAS
Global iflag As Long 'sirogas input flags
Global jflag As Long 'sirogas output indicator
Global iagin As Long 'number of input args
Global argin() As Double 'input values
Global iagout As Long 'number of output args
Global argout() As Double 'output values
Global outtime() As Double 'times at which output values for each chapter apply
Global nouend() As Long 'position in argout of last item for this chapter
Global ichapt As Long 'Number of chapters in SIROGAS inp file specifying output
arguments from the DLL
Global iout As Integer 'current output row
Global ioutold As Integer 'old iout
Global tScadaStart As Double 'Excel time corresponding to SIROGAS time 0
Global tScadaNext As Double 'Excel time of next set of Scada data
Global stub As String * 60 'root of inp eg demo for demo.inp
Global rstr As String * 60 'restart; only if restart case
Global eol$ 'end of line
Global ResumeFileName As String 'file recording time offset and restart file name
Global FlowTranDir$
Global LastFileDelete 'calendar time of last delete
Global DataCount As Integer 'used in GetScadaData
'-------------------------------------------------------------------------------
-----
Sub TrackingBegin()
'This macro executed at start of tracking. It sets up.
If Val(Application.Version) < 7 Then
    MsgBox "Excel Version 7.0 or later required to call the 32 bit SIROGAS.dll;
sorry."
    End
End If
Call FindFlowTran(FlowTranDir$)
LastFileDelete = Now()
eol$ = Chr$(10) + Chr$(13) 'end of line
' . . . . . .
. .
'sets up name of resume file
Dim i As Integer, j As Integer 'General purpose do indexes
'write Scada time corresponding to SIROGAS 0 time, and name of file containing
network dynamic state (restart file)
ResumeFileName = Trim$(Range("ConfigurationFile"))
ResumeFileName = Left$(ResumeFileName, Len(ResumeFileName) - 3) & "dat"
ResumeFile:
i = FreeFile()
On Error Resume Next
Open ResumeFileName For Append As i
```

```
If Err > 0 Then
    'assume file is read only (which it is on demo cd) so use temp file
    If InStr(ResumeFileName, "c:\Track.dat") <> 1 Then
        ResumeFileName = "c:\Track.dat"
        GoTo ResumeFile
    Else
        MsgBox ("Unable to write resume file " & ResumeFileName & "; so please do not
pause tracking.")
    End If
End If
On Error GoTo 0
Close i
' . . . . . .
. .
'Pass SIROGAS file names SGSNAME
Dim comp As String * 2048 'compressor
Dim wsgs As String * 2048 'wsg - may be blank if option -1 not used
Dim prof As String * 2048 'profile
Dim eqns As String * 2048 'equation of state; only for version <2.4 inp
Call GetFileNames(stub, wsgs, comp, prof, eqns, rstr)
If InStr(wsgs, ".wsg") = 0 Then wsgs = Left$(stub, InStr(stub, " ") - 1) & ".wsg"
If Range("CurrentTrackingState").FormulaR1C1 = "Resuming" Then
    'info on resume time should be in .dat file written by TrackingPause macro
    i = FreeFile()
    On Error Resume Next
    Open ResumeFileName For Input As i
    If Err > 0 Then
        MsgBox "Unable to resume as " & ResumeFileName & " not found."
        Range("CurrentTrackingState").FormulaR1C1 = ""
        Exit Sub
    End If
    Input #i, tScadaStart, Tnext, rstr
    Close i
    Kill ResumeFileName
    On Error GoTo 0
Else
    Tnext = 0
    Range("CurrentTrackingState").FormulaR1C1 = "Beginning"
End If
iflag = 8
Dim Lfname As Long 'assume all names have same length
Lfname = Len(stub)
Dim versnm As Double
versnm = -2.61
On Error Resume Next
Call SGNAME(versnm, iflag, stub, wsgs, comp, prof, eqns, rstr, Lfname, Lfname,
Lfname, Lfname, Lfname, Lfname)
i = Err
On Error GoTo 0
Call TestSgError("SGNAME", i, iflag, stub)
jflag = iflag
Select Case Range("CurrentTrackingState").FormulaR1C1
Case "Stopped", "" 'leave Resuming for later
    Range("CurrentTrackingState").FormulaR1C1 = "Beginning"
End Select
' . . . . . .
. .
'Get number of input and output items, and number of chapters
ichapt = 10
ReDim outtime(1 To ichapt) As Double 'output time for each chapter
ReDim nouend(1 To ichapt) As Long 'position in argout of last item for this chapter
'Start SIROGAS and get requirements
On Error Resume Next
Call SGSTRT(iagin, iagout, ichapt, nouend(1))
i = Err
On Error GoTo 0
Call TestSgError("SGSIRT", i, iagin, stub)
Dim msg$
If iagin < 1 Then msg$ = "Cannot proceed as no inputs to SIROGAS specified in
configuration file " & Trim$(stub)
If iagout < 1 Then msg$ = msg$ & eol$ & "Cannot proceed as no outputs from SIROGAS
specified in configuration file " & Trim$(stub)
If iagin < 1 Or iagout < 1 Then
    MsgBox msg$ & eol$ & "Stopping now."
    Range("CurrentTrackingState").FormulaR1C1 = ""
    End
End If
'Redimension to reflect actual requirements for this inp file if required
ReDim argin(1 To iagin) As Double 'input to sirogas
ReDim argout(1 To iagout) As Double 'output from SIROGAS
If UBound(outtime) < ichapt Then ReDim outtime(ichapt), nouend(ichapt)
```

```
' . . . . . .
. .
'Set up Excel worksheets and charts
'args for SGDESC
Dim inout As Long '=1 for input; 2 for output
Dim iaposn As Long 'position of item in SIROGAS array
Dim arrkey As String * 8 'SIROGAS key word for this item
Dim ayaxl As String * 12 'y axis label for this item
Dim aun As String * 12 'units of this item
Dim ipos As Long 'position in network of this item
Dim descrp As String * 120 'description of item
Dim iarrkey As Long 'length of arrkey
iarrkey = Len(arrkey)
Dim iayaxl As Long 'length of ayaxl
iayaxl = Len(ayaxl)
Dim iaun As Long 'length of aun
iaun = Len(aun)
Dim idescrp As Long 'length of descrp
idescrp = Len(descrp)
'Fill in Input and output Headings
Range("InputHeadings") = ""
inout = 1
Range("InputHeadings") = " "
Range("InputHeadings").Cells(5, 1) = "Scada Time"
Range("InputHeadings").Cells(5, 2) = "SIROGAS Time"
Range("InputHeadings").Cells(6, 2) = "seconds"
Range("FlowTranOut").ClearContents
For i = -iagin To iagout
    iaposn = Abs(i)
    If i < 0 Then inout = 1 Else inout = 2
    On Error Resume Next
    Call SGDESC(inout, iaposn, arrkey, ayaxl, aun, ipos, descrp, iarrkey, iayaxl,
iaun, idescrp)
    j = Err
    On Error GoTo 0
    Call TestSgError("SGDESC", j, inout, stub)
    Select Case i
    Case 0
        'run title
        Worksheets("FlowTranInput").Cells(2, 2) = Trim$(descrp)
        Range("FlowTranOut").Cells(3, 1) = Trim$(descrp)
    Case Is < 0
        j = 2 - i
        Range("InputHeadings").Cells(1, j) = iaposn
        Range("InputHeadings").Cells(2, j) = arrkey
        Range("InputHeadings").Cells(3, j) = ipos
        Range("InputHeadings").Cells(4, j) = ayaxl
        Range("InputHeadings").Cells(5, j) = aun
        Range("InputHeadings").Cells(6, j) = Trim$(descrp)
    Case Is > 0
        j = 1 + i
        Range("FlowTranOut").Cells(1, j) = iaposn
        Range("FlowTranOut").Cells(2, j) = arrkey
        Range("FlowTranOut").Cells(3, j) = ipos
        Range("FlowTranOut").Cells(4, j) = ayaxl
        Range("FlowTranOut").Cells(5, j) = aun
        Range("FlowTranOut").Cells(6, j) = Trim$(descrp)
    End Select
Next i
'set time for first run of simulation
Application.OnTime   Now   +   TimeValue("00:00:01"),   "TrackingContinue",   Now   +
TimeValue("00:00:20")
sgtime = -1
End Sub
'-------------------------------------------------------------------------------
-----
Private Sub TrackingContinue()
'This macro gets scada data for new time. We already have data for old time.
'Tells SIROGAS to simulate to new time.
'
'check setup data
'Check TrackingState
Select Case Range("CurrentTrackingState").FormulaR1C1
Case "Stopped", "Paused"
    Exit Sub
Case "Stopping"
    GoTo quit
End Select
'remember current location so can restore
Dim SheetTitle$
Dim OldRange As Range
SheetTitle$ = ActiveSheet.Name
```

```
'On Error Resume Next 'chart does not have cells
Set OldRange = ActiveCell
'Simulate up to latest SCADA data
'Run if possible; see if any data
Dim i As Integer, j As Integer 'general use
'Is it a continuation of a simulation already begun?
If sgtime > -1 Then GoTo ContinueSimulation '.....................................
'First simulation so set startup values
iout = Range("InputHeadings").Rows.Count
ioutold = iout
Const tconvert = 3600 'hours to secs
Dim sec As Double, DT As Double, DLP As Double, FlowIn As Double, FlowOut As Double
Dim tim$, dat$ 'time and date
'Get 1st set of Scada data
ReDim ScadaData(UBound(argin)) As Double
Dim GetErr As Integer
Call GetScadaData(sec, tim$, dat$, ScadaData(), GetErr)
If GetErr <> 0 Then GoTo GetError
tScadaStart = DateValue(dat$) * 3600 * 24 + sec 'convert to Excel secs
'write file for resume
i = FreeFile()
Open ResumeFileName For Output As i
Print #i, tScadaStart, Tnext, Trim$(stub) & ".rst"
Close i
'Put latest data on worksheet
Range("LatestScadaData").Cells(1, 1) = tim$ & " " & dat$
Range("LatestScadaData").Cells(1, 2) = 0
For i = 1 To UBound(argin)
    argin(i) = ScadaData(i)
    Range("LatestScadaData").Cells(1, 2 + i) = argin(i)
Next i
Dim msg$
msg$ = "Descriptions of FlowTran input and outputs written." & eol$
If Range("CurrentTrackingState").FormulaR1C1 = "Resuming" Then
    msg$ = msg$ & "Ready to resume simulation " & Trim$(stub) & " begun at " & dat$ &
" " & tim$
    jflag = 48
Else
    msg$ = msg$ & "Ready to start simulation " & Trim$(stub) & " from " & dat$ & " "
& tim$
    jflag = 64
End If
MsgBox msg$
'set SGRUN input flag
iflag = 64
'Run simuation continuation
Do
    'more data needed; see if more data in file
    Do
        'On Error Resume Next
        ReDim ScadaData(UBound(argin)) As Double
        Call GetScadaData(sec, tim$, dat$, ScadaData(), GetErr)
        If GetErr <> 0 Then GoTo GetError 'normal exit when no more data in file
        Range("CurrentTrackingState").FormulaR1C1 = "Running"
        tScadaNext = DateValue(dat$) * 3600 * 24 + sec - tScadaStart
        For i = 1 To UBound(argin)
            argin(i) = ScadaData(i)
        Next i
    Loop Until tScadaNext > Tnext
    Tnext = tScadaNext
    sgtime = Tnext
    jflag = iflag
    On Error Resume Next
    Call SGRUN(jflag, sgtime, argin(1), iagin, outtime(1), ichapt, argout(1), iagout)
    j = Err
    On Error GoTo 0
    Call TestSgError("SGRUN", j, jflag, stub)
    'put output in sheet
    iout = iout + 1
    Range("FlowTranOut").Cells(iout, 1) = (sgtime + tScadaStart) / (3600# * 24#)
    For i = 1 To UBound(argout)
        Range("FlowTranOut").Cells(iout, i + 1) = argout(i)
    Next i
    If iout > 7 Then
        DT = Range("FlowTranOut").Cells(iout, 1) - Range("FlowTranOut").Cells(iout -
1, 1)
        For i = 1 To 18
            DLP     =     Range("FlowTranOut").Cells(iout,     i     +     13)     -
Range("FlowTranOut").Cells(iout - 1, i + 13)
            FlowIn     =     Range("FlowTranOut").Cells(iout,     i     +     31)     +
Range("FlowTranOut").Cells(iout - 1, i + 31)
```

```
            FlowOut     =     Range("FlowTranOut").Cells(iout,     i     +     49)     +
Range("FlowTranOut").Cells(iout - 1, i + 49)
            Range("ScadaOutput").Cells(iout, i + 5) = (DT * ((FlowIn - FlowOut) / 2)
- DLP) / DT
        Next i
    End If
    If iout > 7 Then
        Kill "C:\GASAPPS\GGT\ggtwrite.txt"
    End If
    If iout > 7 Then
    Close #1
        Open "C:\GASAPPS\GGT\GGTWRITE.TXT" For Append As #1 ' Append creates a file
if it doesn't already exist.
        For i = 1 To 23
            Write #1, Range("ScadaOutput").Cells(iout, i).Value
        Next i
    End If
    Close #1
    '-------------------------------------------------------------------------------
-----
    Dim SendIt
    SendIt = Shell("C:\GASAPPS\GGT\PUTDATA.BAT", vbMinimizedNoFocus)
    Application.Wait TimeSerial(Hour(Now()), Minute(Now()), Second(Now()) + 5)
    '-------------------------------------------------------------------------------
-----
ContinueSimulation:
    If Range("CurrentTrackingState").FormulaR1C1 = "Resuming" Then
        'ensure TrackingState is Running
        Tnext = sgtime
        Range("CurrentTrackingState").FormulaR1C1 = "Running"
    End If
Loop
quit:
'end sirogas
jflag = 0
sgtime = 0
On Error Resume Next
Call SGRUN(jflag, sgtime, argin(1), iagin, outtime(1), ichapt, argout(1), iagout)
Range("CurrentTrackingState").FormulaR1C1 = "Stopped"
Exit Sub

GetError:  'error in getting data; assumed to be because no more data available
'so bring displays up to date
Select Case GetErr
Case Is > 0
    GoTo quit
Case -1
    Dim DeleteRows As Integer
    DeleteRows      =      iout      -      Range("InputHeadings").Rows.Count      -
Range("RecentValuesToKeep")
    If Range("CurrentTrackingState").FormulaR1C1 = "Beginning" Then
        MsgBox "No Scada data available! I will continue to look for it."
        Range("CurrentTrackingState").FormulaR1C1 = "Running"
    End If
    If DeleteRows > 0 Or iout <> ioutold Then
        'put latest input on sheet
        Range("LatestScadaData").Cells(1, 1) = tim$ & " " & dat$
        For i = 1 To UBound(argin)
            Range("LatestScadaData").Cells(1, 2 + i) = argin(i)
        Next i
        Range("LatestScadaData").Cells(1, 2) = Tnext
        'put latest output in plot
        ioutold = iout
        'delete excess rows; note that graph range is changed by Excel
        If DeleteRows > 0 Then
            Dim DeleteRange$
            DeleteRange$ = "A7:A" & LTrim$(Str$(DeleteRows + 6))
            Sheets("FlowTranOutput").Range(DeleteRange$).EntireRow.Delete
            iout = iout - DeleteRows
        End If
    End If
    'set time for next run of simulation
    '
    Dim GrabIt
    GrabIt = Shell("C:\GASAPPS\GGT\GETDATA.BAT", vbMinimizedNoFocus)
    Application.Wait TimeSerial(Hour(Now()), Minute(Now()), Second(Now()) + 5)
    ActiveWorkbook.Save
    Application.OnTime      Now      +      TimeValue(Range("WakeInterval").Text),
"TrackingContinue"
    Reset 'so can delete Scada.dat
    If SheetTitle$ <> ActiveSheet.Name Then Sheets(SheetTitle$).Select
    On Error Resume Next 'chart does not have cells
```

```
    If OldRange <> ActiveCell Then OldRange.Select
    On Error GoTo 0
End Select
'check for delete of restart files; new file written at next SGRUN
Call FileLengthControl(Range("ConfigurationFile") & "rst")
Call FileLengthControl(Range("RestartConfigurationFile") & "rst")
End Sub 'go to sleep until next on time wakes Tracking up
'-------------------------------------------------------------------------------
-----
Sub SetGraphRows(icol, Ch As Chart, PlotStart, PlotEnd)
'set rows to be plotted
Dim LRow$, RRow$, PCol$
LRow$ = LTrim$(Str$(PlotEnd))
RRow$ = LTrim$(Str$(PlotStart))
PCol$ = Chr$(Asc("A") + icol - 1)
Dim RPlot$
RPlot$ = "A" & RRow$ & ":A" & LRow$ 'x values
RPlot$ = RPlot$ & "," & PCol$ & RRow$ & ":" & PCol$ & LRow$ 'y values
Ch.SetSourceData Source:=Sheets("FlowTranOutput").Range(RPlot), PlotBy:=xlColumns
End Sub
'-------------------------------------------------------------------------------
-----
Sub TrackingEnd()
'set to stop tracking at next run of Simulation
If Range("CurrentTrackingState").FormulaR1C1 = "Running" Then
    Range("CurrentTrackingState").FormulaR1C1 = "Stopping"
    Range("RestartConfigurationFile").Font.Bold = False
    Range("ConfigurationFile").Font.Bold = False
Else
    MsgBox "Cannot stop as not running."
End If
End Sub
'-------------------------------------------------------------------------------
-----
Sub TrackingPause()
'set tracking to pause.
'Resume can be at this Excel session - the same SIROGAS calc is continued
' or at a later Excel session - the restart inp file will be used in a restart
SIROGAS case using the rst file named in the .dat file.
If Range("CurrentTrackingState").FormulaR1C1 = "Running" Then
    'set to pause tracking
    Range("CurrentTrackingState").FormulaR1C1 = "Paused"
    MsgBox "Tracking paused and FlowTran license released. You can resume during this
or a later Excel session of the unsaved Tracking.xls."
    End
Else
    MsgBox "Sorry; cannot pause as not running."
End If
End Sub
'-------------------------------------------------------------------------------
-----
Sub TrackingResume()
Select Case Range("CurrentTrackingState").FormulaR1C1
Case "Paused", ""
    'a new SIROGAS calc Beginning from the dynamic state from the restart file.
    Range("CurrentTrackingState").FormulaR1C1 = "Resuming"
    Call TrackingBegin
Case Else
    MsgBox "Sorry; cannot resume as already tracking " &
Range("CurrentTrackingState").FormulaR1C1
End Select
End Sub
'-------------------------------------------------------------------------------
-----
Sub FileLengthControl(fName$)
'Deletes file fName$ at time interval from Setup sheet
If Now() > LastFileDelete + TimeValue(Range("DeleteRestartFile")) Then
    On Error Resume Next
    Kill fName$
    On Error GoTo 0
    LastFileDelete = Now()
End If
End Sub
'-------------------------------------------------------------------------------
-----
Sub GetFileNames(stub$, wsgs$, comp$, prof$, eqns$, rstr$)
'Change to FlowTran directory
Dim i As Integer
'check inp file exists
If Range("CurrentTrackingState").FormulaR1C1 = "Resuming" Then
    Range("RestartConfigurationFile").Font.Bold = True
    Range("ConfigurationFile").Font.Bold = False
```

```
    stub$ = Range("RestartConfigurationFile")
Else
    Range("RestartConfigurationFile").Font.Bold = False
    Range("ConfigurationFile").Font.Bold = True
    stub$ = Range("ConfigurationFile")
End If
'Can only check for inp once as SIROGAS does not release once started.
If InpFileFound = 0 Then
    i = FreeFile()
    On Error Resume Next
    Open stub$ For Input As i
    If Err > 0 Then
        MsgBox "Unable to open file " & stub$ & ". Please check range
'ConfigurationFile'"
        Exit Sub
    End If
    InpFileFound = True
End If
On Error GoTo 0
Close i
i = Len(stub$)
stub$ = Left$(stub$, i - 4)
comp$ = FlowTranDir$ & "compress.cmp"
prof$ = FlowTranDir$ & "profiles.pro"
eqns$ = FlowTranDir$ & "bwrs.eqs"
End Sub
'-------------------------------------------------------------------------------
-----Option Explicit
Dim DataOld(100)
Sub GetScadaData(sec As Double, tim$, dat$, Data() As Double, GetError As Integer)
'This routine must get scada data; all arguments are outputs
'sec = time to which data applies; number of seconds after midnight eg 58033.16
'tim$ = time to which data applies eg  "16:07:13" (this is vb5 Time$ format)
'dat$ = time to which data applies; eg "01-06-1998" (this is vb5 Date$ format)
'Data() = values of scada data in the order specified in the InputVariables chapters
of the SIROGAS configuration (inp) file
'           These scada data are also listed in the .out file
'GetError = 0 if no error; -1 if data may be available later; >0 error, cease
tracking
'This example gets the data from a file, but any method will do.
'Note that procedure writing any Scada data file must not allow the file to grow
indefinitely
Dim i As Integer
Static iscada As Integer 'iscada=0 initially
On Error GoTo GetScadaError
DataCount = DataCount + 1
'
If iscada = 0 Then 'open file containing ScadaData
    i = FreeFile()
    On Error Resume Next
    If DataCount = 1 Then
        Open Range("StartDataFile") For Input As i
    Else
        Open Range("ScadaDataFile") For Input As i
    End If
    If Err > 0 Then GoTo HGetScadaError
    iscada = i
End If
On Error Resume Next
Input #iscada, sec, tim$, dat$
If Err > 0 Then GoTo HGetScadaError
For i = 1 To UBound(Data)
    Input #iscada, Data(i)
    If Err > 0 Then GoTo HGetScadaError
    If Data(i) = -999 Then 'Filter for bad data -999
        Data(i) = DataOld(i)
    End If
Next i
For i = 1 To UBound(Data)
    DataOld(i) = Data(i)
Next i
GetError = 0
Exit Sub

GetScadaError:  'Error occured
Resume HGetScadaError

HGetScadaError:
On Error GoTo 0
Close iscada 'so can be deleted
iscada = 0
GetError = -1
```

```
End Sub
```

APPENDIX B – FLOWTRAN MODEL INPUT FILE

```
Default values for FlowTran wjs97jul22
CONTROLS
 version number                    VERSN     2.610
 netwrk balance                    TOL
1.0000000E 08
 max no. of its                    ITMAX     10
 min dt                            SMIN
5.0000000E-01
 max dt                            SMAX
9.0000000E+09
 target chng                       CTAR
1.0000000E-02
 max change                        CMAX
2.0000000E+00
 max newdt/old                     CINC
2.0000000E+00
 MaxTime & restart                 TMAX
0.0000000E+00
 restart time                      RTIME     not_used
 initial dt                        RDELT     not_used
 freq full print                   XFP       0
 full print after                  TSFP
9.0000000E+09
 freq restart dump                 XFRST     -1
                                             bwrs.eqs
COMPOSITION
BWRSmixA
*Default steady state composition
 METHANE
6.7560928E-01
 ETHYLENE
0.0000000E+00
 ETHANE
1.0584123E-01
 PROPYLENE
0.0000000E+00
 PROPANE
6.6520121E-02
 I BUTANE
3.5071887E-02
 N BUTANE
3.5071887E-02
 I PENTANE
1.0883931E-02
 N-PENTANE
1.0883931E-02
 N HEXANE
2.1666485E 03
 N-HEPTANE
0.0000000E+00
 N-OCTANE
0.0000000E+00
 NITROGEN
2.2541271E-02
 CARBON DIOXIDE
3.5409813E-02
 HYDROGEN SULFIDE
0.0000000E+00
COMPOSITION
BWRSmixB
 METHANE
7.4400793E-01
 ETHYLENE
0.0000000E+00
 ETHANE
1.0444010E-01
 PROPYLENE
0.0000000E+00
 PROPANE
3.5344360E 02
 I-BUTANE
1.5529053E-02
 N BUTANE
1.5529053E-02
 I-PENTANE
3.8553306E-03
 N-PENTANE
3.8553306E-03
 N-HEXANE
4.6048505E 04
 N-HEPTANE
0.0000000E+00
 N OCTANE
0.0000000E+00
 NITROGEN
2.9942323E-02
 CARBON DIOXIDE
4.7036038E-02
 HYDROGEN SULFIDE
0.0000000E+00
COMPOSITION
BWRSmixC
 METHANE
7.6983541E-01
 ETHYLENE
0.0000000E+00
 ETHANE
6.5587523E-02
 PROPYLENE
0.0000000E+00
 PROPANE
1.6831942E-02
 I-BUTANE
3.1694383E-03
 N-BUTANE
3.1694383E-03
 I-PENTANE
1.9671567E-03
 N-PENTANE
1.9671567E-03
 N-HEXANE
0.0000000E+00
 N-HEPTANE
0.0000000E+00
 N-OCTANE
0.0000000E+00
 NITROGEN
5.3472547E 02
 CARBON DIOXIDE
8.3999386E-02
 HYDROGEN SULFIDE
0.0000000E+00
PIPE
Apache_Inlet to Yarraloola
*Original FlowTran Version 1.10 Pipe values
 number of nodes                   N         2
 axial position                    Z          900,
1100,
 altitude                          ALT        50,
50,
 diameter                          DIAM
3.9440000E-01
 roughness                         RGHVAL
0.0000000E+00
 heat transfer coef                HFVAL
4.0000000E+00
 ground temp                       TFCVAL
3.0873000E-02
PIPE
Yarraloola to Wyloo_West
*Original FlowTran Version 1.10 Pipe values
*
*
 number of nodes                   N         138
 axial position                    Z          1100,
2114.5445,  3129.0923,

4143.6368,  5158.1813,

6172.7258,  7187.2736,

8201.8181,  9216.3625,

10230.91,  11245.455,

12259.999,  13274.544,

14289.092,  15303.636,

16318.181,  17332.728,

18347.273,  19361.817,

20375.365,  21390.91,

22405.454,  23419.999,

24434.546,  25449.091,

26463.635,  27478.183,

28492.728,  29507.272,

30521.817,  31536.361,

32550.909,  33565.457,

34580.001,  35594.546,

36609.09,  37623.635,

38638.183,  39652.727,

40667.275,  41681.819,

42696.364,  43710.908,

44725.453,  45740.001,

46754.545,  47769.093,

48783.637,  49798.182,

50812.726,  51827.271,

52841.819,  53856.363,

54870.908,  55885.456,  56900,

57904.879,  58909.757,

59914.633,  60919.511,

61924.39,  62929.268,

63934.148,  64939.022,

65943.902,  66948.781,

67953.66,  68958.537,

69963.416,  70968.292,

71973.171,  72978.048,

73982.927,  74987.803,

75992.682,  76997.561,

78002.439,  79007.32,
```

80012.197, 81017.074,

82021.952, 83026.829,

84031.707, 85036.584,

86041.461, 87046.342,

88051.219, 89056.096,

90060.978, 91065.855,

92070.733, 93075.61,

94080.487, 95085.365,

96090.242, 97095.123, 98100,

99104.877, 100109.75,

101114.64, 102119.51,

103124.39, 104129.27,

105134.14, 106139.03,

107143.9, 108148.78,

109153.66, 110158.53,

111163.42, 112168.29,

113173.17, 114178.05,

115182.93, 116187.81,

117192.68, 118197.56,

119202.44, 120207.32,

121212.19, 122217.07,

123221.95, 124226.83,

125231.71, 126236.58,

127241.47, 128246.34,

129251.22, 130256.1,

131260.97, 132265.86,

133270.73, 134275.61,

135280.49, 136285.36,

137290.25, 138295.12, 139300,

altitude ALT 50,

51.6909103393555,

53.3818206787109,

55.0727310180664,

56.7636299133301,

58.4545402526855,

60.145450592041,

61.8363609313965,

63.527271270752,

65.2181930541992,

66.9090881347656,

68.5999984741211,

70.2909088134766,

71.981819152832,

73.6727294921875,

75.3636322021484,

77.0545501708984,

78.7454528808594,

80.4363632202148,

82.1272735595703,

83.8181762695313,

85.5090866088867,

87.1999969482422,

88.8909072875977,

90.5818176269531,

92.2727279663086,

93.9636383056641,

95.6545486450195,

97.3454513549805,

99.0363616943359,

100.72730255127,

102.418197631836,

104.109100341797,

105.800003051758,

107.490858132324,

109.181800842285,

110.872703552246,

112.563598632813,

114.254501342773,

115.945503234863,

117.63639831543,

119.327301025391,

121.018203735352,

122.709098815918,

124.400001525879,

126.090896606445,

127.781799316406,

129.472702026367,

131.163604736328,

132.854598999023,

134.545501708984,

136.236404418945,

137.927307128906,

139.618194580078,

141.309097290039, 143,

143.463394165039,

143.926803588867,

144.390197753906,

144.853698730469,

145.317092895508,

145.780502319336,

146.243896484375,

146.707305908203,

147.170700073242,

147.634094238281,

148.097595214844,

148.561004638672,

149.024398803711,

149.48779296875,

149.951202392578,

150.414596557617,

150.87809753418,

151.341506958008,

151.804901123047,

152.268295288086,

152.731704711914,

153.195098876953,

153.658493041992,

154.12190246582,

154.585403442383,

155.048797607422,

155.51220703125,

155.975601196289,

156.438995361328,

156.902404785156,

157.365798950195,

157.829299926758,

158.292694091797,

158.756103515625,

159.219497680664,

159.682907104492,

160.146301269531,

160.609802246094,

161.073196411133,

161.536605834961, 162,

162.463394165039,

162.926803588867,

163.390197753906,

163.853698730469,

164.317092895508,

164.780502319336,

165.243896484375,

165.707305908203,

166.170700073242,

166.634201049805,

167.097595214844,

167.561004638672,

168.024398803711,

168.48779296875,

168.951202392578,

169.414596557617,

169.87809753418,

170.341506958008,

170.804901123047,

171.268295288086,

171.731704711914,

172.195098876953,

172.658493041992,

173.12190246582,

173.585403442383,

174.048797607422,

174.51220703125,

174.975601196289,

175.438995361328,

175.902404785156,

176.365905761719,

176.829299926758,

177.292694091797,

177.756103515625,

178.219497680664,

178.682907104492,

179.146301269531,

179.609802246094,

180.073196411133,

180.536605834961, 181.
 diameter DIAM
3.9440000E 01
 roughness RGHVAL
5.9000000E-05
 heat transfer coef HFVAL
4.0000000E+00
 ground temp TFCVAL
3.0873000E+02
PIPE
Wyloo West to Paraburdoo
*Original FlowTran Version 1.10 Pipe values
*
 number of nodes N 165
 axial position Z 139300,
140305.81, 141311.63,

142317.44, 143323.26,

144329.07, 145334.88,

146340.7, 147346.51,

148352.32, 149358.14,

150363.95, 151369.77,

152375.58, 153381.4,

154387.21, 155393.03,

156398.84, 157404.65,

158410.46, 159416.28,

160422.09, 161427.91,

162433.72, 163439.54,

164445.35, 165451.16,

166456.97, 167462.79,

168468.6, 169474.42,

170480.23, 171486.05,

172491.86, 173497.68,

174503.49, 175509.3,

176515.12, 177520.93,

178526.74, 179532.56,

180538.37, 181544.19, 182550,

183555.81, 184561.63,

185567.45, 186573.26,

187579.08, 188584.89,

189590.71, 190596.52,

191602.32, 192608.14,

193613.95, 194619.77,

195625.58, 196631.39,

197637.2, 198643.02,

199648.83, 200654.65,

201660.46, 202666.28,

203672.09, 204677.91,

205683.72, 206689.54,

207695.35, 208701.17,

209706.98, 210712.8, 211718.6,

212724.42, 213730.23,

214736.05, 215741.86,

216747.68, 217753.49,

218759.31, 219765.11,

220770.92, 221776.74,

222782.55, 223788.37,

224794.18, 225800, 226801.28,

227802.56, 228803.84,

229805.13, 230806.41,

231807.69, 232808.97,

233810.26, 234811.53,

235812.82, 236814.1,

237815.39, 238816.66,

239817.95, 240819.23,

241820.52, 242821.79,

243823.08, 244824.36,
245825.65, 246826.92,
247828.2, 248829.49,
249830.78, 250832.05,
251833.33, 252834.62,
253835.9, 254837.18,
255838.46, 256839.74,
257841.03, 258842.31,
259843.58, 260844.87,
261846.16, 262847.44,
263848.71, 264850, 265851.28,
266852.56, 267853.85,
268855.13, 269856.41,
270857.69, 271858.98,
272860.26, 273861.54,
274862.82, 275864.1,
276865.38, 277866.67,
278867.95, 279869.23,
280870.51, 281871.8,
282873.08, 283874.36,
284875.64, 285876.92,
286878.2, 287879.49,
288880.77, 289882.05,
290883.33, 291884.62,
292885.9, 293887.18,
294888.46, 295889.74,
296891.02, 297892.31,
298893.59, 299894.87,
300896.15, 301897.44,
302898.72, 303900,
altitude ALT 181,
181.965103149414,
182.930206298828,
183.895401000977,
184.860504150391,
185.825607299805,
186.79069519043,
187.755798339844,
188.720901489258,
189.686004638672,
190.651199340820,
191.616302490234,
192.581405639648,
193.546493530273,
194.511596679688,
195.476699829102,
196.44189453125,
197.406997680664,
198.372100830078,
199.337203979492,
200.302307128906,
201.267395019531,
202.232604980469,
203.197692871094,
204.162796020508,
205.127899169922,
206.093002319336,
207.058105468750,
208.023300170898,
208.988403320313,
209.953506469727,
210.918594360352,
211.883697509766,
212.84880065918,
213.813903808594,
214.779098510742,
215.744201660156,
216.70930480957,
217.674392700195,
218.639495849609,
219.604598999023,
220.569793701172,
221.534896850586, 222.5,
223.465103149414,
224.430206298828,
225.395401000977,
226.360504150391,
227.325607299805,
228.29069519043,
229.255798339844,
230.220901489258,
231.186004638672,
232.15119934082,
233.116302490234,
234.081405639648,
235.046493530273,
236.011596679688,
236.976699829102,
237.941802978516,
238.906997680664,
239.872100830078,
240.837203979492,
241.802307128906,
242.767395019531,
243.732604980469,
244.697692871094,
245.662796020508,
246.627899169922,
247.593002319336,
248.558197021484,
249.523300170898,
250.488403320313,
251.453506469727,
252.418594360352,
253.383697509766,
254.34880065918,
255.313995361328,
256.279113769531,
257.244201660156,
258.209289550781,
259.174407958984,

260.139495849609,

261.104614257813,

262.069793701172,

263.034912109375, 264,

264.730804443359,

265.461486816406,

266.192291259766,

266.923095703125,

267.65380859375,

268.384613037109,

269.115386962891,

269.84619140625,

270.576904296875,

271.307708740234,

272.038513183594,

272.769195556641, 273.5,

274.230804443359,

274.961486816406,

275.692291259766,

276.423095703125,

277.15380859375,

277.884613037109,

278.615386962891,

279.34619140625,

280.076904296875,

280.807708740234,

281.538513183594,

282.269195556641, 283,

283.730804443359,

284.461486816406,

285.192291259766,

285.923095703125,

286.65380859375,

287.384613037109,

288.115386962891,

288.846099853516,

289.576904296875,

290.307708740234,

291.038513183594,

291.769195556641, 292.5,

293.230804443359,

293.961486816406,

294.692291259766,

295.423095703125,

296.153900146484,

296.884613037109,

297.615386962891,

298.34619140625,

299.076904296875,

299.807708740234,

300.538513183594,

301.269195556641, 302,

302.730804443359,

303.461486816406,

304.192291259766,

304.923095703125,

305.65380859375,

306.384613037109,

307.115386962891,

307.84619140625,

308.576904296875,

309.307708740234,

310.038513183594,

310.769195556641, 311.5,

312.230804443359,

312.961486816406,

313.692291259766,

314.423095703125,

315.153900146484,

315.884613037109,

316.615386962891,

317.34619140625,

318.076904296875,

318.807708740234,

319.538513183594,

320.269195556641, 321,

```
 diameter                        DIAM
3.9440000E-01
 roughness                       RGHVAL
1.0000000E-05
 heat transfer coef              HFVAL
4.0000000E+00
 ground temp                     TFCVAL
3.0863000E+02
PIPE
Paraburdoo to Turee_Creek
*Original FlowTran Version 1.10 Pipe values
*
 number of nodes                 N          160
 axial position                  Z           303900,
```

304906.93, 305913.86,

306920.79, 307927.72,

308934.65, 309941.58,

310948.51, 311955.44,

312962.37, 313969.3,

314976.24, 315983.17,

316990.1, 317997.03,

319003.96, 320010.89,

321017.82, 322024.75,

323031.68, 324038.61,

325045.54, 326052.47,

327059.41, 328066.34,

329073.27, 330080.2,

331087.13, 332094.06,

333100.99, 334107.92,

335114.85, 336121.78,

337128.72, 338135.65,

339142.58, 340149.51,

341156.44, 342163.37,

343170.3, 344177.23,

345184.16, 346191.09,

347198.02, 348204.95,

349211.88, 350218.81,

351225.74, 352232.67,

353239.6, 354246.53,

355253.48, 356260.38,

357267.34, 358274.24,

359281.2, 360288.12,
361295.05, 362301.98,
363308.91, 364315.84,
365322.77, 366329.7,
367336.63, 368343.56,
369350.49, 370357.44,
371364.35, 372371.3,
373378.21, 374385.16,
375392.07, 376399.02,
377405.93, 378412.88,
379419.79, 380426.74,
381433.67, 382440.6,
383447.53, 384454.46,
385461.39, 386468.32,
387475.25, 388482.17,
389489.1, 390496.03,
391502.96, 392509.89,
393516.82, 394523.75,
395530.71, 396537.62,
397544.56, 398551.49,
399558.42, 400565.35,
401572.28, 402579.21,
403586.14, 404593.07, 405600,
406605.18, 407610.34,
408615.52, 409620.7,
410625.86, 411631.04,
412636.22, 413641.37,
414646.55, 415651.71,
416656.89, 417662.08,
418667.25, 419672.41,
420677.59, 421682.75,
422687.93, 423693.1,
424698.29, 425703.45,
426708.62, 427713.78,
428718.97, 429724.15,
430729.32, 431734.48,
432739.64, 433744.81, 434750,
435755.17, 436760.35,
437765.52, 438770.69,
439775.86, 440781.03,
441786.21, 442791.38,
443796.55, 444801.72,
445806.9, 446812.07,
447817.24, 448822.41,
449827.59, 450832.76,
451837.93, 452843.1,
453848.28, 454853.45,
455858.62, 456863.79,
457868.97, 458874.14,
459879.31, 460884.48,
461889.65, 462894.83, 463900,
altitude ALT 321,
322.762390136719,
324.524688720703,
326.287109375,
328.049499511719,
329.811889648438,
331.574188232422,
333.336608886719,
335.098999023438,
336.861389160156,
338.623687744141,
340.386108398438,
342.148498535156,
343.910888671875,
345.673309326172,
347.435607910156,
349.197998046875,
350.960388183594,
352.722808837891,
354.485198974609,
356.247497558594,
358.009887695313,
359.772308349609,
361.534606933594,
363.296997070313,
365.059387207031,
366.821807861328,
368.584197998047,
370.346496582031,
372.10888671875,
373.871307373047,
375.633697509766,
377.396087646484,
379.158386230469,
380.920806884766,
382.683197021484,
384.445587158203,
386.207885742188,
387.970306396484,
389.732696533203,
391.495086669922,
393.257385253906,
395.019805908203,
396.782196044922,
398.544586181641,
400.306884765625,
402.069305419922,
403.831695556641,
405.594085693359,
407.356414794922,
409.118804931641,
410.881195068359,
412.643585205078,
414.405914306641,
416.168304443359,
417.930694580078,
419.693115234375,
421.455413818359,
423.217803955078,
424.980194091797,

```
426.742614746094,
428.505004882813,
430.267303466797,
432.029693603516,
433.792114257813,
435.554412841797,
437.316802978516,
439.079193115234,
440.841613769531,
442.603912353516,
444.366394042969,
446.128692626953,
447.89111328125,
449.653503417969,
451.415893554688,
453.178192138672,
454.940612792969,
456.703002929688,
458.465301513672,
460.227691650391,
461.990112304688,
463.752502441406,
465.514892578125,
467.277191162109,
469.039611816406,
470.802001953125,
472.564392089844,
474.326690673828,
476.089111328125,
477.851501464844,
479.613800048828,
481.376312255859,
483.138610839844,
484.901000976563,
486.663391113281,
488.425811767578,
490.188110351563,
491.950500488281,
493.712890625,
495.475311279297,
497.237609863281,  499,  501,
                                        503,
505,  507,  509,  511,
                                        513,
515,  517,  519,  521,
                                        523,
525,  527,  529,  531,
                                        533,
535,  537,  539,  541,
                                        543,
545,  547,  549,  551,
                                        553,
555,  557,  559,  561,
                                        563,
565,  567,  569,  571,
                                        573,
575,  577,  579,  581,
                                        583,
585,  587,  589,  591,
                                        593,
595,  597,  599,  601,
                                        603,
605,  607,  609,  611,
                                        613,
615,
 diameter                       DIAM
3.944000CE 01
 roughness                      RGHVAL
7.000000CE-06
 heat transfer coef             HFVAL
4.0000000E+00
 ground temp                    TFCVAL
3.0695000E+02
PIPE
Turee_Creek to Newman
*Original FlowTran Version 1.10 Pipe values
 number of nodes                N          57
 axial position                 Z          463900,
464907.14,  465914.28,
466921.43,  467928.57,
468935.72,  469942.86,  470950,
471957.14,  472964.28,
473971.43,  474978.57,
475985.72,  476992.86,  478000,
479007.14,  480014.28,
481021.43,  482028.57,
483035.72,  484042.86,  485050,
486057.14,  487064.28,
488071.43,  489078.57,
490085.72,  491092.86,  492100,
493107.14,  494114.27,
495121.44,  496128.56,
497135.73,  498142.86,  499150,
500157.14,  501164.27,
502171.44,  503178.56,
504185.73,  505192.86,  506200,
507207.14,  508214.28,
509221.44,  510228.56,
511235.72,  512242.86,  513250,
514257.14,  515264.28,
516271.42,  517278.58,
518285.72,  519292.86,  520300,
 altitude                       ALT        615,
614.892883300781,
614.785705566406,
614.678588867188,
614.571411132813,
614.464294433594,
614.357116699219,  614.25,
614.142883300781,
614.035705566406,
613.928588867188,
613.821411132813,
613.714294433594,
613.607177734375,  613.5,
613.392822265625,
613.285705566406,
613.178588867188,
613.071411132813,
612.964294433594,
612.857177734375,  612.75,
612.642822265625,
612.535705566406,
612.428588867188,
612.321411132813,
612.214172363281,
612.107177734375,  612,
611.892822265625,
611.785705566406,
611.678588867188,
```

```
611.571411132813,
611.464294433594,
611.357116699219,  611.25,
611.142883300781,
611.035705566406,
610.928588867188,
610.821411132813,
610.714294433594,
610.607116699219,  610.5,
610.392822265625,
610.285705566406,
610.178588867188,
610.071411132813,
609.964294433594,
609.857177734375,  609.75,
609.642883300781,
609.535705566406,
609.428588867188,
609.321411132813,
609.214294433594,
609.107116699219,  609,
 diameter                          DIAM
3.9440000E-01
 roughness                         RGHVAL
0.0000000E+00
 heat transfer coef                HFVAL
4.0000000E+00
 ground temp                       TFCVAL
3.0738000E-02
PIPE
Newman to NewmanT
*Original FlowTran Version 1.10 Pipe values
*
 number of nodes                   N          2
 axial position                    Z          520300,
567945,
 altitude                          ALT        609,
609,
 diameter                          DIAM
2.1030000E-01
 roughness                         RGHVAL
1.2000000E-05
 heat transfer coef                HFVAL
4.0000000E+00
 ground temp                       TFCVAL
3.0738000E+02
PIPE
Newman to Ilgarari_In
*Original FlowTran Version 1.10 Pipe values
*
 number of nodes                   N          82
 axial position                    Z          520300,
521317.89,  522335.78,
523353.67,  524371.56,
525389.46,  526407.32,
527425.23,  528443.12,  529461,
530478.89,  531496.78,
532514.67,  533532.56,
534550.46,  535568.32,
536586.23,  537604.12,  538622,
539639.89,  540657.78,
541675.67,  542693.56,
543711.46,  544729.32,
545747.23,  546765.12,  547783,
548800.89,  549818.78,
550836.67,  551854.56,
552872.46,  553890.32,
554908.23,  555926.12,  555944,
                                    557962,
558980.  559998.
                                    561016,
562034.02,  563051.98,
564070.01,  565088,  566106,
567123.89,  568141.78,
569159.67,  570177.56,
571195.46,  572213.32,
573231.23,  574249.12,  575267,
576284.89,  577302.78,
578320.67,  579338.56,
580356.46,  581374.32,
582392.23,  583410.12,  584428,
585445.89,  586463.78,
587481.67,  588499.56,
589517.46,  590535.32,
591553.23,  592571.12,  593589,
594606.89,  595624.79,
596642.65,  597660.57,
598678.44,  599696.33,
600714.22,  601732.11,  602750,
 altitude                          ALT        609,
608.987670898438,
608.975280761719,
608.963012695313,
608.95068359375,
608.938415527344,
608.926025390625,
608.91357421875,
608.901428222656,
608.888977050781,
608.876708984375,
608.864318847656,
608.851989746094,
608.839721679688,
608.827392578125,
608.815002441406,
608.802673339844,
608.790405273438,
608.778015136719,
608.765686035156,
608.75341796875,
608.741027832031,
608.728576660156,
608.716369628906,
608.703979492188,
608.69171142578l,
608.679382324219,
608.6669921875,
608.654724121094,
608.642272949219,
608.630004882813,
608.61767578125,
608.605285644531,
608.593017578125,
608.580688476563,
608.568420410156,
608.556030273438,
608.543701171875,
608.531372070313,
608.518981933594,
```

```
608.506713867188,
608.494384765625,
608.481994628906,
608.4697265625,
608.457397460938,
608.445007324219,
608.4326171875,
608.420104980469,
608.40771484375,
608.395324707031, 608.3828125,
608.370422363281,
608.35791015625,
608.345520019531,
608.3330078125,
608.320678710938,
608.308288574219,
608.296020507813,
608.28369140625,
608.271423339844,
608.258972167969,
608.246704101563, 608.234375,
608.221984863281,
608.209716796875,
608.197326660156.
608.184997558594.
608.172729492188.
608.160400390625,
608.147888183594.
608.135681152344.
608.123413085938.
608.111022949219,
608.098693847656,
608.08642578125,
608.073974609375,
608.061706542969,
608.04931640625,
608.036987304688,
608.024719238281,
608.012329101563. 608,
 diameter                        DIAM
3.4500000E 01
 roughness                       RGHVAL
9.0000000E 06
 heat transfer coef              HFVAL
4.0000000E+00
 ground temp                     TFCVAL
3.0653000E+02
PIPE
Ilgarari_In to Ilgarari
*Original FlowTran Version 1.10 Pipe values
*
*
 number of nodes                 N         2
 axial position                  Z          602750,
602800.
 altitude                        ALT        608.
608,
 diameter                        DIAM
3.4500000E 01
 roughness                       RGHVAL
0.0000000E+00
 heat transfer coef              HFVAL
4.0000000E+00
 ground temp                     TFCVAL
3.0653000E+02
PIPE
Ilgarari to Three_Rivers
*Original FlowTran Version 1.10 Pipe values
 number of nodes                 N         101
 axial position                  Z          602800,
603806.01, 604812.01,
605818.02, 606823.99,
607829.99, 608836, 609842,
610848.01, 611853.98,
612859.99, 613865.99, 614872,
                                            615878,
616884.01, 617890.02,
618896.02, 619901.99, 620908,
                                            621914,
622920.01, 623926.01,
624931.98, 625937.99,
626943.99, 627950, 628956,
629962.02, 630968.02,
631974.02, 632980, 633986,
                                            634992,
635997.98, 637003.98,
638009.98, 639016, 640022,
                                            641028,
642034, 643040.02,
644046.02, 645052.02, 646058,
                                            647064,
648070, 649075.98,
650081.98, 651087.98, 652094,
                                            653100,
654106, 655112,
                                            656118,
657124, 658130,
                                            659136,
660142, 661148,
                                            662154,
663160, 664166,
                                            665172,
666178, 667184,
                                            668190,
669196, 670202,
                                            671208,
672214, 673220,
                                            674226,
675232, 676238,
                                            677244,
678250, 679256,
                                            680262,
681268, 682274,
                                            683280,
684286, 685292,
                                            686298,
687304, 688310,
                                            689316,
690322, 691328,
                                            692334,
693340, 694346,
                                            695352,
696358, 697364,
                                            698370,
699376, 700382,
                                            701388,
702394, 703400,
 altitude                        ALT        608,
608, 608, 608, 608,
                                            608,
608, 608, 608, 608,
                                            608,
608, 608, 608, 608,
                                            608,
608, 608, 608, 608,
                                            608,
608, 608, 608, 608,
                                            608,
608, 608, 608, 608,
                                            608,
608, 608, 608, 608,
                                            608,
608, 608, 608, 608,
                                            608,
608, 608, 608, 608,
                                            608,
608, 608, 608, 608,
                                            608,
608, 608, 608, 608,
                                            608,
608, 608, 608, 608,
                                            608,
608, 608, 608, 608,
                                            608,
608, 608, 608, 608,
                                            608,
608, 608, 608, 608,
                                            608,
608, 608, 608, 608,
                                            608,
608, 608, 608, 608,
                                            608,
608, 608, 608, 608,
                                            608,
608, 608, 608, 608,
                                            608,
608, 608, 608, 608,
                                            608,
```

```
 diameter                          DIAM
3.4500000E 01
 roughness                         RGHVAL
0.0000000E+00
 heat transfer coef                HFVAL
4.0000000E+00
 ground temp                       TFCVAL
3.0628000E+02
PIPE
Three_Rivers to PlutonicT
*Original FlowTran Version 1.10 Pipe values
 number of nodes                   N          2
 axial position                    Z          703400,
703420,
 altitude                          ALT        608,
608,
 diameter                          DIAM
1.0470000E-01
 roughness                         RGHVAL
1.2000000E-05
 heat transfer coef                HFVAL
4.0000000E+00
 ground temp                       TFCVAL
3.0628000E+02
PIPE
Three_Rivers to Ned's_Creek
*Original FlowTran Version 1.10 Pipe values
 number of nodes                   N          37
 axial position                    Z          703400,
704413.89,  705427.78,

706441.67,  707455.56,

708469.44,  709483.33,

710497.22,  711511.11,  712525,

713538.89,  714552.78,

715566.67,  716580.56,

717594.44,  718608.33,

719622.22,  720636.11,  721650,

722663.89,  723677.8,

724691.69,  725705.56,

726719.44,  727733.31,

728747.2,  729761.11,  730775,

731788.9,  732802.8,  733816.66,

734830.56,  735844.45,

736858.35,  737872.2,  738886.1,
                                    739900,
 altitude                          ALT        608,
606.166625976563,

604.333374023438,  602.5,

600.666687011719,

598.833312988281,  597,

595.166687011719,

593.333312988281,  591.5,

589.666687011719,

587.833312988281,  586,

584.166687011719,

582.333312988281,  580.5,

578.666687011719,

576.833312988281,  575,

573.166687011719,

571.333374023438,  569.5,

567.666687011719,

565.833312988281,  564,

562.166625976563,

560.333312988281,  558.5,

556.666687011719,

554.833312988281,  553,

551.166687011719,

549.333312988281,  547.5,

545.666687011719,

543.833374023438,  542,
 diameter                          DIAM
3.4500000E-01
 roughness                         RGHVAL
8.0000000E-06
 heat transfer coef                HFVAL
4.0000000E+00
 ground temp                       TFCVAL
3.0628000E+02
PIPE
Ned's_Creek to Wiluna
*Original FlowTran Version 1.10 Pipe values
*
 number of nodes                   N          125
 axial position                    Z          739900,
740901.79,  741903.57,

742905.36,  743907.14,

744908.93,  745910.71,

746912.5,  747914.29,

748916.07,  749917.86,

750919.64,  751921.43,

752923.21,  753925,  754926.79,

755928.57,  756930.36,

757932.14,  758933.93,

759935.71,  760937.5,

761939.29,  762941.07,

763942.86,  764944.64,

765946.43,  766948.21,  767950,

768951.79,  769953.55,

770955.38,  771957.12,

772958.95,  773960.71,

774962.5,  775964.29,

776966.05,  777967.88,

778969.62,  779971.45,

780973.21,  781975,  782976.77,

783978.56,  784980.38,

785982.12,  786983.94,

787985.73,  788987.5,

789989.28,  790991.06,

791992.84,  792994.66,

793996.44,  794998.22,  796000,

797004.4,  798008.8,  799013.25,

800017.65,  801022.05,

802026.45,  803030.9,  804035.3,

805039.71,  806044.11,

807048.51,  808052.95,

809057.35,  810061.75,

811066.2,  812070.6,  813075,

814079.41,  815083.8,

816088.21,  817092.65,

818097.06,  819101.49,

820105.91,  821110.29,

822114.71,  823119.09,

824123.51,  825127.94,

826132.35,  827136.79,

828141.2,  829145.59,  830150,

831154.41,  832158.83,

833163.23,  834167.65,

835172.06,  836176.47,

837180.88,  838185.29,

839189.71,  840194.12,

841198.53,  842202.94,

843207.35,  844211.77,

845216.17,  846220.59,  847225,
```

848229.41, 849233.83,

850238.23, 851242.65,

852247.06, 853251.47,

854255.88, 855260.29,

856264.71, 857269.12,

858273.53, 859277.94,

860282.35, 861286.77,

862291.17, 863295.59, 864300,

altitude ALT 542,

542.517822265625,

543.035705566406,

543.553588867188,

544.071411132813,

544.589294433594,

545.107116699219, 545.625,

546.142883300781,

546.660705566406,

547.178588867188,

547.696411132813,

548.214294433594,

548.732116699219, 549.25,

549.767883300781,

550.285705566406,

550.803588867188,

551.321411132813,

551.839294433594,

552.357116699219, 552.875,

553.392883300781,

553.910705566406,

554.428588867188,

554.946411132813,

555.464294433594,

555.982177734375, 556.5,

557.017822265625,

557.535705566406,

558.053588867188,

558.571411132813,

559.089294433594,

559.607177734375, 560.125,

560.642822265625,

561.160705566406,

561.678588867188,

562.196411132813,

562.714294433594,

563.232177734375, 563.75,

564.267822265625,

564.785705566406,

565.303588867188,

565.821411132813,

566.339294433594,

566.857177734375, 567.375,

567.892822265625,

568.410705566406,

568.928588867188,

569.446411132813,

569.964294433594,

570.482177734375, 571,

570.058776855469,

569.117614746094,

568.176513671875,

567.235290527344,

566.294128417969,

565.352905273438,

564.411682128906,

563.470581054688,

562.529418945313,

561.588195800781,

560.64697265625,

559.705871582031,

558.764709472656,

557.823486328125,

556.882385253906,

555.941223144531, 555,

554.058776855469,

553.117614746094,

552.176513671875,

551.235290527344,

550.294128417969,

549.35302734375,

548.411804199219,

547.470581054688,

546.529418945313,

545.588195800781,

544.64697265625,

543.705871582031,

542.764709472656,

541.823486328125,

540.882385253906,

539.941223144531, 539,

538.058776855469,

537.11767578125,

536.176513671875,

535.235290527344,

534.294128417969,

533.35302734375,

532.411682128906,

531.470581054688,

530.529418945313,

529.588317871094,

528.64697265625,

527.705871582031,

526.764709472656,

525.823486328125,

524.88232421875,

523.941223144531, 523,

522.058776855469,

521.117614746094,

520.176513671875,

519.235290527344,

518.294128417969,

517.35302734375,

```
516.411682128906,

515.470581054688,

514.529418945313,

513.588317871094,

512.64697265625,

511.705902099609,

510.764709472656,

509.823486328125,

508.882385253906,

507.941192626953,  507,
 diameter                       DIAM
3.450000CE-01
 roughness                      RGHVAL
7.000000CE-06
 heat transfer coef             HFVAL
4.000000E+00
 ground temp                    TFCVAL
3.064300E+02
PIPE
Wiluna to Wil_JunT
*Original FlowTran Version 1.10 Pipe values
*
*
 number of nodes                N          2
 axial position                 Z          864300,
864320,
 altitude                       ALT        507,
507,
 diameter                       DIAM
2.100000E-01
 roughness                      RGHVAL
1.200000CE-05
 heat transfer coef             HFVAL
4.000000CE+00
 ground temp                    TFCVAL
3.045700E+02
PIPE
Wiluna to Mt_Keith
*Original FlowTran Version 1.10 Pipe values
 number of nodes                N          83
 axial position                 Z          864300,
865301.22,  866302.44,

867303.66,  868304.88,

869306.1,  870307.32,

871308.53,  872309.76,

873310.98,  874312.2,

875313.41,  876314.63,

877315.86,  878317.07,

879318.29,  880319.51,

881320.73,  882321.95,

883323.17,  884324.39,

885325.61,  886326.83,

887328.05,  888329.27,

889330.49,  890331.71,

891332.93,  892334.14,

893335.37,  894336.59,

895337.8,  896339.02,

897340.24,  898341.47,

899342.68,  900343.9,

901345.12,  902346.34,

903347.56,  904348.78,  905350,

906351.22,  907352.41,

908353.63,  909354.88,

910356.1,  911357.32,

912358.57,  913359.78,

914360.98,  915362.2,

916363.41,  917364.61,

918365.83,  919367.04,

920368.29,  921369.51,

922370.76,  923371.98,

924373.2,  925374.39,

926375.61,  927376.81,

928378.02,  929379.28,

930380.49,  931381.71,

932382.91,  933384.17,

934385.38,  935386.6,  936387.8,

937389.01,  938390.22,

939391.48,  940392.69,

941393.9,  942395.11,

943396.32,  944397.58,

945398.79,  946400,
 altitude                       ALT        507,
507.243896484375,

507.48779296875,

507.731689453125,

507.9755859375,

508.219512939453,

508.463409423828,

508.707305908203,

508.951202392578,

509.195098876953,

509.438995361328,

509.682891845703,

509.926788330078,

510.170684814453,

510.414611816406,

510.658508300781,

510.902404785156,

511.146392822266,

511.390289306641,

511.634185791016,

511.878112792969,

512.121887207031,

512.365783691406,

512.609680175781,

512.853576660156,

513.097473144531,

513.341369628906,

513.585327148438,

513.829223632813,

514.073181152344,

514.317077636719,

514.560974121094,

514.804870605469,

515.048828125,

515.292724609375,

515.53662109375,

515.780517578125,

516.0244140625,

516.268310546875,

516.51220703125,

516.756103515625,  517,

517.243896484375,

517.48779296875,

517.731689453125,

517.9755859375,

518.219482421875,
```

518.46337890625,

518.707275390625,

518.951171875,

519.195129394531,

519.439025878906,

519.682922363281,

519.926818847656,

520.170715332031,

520.414611816406,

520.658508300781,

520.902526855469,

521.146423339844,

521.390319824219,

521.634216308594,

521.878112792969,

522.121887207031,

522.365783691406,

522.609680175781,

522.853698730469,

523.097595214844,

523.341491699219,

523.585327148438,

523.829284667969,

524.073181152344,

524.317077636719,

524.560974121094,

524.804870605469,

525.048828125,

525.292724609375,

525.53662109375,

525.780517578125,

526.0244140625,

526.268310546875,

526.512207031250,

526.756103515625, 527,
 diameter DIAM
3.4500000E-01
 roughness RGHVAL
0.0000000E+00
 heat transfer coef HFVAL
4.0000000E+00
 ground temp TFCVAL
3.0457000E+02
PIPE
Mt_Keith to Mt_KeithT
*Original FlowTran Version 1.10 Pipe values
*
 number of nodes N 2
 axial position Z 946400,
954400,
 altitude ALT 527,
527,
 diameter DIAM
2.1030000E-01
 roughness RGHVAL
1.2000000E-05
 heat transfer coef HFVAL
4.0000000E+00
 ground temp TFCVAL
3.0457000E+02
PIPE
Mt_Keith to Leinster
*Original FlowTran Version 1.10 Pipe values
 number of nodes N 66
 axial position Z 946400,
947403.08, 948406.15,

949409.23, 950412.31,

951415.38, 952418.46,

953421.54, 954424.61,

955427.69, 956430.77,

957433.85, 958436.92, 959440,

960443.08, 961446.15,

962449.23, 963452.31,

964455.38, 965458.46,

966461.54, 967464.61,

968467.69, 969470.77,

970473.84, 971476.92, 972480,

973483.08, 974486.15,

975489.23, 976492.31,

977495.38, 978498.46,

979501.57, 980504.59,

981507.72, 982510.74,

983513.88, 984516.89,

985520.03, 986523.05,

987526.18, 988529.2,

989532.34, 990535.35,

991538.49, 992541.51,

993544.64, 994547.66,

995550.78, 996553.86,

997556.94, 998560.01,

999563.09, 1000566.2,

1001569.2, 1002572.3,

1003575.4, 1004578.5,

1005581.5, 1006584.6,

1007587.7, 1008590.8,

1009593.8, 1010596.9, 1011600,
 altitude ALT 527,
526.799987792969,

526.599975585938,

526.400024414063,

526.200012207031, 526,

525.799987792969,

525.599975585938,

525.400024414063,

525.200012207031, 525,

524.799987792969,

524.599975585938,

524.400024414063,

524.200012207031, 524,

523.799987792969,

523.599975585938,

523.400024414063,

523.200012207031, 523,

522.799987792969,

522.599975585938,

522.400024414063,

522.200012207031, 522,

521.799987792969,

521.599975585938,

521.400024414063,

521.200012207031, 521,

520.799987792969,

520.599975585938,

520.400024414063,

520.200012207031, 520,

519.799987792969,

```
519.599975585938,
519.400024414063,
519.200012207031,  519.
518.799987792969,
518.599975585938,
518.400024414063,
518.200012207031,  518.
517.799987792969,
517.599975585938,
517.400024414063,
517.200012207031,  517.
516.799987792969,
516.599975585938,
516.400024414063,
516.200012207031,  516.
515.799987792969,
515.599975585938,
515.400024414063,
515.200012207031,  515.
514.799987792969,
514.599975585938,
514.400024414063,
514.200012207031,  514.
 diameter                          DIAM
3.4500000E 01
 roughness                         RGHVAL
1.5000000E-05
 heat transfer coef                HFVAL
4.0000000E+00
 ground temp                       TFCVAL
3.0634000E-02
PIPE
Leinster to LeinsterT
*Original FlowTran Version 1.10 Pipe values
*
 number of nodes                   N          2
 axial position                    Z
1011600,  1016600,
 altitude                          ALT        514,
514,
 diameter                          DIAM
2.1030000E-01
 roughness                         RGHVAL
1.2000000E-05
 heat transfer coef                HFVAL
4.0000000E-00
 ground temp                       TFCVAL
3.0634000E-02
PIPE
Leinster to Anaconda
*Original FlowTran Version 1.10 Pipe values
*
 number of nodes                   N          131
 axial position                    Z
1011600,  1012607.1,  1013614.3,
1014621.4,  1015628.6,
1016635.7,  1017642.9,  1018650,
1019657.1,  1020664.3,
1021671.4,  1022678.6,
1023685.7,  1024692.9,  1025700,
1026707.1,  1027714.3,
1028721.4,  1029728.6,
1030735.7,  1031742.9,  1032750,
1033757.1,  1034764.3,
1035771.4,  1036778.6,
1037785.7,  1038792.9,  1039800,
1040807.1,  1041814.3,
1042821.4,  1043828.6,
1044835.7,  1045842.9,  1046850,
1047857.1,  1048864.3,
1049871.5,  1050878.6,
1051885.7,  1052892.9,  1053900,
1054907.1,  1055914.3,
1056921.4,  1057928.6,
1058935.7,  1059942.8,  1060950,
1061957.2,  1062964.3,
1063971.4,  1064978.6,
1065985.7,  1066992.8,  1068000,
1069007.1,  1070014.3,
1071021.4,  1072028.6,
1073035.7,  1074042.9,  1075050,
1076057.2,  1077064.3,
1078071.4,  1079078.5,
1080085.7,  1081092.8,  1082100,
1083111.7,  1084123.3,  1085135,
1086146.7,  1087158.4,  1088170,
1089181.7,  1090193.3,  1091205,
1092216.7,  1093228.3,  1094240,
1095251.6,  1096263.3,  1097275,
1098286.7,  1099298.4,  1100310,
1101321.7,  1102333.3,  1103345,
1104356.7,  1105368.3,  1106380,
1107391.7,  1108403.3,  1109415,
1110426.6,  1111438.3,  1112450,
1113461.7,  1114473.3,  1115485,
1116496.7,  1117508.3,  1118520,
1119531.7,  1120543.3,  1121555,
1122566.7,  1123578.3,  1124590,
1125601.7,  1126613.3,  1127625,
1128636.7,  1129648.3,  1130660,
1131671.7,  1132683.3,  1133695,
1134706.7,  1135718.3,  1136730,
1137741.7,  1138753.3,  1139765,
1140776.7,  1141788.3,  1142800,
 altitude                          ALT        514,
512.528625488281,
511.057189941406,
509.585693359375,
508.114288330078,
506.642913818359,
505.17138671875,
503.700012207031,
502.228607177734,
500.757110595703,
499.285705566406,
497.814300537109,
496.342803955078,
494.871398925781,
493.399993896484,
491.928588867188,
490.457092285156,
488.985687255859,
487.514312744141,
486.042907714844,
484.571411132813,
483.100006103516,
481.628601074219,
```

```
480.157196044922,
478.685699462891,
477.214294433594,
475.742889404297,
474.271392822266,
472.799987792969,
471.32861328125,
469.857086181641,
468.385711669922,
466.914306640625,
465.442810058594,
463.971405029297,  462.5,
461.028594970703,
459.557098388672,
458.085784912109,
456.614288330078,
455.142913818359,
453.67138671875,
452.200012207031,
450.728607177734,
449.257110595703,
447.785705566406,
446.314300537109,
444.842895507813,
443.371398925781,
441.899993896484,
440.428588867188,
438.957214355469,
437.485687255859,
436.014312744141,
434.542907714844,
433.071411132813,
431.600006103516,
430.128601074219,
428.657104492188,
427.185699462891,
425.714294433594,
424.242889404297,
422.771392822266,
421.299987792969,
419.82861328125,
418.357086181641,
416.885711669922,
415.414306640625,
413.942901611328,
412.471405029297,  411,
410.799987792969,
410.600006103516,
410.399993896484,
410.200012207031,  410,
409.799987792969,
409.600006103516,
409.399993896484,
409.200012207031,  409,
408.799987792969,
408.600006103516,
408.399993896484,
408.200012207031,  408,
407.799987792969,
407.600006103516,
407.399993896484,
407.200012207031,  407,
406.799987792969,
406.600006103516,
406.399993896484,
406.200012207031,  406,
405.799987792969,
405.600006103516,
405.399993896484,
405.200012207031,  405,
404.799987792969,
404.600006103516,
404.399993896484,
404.200012207031,  404,
403.799987792969,
403.600006103516,
403.399993896484,
403.200012207031,  403,
402.799987792969,
402.600006103516,
402.399993896484,
402.200012207031,  402,
401.799987792969,
401.600006103516,
401.399993896484,
401.200012207031,  401,
400.799987792969,
400.600006103516,
400.399993896484,
400.200012207031,  400,
399.799987792969,
399.600006103516,
399.399993896484,
399.200012207031,  399,
 diameter                        DIAM
3.45000006-01
 roughness                       RGHVAL
0.00000000E+00
 heat transfer coef              HFVAL
4.00000000E+00
 ground temp                     TFCVAL
3.06030006+02
PIPE
Anaconda to AnacondaT
*Original FlowTran Version 1.10 Pipe values
*
*
 number of nodes                 N          2
 axial position                  Z
1142800,  1142820,
 altitude                        ALT        399,
399,
 diameter                        DIAM
2.10300006-01
 roughness                       RGHVAL
1.20000006-05
 heat transfer coef              HFVAL
4.00000006+00
 ground temp                     TFCVAL
3.06030006+02
PIPE
Anaconda to Leonora
*Original FlowTran Version 1.10 Pipe values
*
*
 number of nodes                 N          12
```

```
 axial position                    Z
1142800,  1143809.1,  1144818.2,

1145827.3,  1146836.4,

1147845.5,  1148854.5,

1149863.6,  1150872.8,

1151881.8,  1152890.9,  1153900,
 altitude                          ALT         399,
398.818206787109,

398.636413574219,

398.454498291016,

398.272705078125,

398.090911865234,

397.909088134766,

397.727294921875,

397.545501708984,

397.363586425781,

397.181793212891,  397,
 diameter                          DIAM
3.4500000E 01
 roughness                         RGHVAL
1.7600000E-03
 heat transfer coef                HFVAL
4.0000000E+00
 ground temp                       TFCVAL
3.0600000E+02
PIPE
Leonora to Jeedamya
*Original FlowTran Version 1.10 Pipe values
 number of nodes                   N           52
 axial position                    Z
1153900,  1154905.9,  1155911.8,

1156917.6,  1157923.5,

1158929.4,  1159935.3,

1160941.2,  1161947.1,

1162952.9,  1163958.8,

1164964.7,  1165970.6,

1166976.5,  1167982.4,

1168988.2,  1169994.1,  1171000,

1172005.9,  1173011.8,

1174017.6,  1175023.5,

1176029.4,  1177035.3,

1178041.2,  1179047.1,

1180052.9,  1181058.9,

1182064.7,  1183070.6,

1184076.4,  1185082.4,

1186088.2,  1187094.2,  1188100,

1189105.9,  1190111.7,

1191117.7,  1192123.5,

1193129.4,  1194135.3,

1195141.2,  1196147.1,  1197153,

1198158.8,  1199164.7,

1200170.6,  1201176.5,

1202182.4,  1203188.2,

1204194.1,  1205200,
 altitude                          ALT         397,
397.019592285156,

397.039215087891,

397.058807373047,

397.078399658203,

397.097991943359,

397.117614746094,

397.13720703125,

397.156890869141,

397.176513671875,

397.196105957031,

397.215698242188,

397.235290527344,

397.254913330078,

397.274505615234,

397.294097900391,

397.313690185547,

397.333312988281,

397.352905273438,

397.372589111328,

397.392211914063,

397.411712646484,

397.431396484375,

397.450988769531,

397.470611572266,

397.490203857422,

397.509796142578,

397.529388427734,

397.549011230469,

397.568603515625,

397.588195800781,

397.607788085938,

397.627410888672,

397.647094726563,

397.666687011719,

397.686309814453,

397.705902099609,

397.725494384766,

397.745086669922,

397.764709472656,

397.784301757813,

397.803894042969,

397.823486328125,

397.843109130859,

397.86279296875,

397.882385253906,

397.902008056641,

397.921600341797,

397.941192626953,

397.960784912109,

397.980407714844,  398,
 diameter                          DIAM
3.4500000E-01
 roughness                         RGHVAL
0.0000000E-00
 heat transfer coef                HFVAL
4.0000000E-00
 ground temp                       TFCVAL
3.0572000E-02
PIPE
Jeedamya to Cawse
*
*
 number of nodes                   N           112
 axial position                    Z
1205200,  1206209.8,  1207219.6,

1208229.3,  1209239.1,

1210248.9,  1211258.7,

1212268.5,  1213278.3,  1214288,

1215297.8,  1216307.6,

1217317.4,  1218327.2,  1219337,

1220346.7,  1221356.5,

1222366.3,  1223376.1,
```

1224385.9, 1225395.7,

1226405.4, 1227415.2, 1228425,

1229434.8, 1230444.6,

1231454.3, 1232464.1,

1233473.9, 1234483.7,

1235493.5, 1236503.3, 1237513,

1238522.8, 1239532.6,

1240542.4, 1241552.2, 1242562,

1243571.7, 1244581.5,

1245591.3, 1246601.1,

1247610.9, 1248620.7,

1249630.4, 1250640.2, 1251650,

1252659.8, 1253669.6,

1254679.3, 1255689.1,

1256698.9, 1257708.7,

1258718.5, 1259728.2,

1260738.1, 1261747.8,

1262757.6, 1263767.4,

1264777.2, 1265786.9,

1266796.8, 1267806.5,

1268816.3, 1269826.1,

1270835.9, 1271845.7,

1272855.4, 1273865.2, 1274875,

1275884.8, 1276894.6,

1277904.3, 1278914.1,

1279923.9, 1280933.7,

1281943.5, 1282953.2,

1283963.1, 1284972.8,

1285982.6, 1286992.4,

1288002.2, 1289012, 1290021.8,

1291031.5, 1292041.3,

1293051.1, 1294060.9,

1295070.7, 1296080.4,

1297090.2, 1298100, 1299115.3,

1300130.5, 1301145.8, 1302161,

1303176.3, 1304191.6,

1305206.8, 1306222.1,

1307237.4, 1308252.6,

1309267.9, 1310283.2,

1311298.4, 1312313.7,

1313328.9, 1314344.2,

1315359.5, 1316374.7, 1317390,

altitude ALT 398,

398.146789550781,

398.293487548828,

398.440185546875,

398.5869140625,

398.733703613281,

398.880401611328,

399.027191162109,

399.173889160156,

399.320587158203,

399.467407226563,

399.614105224609,

399.760894775391,

399.907592773438,

400.054412841797,

400.201110839844,

400.347808837891,

400.494598388672,

400.641296386719,

400.7880859375,

400.934814453125,

401.081512451172,

401.228302001953, 401.375,

401.521697998047,

401.668487548828,

401.815185546875,

401.9619140625,

402.108703613281,

402.255401611328,

402.402191162109,

402.548889160156,

402.695587158203,

402.842407226563,

402.989105224609,

403.135894775391,

403.282592773438,

403.429290771484,

403.576110839844,

403.722808837891,

403.869598388672,

404.016296386719,

404.162994384766,

404.309814453125,

404.456512451172,

404.603302001953, 404.75,

404.896697998047,

405.043487548828,

405.190185546875,

405.337005615234,

405.483703613281,

405.630401611328,

405.777191162109,

405.923889160156,

406.070709228516,

406.217407226563,

406.364105224609,

406.510894775391,

406.657592773438,

406.804290771484,

406.951110839844,

407.097808837891,

407.244598388672,

407.391296386719,

407.5380859375,

407.684814453125,

407.831512451172,

407.978210449219, 408.125,

408.271789550781,

408.418487548828,

```
408.565185546875,
408.7119140625,
408.858703613281,
409.005401611328,
409.152191162109,
409.298889160156,
409.445709228516,
409.592407226563,
409.739196777344,
409.885803222656,
410.032592773438,
410.179412841797,
410.326110839844,
410.472808837891,
410.619598388672,
410.766296386719,
410.9130859375,
411.059814453125,
411.206512451172,
411.353210449219,  411.5,
411.578887939453,
411.657897949219,
411.736785888672,
411.815795898438,
411.894714355469,
411.973693847656,
412.052612304688,
412.131591796875,
412.210510253906,
412.289489746094,
412.368408203125,
412.447387695313,
412.526306152344,
412.605285644531,
412.684204101563,
412.763214111328,
412.842102050781,
412.921112060547,  413,
 diameter                        DIAM
3.4500000E 01
 roughness                       RGHVAL
3.0000000E-06
 heat transfer coef              HFVAL
4.0000000E-00
 ground temp                     TFCVAL
2.9958000E-02
PIPE
Cawse to CawseT
*Original FlowTran Version 1.10 Pipe values
*
*
 number of nodes                 N          2
 axial position                  Z
1317390,  1317410,
 altitude                        ALT        413,
413,
 diameter                        DIAM
1.5000000E-01
 roughness                       RGHVAL
1.2000000E-05
 heat transfer coef              HFVAL
4.0000000E+00
 ground temp                     TFCVAL
2.9958000E+02
PIPE
Cawse to Kal_North
*Original FlowTran Version 1.10 Pipe values
*
 number of nodes                 N          38
 axial position                  Z
1317390,  1318409.2,  1319428.4,
1320447.6,  1321466.8,
1322485.9,  1323505.1,
1324524.3,  1325543.5,
1326562.7,  1327581.9,
1328601.1,  1329620.3,
1330639.5,  1331658.6,
1332677.8,  1333697,  1334716.2,
1335735.4,  1336754.6,
1337773.8,  1338793,  1339812.2,
1340831.4,  1341850.5,
1342869.7,  1343888.9,
1344908.1,  1345927.3,
1346946.5,  1347965.7,
1348984.8,  1350004.1,
1351023.3,  1352042.4,
1353061.6,  1354080.8,  1355100,
 altitude                        ALT        413,
412.297302246094,
411.594604492188,
410.891906738281,
410.189208984375,
409.486511230469,
408.783813476563,
408.081085205078,
407.378387451172,
406.675689697266,
405.972991943359,
405.270294189453,
404.567596435547,
403.864898681641,
403.162200927734,
402.459503173828,
401.756805419922,
401.054107666016,
400.351409912109,
399.648590087891,
398.946014404297,
398.243286132813,
397.540496826172,
396.837799072266,
396.135101318359,
395.432403564453,
394.729705810547,
394.027008056641,
393.324310302734,
392.621612548828,
391.918914794922,
391.216186523438,
390.513488769531,
389.810791015625,
389.108093261719,
388.405395507813,
387.702697753906,  387,
 diameter                        DIAM
3.4500000E-01
 roughness                       RGEVAL
5.4000000E-05
 heat transfer coef              HFVAL
4.0000000E+00
```

```
 ground temp                          TFCVAL
2.9958000E+02
PIPE
Kal_North to Kal_NorthT
*Original FlowTran Version 1.10 Pipe values
*
 number of nodes                      N          2
 axial position                       Z
1355100,  1363100,
 altitude                             ALT        387,
387.
 diameter                             DIAM
2.1030000E-01
 roughness                            RGHVAL
1.2000000E 05
 heat transfer coef                   HFVAL
4.0000000E+00
 ground temp                          TFCVAL
2.9958000E+02
PIPE
Kal_North to Kal_West
*Original FlowTran Version 1.10 Pipe values
 number of nodes                      N          12
 axial position                       Z
1355100,  1356136.4,  1357172.7,

1358209.1,  1359245.5,

1360281.8,  1361318.1,

1362354.5,  1363390.9,

1364427.3,  1365463.6,  1366500,
 altitude                             ALT        387,
386.090911865234,

385.181793212891,

384.272705078125,

383.363586425781,

382.454498291016,

381.545501708984,

380.636413574219,

379.727294921875,

378.818206787109,

377.909088134766,  377,
 diameter                             DIAM
3.4500000E 01
 roughness                            RGHVAL
0.0000000E+00
 heat transfer coef                   HFVAL
4.0000000E+00
 ground temp                          TFCVAL
3.0043000E+02
PIPE
Kal_West to Kal_SouthT
*Original FlowTran Version 1.10 Pipe values
*
 number of nodes                      N          2
 axial position                       Z
1366500,  1377680,
 altitude                             ALT        377,
354,
 diameter                             DIAM
3.4500000E-01
 roughness                            RGHVAL
1.2000000E-05
 heat transfer coef                   HFVAL
4.0000000E+00
 ground temp                          TFCVAL
3.0043000E+02
DEVICE
Inpipe1003
 in pipe type - valve                 IPDTYP     1
 pipe containing valve                IPIPE      3
 segment in this pipe                 ISEG       1
 valve type                           IVTYP      2
 valve initial state                  LMODV      1
 time to start closing                TSCLV
1.0000000E-09
 inlet p to trigger close             PINCL
0.0000000E-00
 dPin/dt to trig closing              PIRCL
1.0000000E-09
 pressure to trigger closing          PVOS
1.0000000E-09
     in pipe                          IPIPV      1
     node # from start of pipe        INODE      1
 time interval to close               DTVCL
1.2000000E-03
 time to start opening                TSOPV
1.0000000E-09
 Pin to trigger opening               PINOP
1.0000000E-09
 Pout to trigger opening              POUTOP
0.0000000E-00
 dPin/dt to trig opening              PIROP      -
1.0000000E-09
 dPout/dt to trig opening             POROP
1.0000000E-09
 time interval to open                DTVOP
1.2000000E-03
DEVICE
Inpipe1004
 in pipe type   valve                 IPDTYP     1
 pipe containing valve                IPIPE      4
 segment in this pipe                 ISEG       1
 valve type                           IVTYP      2
 valve initial state                  LMODV      1
 time to start closing                TSCLV
1.0000000E+09
 inlet p to trigger close             PINCL
0.0000000E+00
 dPin/dt to trig closing              PIRCL
1.0000000E+09
 pressure to trigger closing          PVOS
1.0000000E+09
     in pipe                          IPIPV      1
     node # from start of pipe        INODE      1
 time interval to close               DTVCL
1.2000000E+03
 time to start opening                TSOPV
1.0000000E+09
 Pin to trigger opening               PINOP
1.0000000E+09
 Pout to trigger opening              POUTOP
0.0000000E+00
 dPin/dt to trig opening              PIROP      -
1.0000000E+09
 dPout/dt to trig opening             POROP
1.0000000E+09
 time interval to open                DTVOP
1.2000000E+03
DEVICE
Inpipe1005
 in pipe type - valve                 IPDTYP     1
 pipe containing valve                IPIPE      5
 segment in this pipe                 ISEG       1
 valve type                           IVTYP      2
 valve initial state                  LMODV      1
 time to start closing                TSCLV
1.0000000E+09
 inlet p to trigger close             PINCL
0.0000000E-00
 dPin/dt to trig closing              PIRCL
1.0000000E-09
 pressure to trigger closing          PVOS
1.0000000E-09
     in pipe                          IPIPV      1
     node # from start of pipe        INODE      1
 time interval to close               DTVCL
1.2000000E+03
 time to start opening                TSOPV
1.0000000E+09
 Pin to trigger opening               PINOP
1.0000000E+09
 Pout to trigger opening              POUTOP
0.0000000E+00
 dPin/dt to trig opening              PIROP      -
1.0000000E+09
 dPout/dt to trig opening             POROP
1.0000000E+09
 time interval to open                DTVOP
1.2000000E+03
DEVICE
Inpipe1006
*Original FlowTran Version 1.31 In Pipe Control
values
 in pipe type - valve                 IPDTYP     1
 pipe containing valve                IPIPE      6
 segment in this pipe                 ISEG       1
 valve type                           IVTYP      2
 valve initial state                  LMODV      1
 time to start closing                TSCLV
1.0000000E+09
 inlet p to trigger close             PINCL
0.0000000E+00
 dPin/dt to trig closing              PIRCL
1.0000000E+09
 pressure to trigger closing          PVOS
1.0000000E+09
     in pipe                          IPIPV      1
     node # from start of pipe        INODE      1
 time interval to close               DTVCL
1.2000000E+03
 time to start opening                TSOPV
1.0000000E+09
 Pin to trigger opening               PINOP
1.0000000E+09
 Pout to trigger opening              POUTOP
0.0000000E+00
 dPin/dt to trig opening              PIROP      -
1.0000000E+09
 dPout/dt to trig opening             POROP
1.0000000E+09
 time interval to open                DTVOP
1.2000000E+03
DEVICE
Inpipe1007
 in pipe type   valve                 IPDTYP     1
 pipe containing valve                IPIPE      7
 segment in this pipe                 ISEG       1
 valve type                           IVTYP      2
 valve initial state                  LMODV      1
 time to start closing                TSCLV
1.0000000E+09
 inlet p to trigger close             PINCL
0.0000000E+00
 dPin/dt to trig closing              PIRCL
1.0000000E+09
 pressure to trigger closing          PVOS
1.0000000E+09
     in pipe                          IPIPV      1
```

```
     node # from start of pipe     INODE      1
 time interval to close            DTVCL
1.2000000E-03
 time to start opening             TSOPV
1.0000000E-09
 Pin to trigger opening            PINOP
1.0000000E-09
 Pout to trigger opening           POUTOP
0.0000000E-00
 dPin/dt to trig opening           PIROP      -
1.0000000E-09
 dPout/dt to trig opening          POROP
1.0000000E-09
 time interval to open             DTVOP
1.2000000E+03
DEVICE
Inpipe1008
*Original FlowTran Version 1.31 In-Pipe Control
values
 in pipe type - valve              IPDTYP     1
 pipe containing valve             IPIPE      8
 segment in this pipe              ISEG       1
 valve type                        IVTYP      2
 valve initial state               LMODV      1
 time to start closing             TSCLV
1.0000000E+09
 inlet p to trigger close          PINCL
0.0000000E+00
 dPin/dt to trig closing           PIRCL
1.0000000E+09
 pressure to trigger closing       PVOS
1.0000000E+09
     in pipe                       IPIPV      1
     node # from start of pipe     INODE      1
 time interval to close            DTVCL
1.2000000E+03
 time to start opening             TSOPV
1.0000000E+09
 Pin to trigger opening            PINOP
1.0000000E+09
 Pout to trigger opening           POUTOP
0.0000000E+00
 dPin/dt to trig opening           PIROP      -
1.0000000E+09
 dPout/dt to trig opening          POROP
1.0000000E+09
 time interval to open             DTVOP
1.2000000E+03
DEVICE
Inpipe1009
 in pipe type - valve              IPDTYP     1
 pipe containing valve             IPIPE      9
 segment in this pipe              ISEG       1
 valve type                        IVTYP      2
 valve initial state               LMODV      1
 time to start closing             TSCLV
1.0000000E+09
 inlet p to trigger close          PINCL
0.0000000E+00
 dPin/dt to trig closing           PIRCL
1.0000000E+09
 pressure to trigger closing       PVOS
1.0000000E+09
     in pipe                       IPIPV      1
     node # from start of pipe     INODE      1
 time interval to close            DTVCL
1.2000000E+03
 time to start opening             TSOPV
1.0000000E+09
 Pin to trigger opening            PINOP
1.0000000E+09
 Pout to trigger opening           POUTOP
0.0000000E+00
 dPin/dt to trig opening           PIROP      -
1.0000000E+09
 dPout/dt to trig opening          POROP
1.0000000E+09
 time interval to open             DTVOP
1.2000000E+03
DEVICE
Inpipe1010
*Original FlowTran Version 1.31 In-Pipe Control
values
 in pipe type - valve              IPDTYP     1
 pipe containing valve             IPIPE      10
 segment in this pipe              ISEG       1
 valve type                        IVTYP      2
 valve initial state               LMODV      1
 time to start closing             TSCLV
1.0000000E+09
 inlet p to trigger close          PINCL
0.0000000E+00
 dPin/dt to trig closing           PIRCL
1.0000000E+09
 pressure to trigger closing       PVOS
1.0000000E+09
     in pipe                       IPIPV      1
     node # from start of pipe     INODE      1
 time interval to close            DTVCL
1.2000000E+03
 time to start opening             TSOPV
1.0000000E+09
 Pin to trigger opening            PINOP
1.0000000E+09
 Pout to trigger opening           POUTOP
0.0000000E+00
 dPin/dt to trig opening           PIROP      -
1.0000000E+09
 dPout/dt to trig opening          POROP
1.0000000E+09
 time interval to open             DTVOP
1.2000000E+03
DEVICE
Inpipe1011
 in pipe type - valve              IPDTYP     1
 pipe containing valve             IPIPE      11
 segment in this pipe              ISEG       1
 valve type                        IVTYP      2
 valve initial state               LMODV      1
 time to start closing             TSCLV
1.0000000E+09
 inlet p to trigger close          PINCL
0.0000000E+00
 dPin/dt to trig closing           PIRCL
1.0000000E+09
 pressure to trigger closing       PVOS
1.0000000E+09
     in pipe                       IPIPV      1
     node # from start of pipe     INODE      1
 time interval to close            DTVCL
1.2000000E+03
 time to start opening             TSOPV
1.0000000E+09
 Pin to trigger opening            PINOP
1.0000000E+09
 Pout to trigger opening           POUTOP
0.0000000E+00
 dPin/dt to trig opening           PIROP      -
1.0000000E+09
 dPout/dt to trig opening          POROP
1.0000000E+09
 time interval to open             DTVOP
1.2000000E+03
DEVICE
Inpipe1012
 in pipe type - valve              IPDTYP     1
 pipe containing valve             IPIPE      12
 segment in this pipe              ISEG       1
 valve type                        IVTYP      2
 valve initial state               LMODV      1
 time to start closing             TSCLV
1.0000000E+09
 inlet p to trigger close          PINCL
0.0000000E+00
 dPin/dt to trig closing           PIRCL
1.0000000E+09
 pressure to trigger closing       PVOS
1.0000000E+09
     in pipe                       IPIPV      1
     node # from start of pipe     INODE      1
 time interval to close            DTVCL
1.2000000E+03
 time to start opening             TSOPV
1.0000000E+09
 Pin to trigger opening            PINOP
1.0000000E+09
 Pout to trigger opening           POUTOP
0.0000000E+00
 dPin/dt to trig opening           PIROP
1.0000000E+09
 dPout/dt to trig opening          POROP
1.0000000E+09
 time interval to open             DTVOP
1.2000000E+03
DEVICE
Inpipe1013
*Original FlowTran Version 1.31 In-Pipe Control
values
 in pipe type - valve              IPDTYP     1
 pipe containing valve             IPIPE      13
 segment in this pipe              ISEG       1
 valve type                        IVTYP      2
 valve initial state               LMODV      1
 time to start closing             TSCLV
1.0000000E-09
 inlet p to trigger close          PINCL
0.0000000E-00
 dPin/dt to trig closing           PIRCL
1.0000000E-09
 pressure to trigger closing       PVOS
1.0000000E-09
     in pipe                       IPIPV      1
     node # from start of pipe     INODE      1
 time interval to close            DTVCL
1.2000000E+03
 time to start opening             TSOPV
1.0000000E+09
 Pin to trigger opening            PINOP
1.0000000E+09
 Pout to trigger opening           POUTOP
0.0000000E+00
 dPin/dt to trig opening           PIROP      -
1.0000000E+09
 dPout/dt to trig opening          POROP
1.0000000E+09
 time interval to open             DTVOP
1.2000000E+03
DEVICE
Inpipe1014
 in pipe type - valve              IPDTYP     1
 pipe containing valve             IPIPE      14
 segment in this pipe              ISEG       1
 valve type                        IVTYP      2
 valve initial state               LMODV      1
 time to start closing             TSCLV
1.0000000E+09
 inlet p to trigger close          PINCL
0.0000000E+00
 dPin/dt to trig closing           PIRCL
1.0000000E+09
```

```
 pressure to trigger closing      PVOS
1.0000000E+09
     in pipe                      IPIPV     1
     node # from start of pipe    INODE     1
 time interval to close           DTVCL
1.2000000E+03
 time to start opening            TSOPV
1.0000000E+09
 Pin to trigger opening           PINOP
1.0000000E+09
 Pout to trigger opening          POUTOP
0.0000000E+00
 dPin/dt to trig opening          PIROP
1.0000000E+09
 dPout/dt to trig opening         POROP
1.0000000E+09
 time interval to open            DTVOP
1.2000000E+03
DEVICE
Inpipe1015
*Original FlowTran Version 1.31 In-Pipe Control
values
 in pipe type - valve             IPDTYP    1
 pipe containing valve            IPIPE      15
 segment in this pipe             ISEG       1
 valve type                       IVTYP     2
 valve initial state              LMODV     1
 time to start closing            TSCLV
1.0000000E+09
 inlet p to trigger close         PINCL
0.0000000E+00
 dPin/dt to trig closing          PIRCL
1.0000000E+09
 pressure to trigger closing      PVCS
1.0000000E+09
     in pipe                      IPIPV     1
     node # from start of pipe    INODE     1
 time interval to close           DTVCL
1.2000000E+03
 time to start opening            TSOPV
1.0000000E+09
 Pin to trigger opening           PINOP
1.0000000E+09
 Pout to trigger opening          POUTOP
0.0000000E+00
 dPin/dt to trig opening          PIROP
1.0000000E+09
 dPout/dt to trig opening         POROP
1.0000000E+09
 time interval to open            DTVOP
1.2000000E+03
DEVICE
Inpipe1016
 in pipe type - valve             IPDTY2    1
 pipe containing valve            IPIPE      16
 segment in this pipe             ISEG       1
 valve type                       IVTYP     2
 valve initial state              LMODV     1
 time to start closing            TSCLV
1.0000000E+09
 inlet p to trigger close         PINCL
0.0000000E+00
 dPin/dt to trig closing          PIRCL
1.0000000E+09
 pressure to trigger closing      PVCS
1.0000000E+09
     in pipe                      IPIPV     1
     node # from start of pipe    INODE     1
 time interval to close           DTVCL
1.2000000E+03
 time to start opening            TSOPV
1.0000000E+09
 Pin to trigger opening           PINOP
1.0000000E+09
 Pout to trigger opening          POUTOP
0.0000000E+00
 dPin/dt to trig opening          PIROP
1.0000000E+09
 dPout/dt to trig opening         POROP
1.0000000E+09
 time interval to open            DTVOP
1.2000000E+03
DEVICE
Inpipe1017
*Original FlowTran Version 1.31 In-Pipe Control
values
 in pipe type - valve             IPDTYP    1
 pipe containing valve            IPIPE      17
 segment in this pipe             ISEG       1
 valve type                       IVTYP     2
 valve initial state              LMODV     1
 time to start closing            TSCLV
1.0000000E+09
 inlet p to trigger close         PINCL
0.0000000E+00
 dPin/dt to trig closing          PIRCL
1.0000000E+09
 pressure to trigger closing      PVCS
1.0000000E+09
     in pipe                      IPIPV     1
     node # from start of pipe    INODE     1
 time interval to close           DTVCL
1.2000000E+03
 time to start opening            TSOPV
1.0000000E+09
 Pin to trigger opening           PINOP
1.0000000E+09
 Pout to trigger opening          POUTOP
0.0000000E+00
 dPin/dt to trig opening          PIROP      -
1.0000000E+09
 dPout/dt to trig opening         POROP
1.0000000E+09
 time interval to open            DTVOP
1.2000000E+03
DEVICE
Inpipe1018
 in pipe type - valve             IPDTYP    1
 pipe containing valve            IPIPE      18
 segment in this pipe             ISEG       1
 valve type                       IVTYP     2
 valve initial state              LMODV     1
 time to start closing            TSCLV
1.0000000E+09
 inlet p to trigger close         PINCL
0.0000000E+00
 dPin/dt to trig closing          PIRCL
1.0000000E+09
 pressure to trigger closing      PVOS
1.0000000E+09
     in pipe                      IPIPV     1
     node # from start of pipe    INODE     1
 time interval to close           DTVCL
1.2000000E+03
 time to start opening            TSOPV
1.0000000E+09
 Pin to trigger opening           PINOP
1.0000000E+09
 Pout to trigger opening          POUTOP
0.0000000E+00
 dPin/dt to trig opening          PIROP      -
1.0000000E+09
 dPout/dt to trig opening         POROP
1.0000000E+09
 time interval to open            DTVOP
1.2000000E+03
DEVICE
Inpipe1019
*Original FlowTran Version 1.31 In-Pipe Control
values
 in pipe type - valve             IPDTYP    1
 pipe containing valve            IPIPE      19
 segment in this pipe             ISEG       1
 valve type                       IVTYP     2
 valve initial state              LMODV     1
 time to start closing            TSCLV
1.0000000E+09
 inlet p to trigger close         PINCL
0.0000000E+00
 dPin/dt to trig closing          PIRCL
1.0000000E+09
 pressure to trigger closing      PVOS
1.0000000E+09
     in pipe                      IPIPV     1
     node # from start of pipe    INODE     1
 time interval to close           DTVCL
1.2000000E+03
 time to start opening            TSOPV
1.0000000E+09
 Pin to trigger opening           PINOP
1.0000000E+09
 Pout to trigger opening          POUTOP
0.0000000E+00
 dPin/dt to trig opening          PIROP      -
1.0000000E+09
 dPout/dt to trig opening         POROP
1.0000000E+09
 time interval to open            DTVOP
1.2000000E+03
DEVICE
Inpipe1020
 in pipe type - valve             IPDTYP    1
 pipe containing valve            IPIPE      20
 segment in this pipe             ISEG       1
 valve type                       IVTYP     2
 valve initial state              LMODV     1
 time to start closing            TSCLV
1.0000000E+09
 inlet p to trigger close         PINCL
0.0000000E+00
 dPin/dt to trig closing          PIRCL
1.0000000E+09
 pressure to trigger closing      PVOS
1.0000000E+09
     in pipe                      IPIPV     1
     node # from start of pipe    INODE     1
 time interval to close           DTVCL
1.2000000E+03
 time to start opening            TSOPV
1.0000000E+09
 Pin to trigger opening           PINOP
1.0000000E+09
 Pout to trigger opening          POUTOP
0.0000000E+00
 dPin/dt to trig opening          PIROP
1.0000000E+09
 dPout/dt to trig opening         POROP
1.0000000E+09
 time interval to open            DTVOP
1.2000000E+03
DEVICE
Inpipe1021
 in pipe type - valve             IPDTYP    1
 pipe containing valve            IPIPE      21
 segment in this pipe             ISEG       1
 valve type                       IVTYP     2
 valve initial state              LMODV     1
 time to start closing            TSCLV
1.0000000E+09
```

```
 inlet p to trigger close          PINCL
0.0000000E+00
 dPin/dt to trig closing           PIRCL
1.0000000E+09
 pressure to trigger closing       PVOS
1.0000000E+09
      in pipe                      IPIPV     1
      node # from start of pipe    INODE     1
 time interval to close            DTVCL
1.2000000E+03
 time to start opening             TSOPV
1.0000000E+09
 Pin to trigger opening            PINOP
1.0000000E+09
 Pout to trigger opening           POUTOP
0.0000000E+00
 dPin/dt to trig opening           PIROP
1.0000000E+09
 dPout/dt to trig opening          POROP
1.0000000E+09
 time interval to open             DTVOP
1.2000000E+03
DEVICE
Inpipe1022
 in pipe type   valve              IPDTYP    1
 pipe containing valve             IPIPE      22
 segment in this pipe              ISEG       1
 valve type                        IVTYP     2
 valve initial state               LMODV     1
 time to start closing             TSCLV
1.0000000E+09
 inlet p to trigger close          PINCL
0.0000000E+00
 dPin/dt to trig closing           PIRCL
1.0000000E+09
 pressure to trigger closing       PVOS
1.0000000E+09
      in pipe                      IPIPV     1
      node # from start of pipe    INODE     1
 time interval to close            DTVCL
1.2000000E+03
 time to start opening             TSOPV
1.0000000E+09
 Pin to trigger opening            PINOP
1.0000000E+09
 Pout to trigger opening           POUTOP
0.0000000E+00
 dPin/dt to trig opening           PIROP     -
1.0000000E+09
 dPout/dt to trig opening          POROP
1.0000000E+09
 time interval to open             DTVOP
1.2000000E+03
DEVICE
Inpipe1023
*Original FlowTran Version 1.31 In-Pipe Control
values
 in pipe type   valve              IPDTYP    1
 pipe containing valve             IPIPE      23
 segment in this pipe              ISEG       1
 valve type                        IVTYP     2
 valve initial state               LMODV     1
 time to start closing             TSCLV
1.0000000E-09
 inlet p to trigger close          PINCL
0.0000000E-00
 dPin/dt to trig closing           PIRCL
1.0000000E+09
 pressure to trigger closing       PVOS
1.0000000E-09
      in pipe                      IPIPV     1
      node # from start of pipe    INODE     1
 time interval to close            DTVCL
1.2000000E+03
 time to start opening             TSOPV
1.0000000E+09
 Pin to trigger opening            PINOP
1.0000000E+09
 Pout to trigger opening           POUTOP
0.0000000E+00
 dPin/dt to trig opening           PIROP     -
1.0000000E+09
 dPout/dt to trig opening          POROP
1.0000000E+09
 time interval to open             DTVOP
1.2000000E+03
DEVICE
Inpipe1024
 in pipe type - valve              IPDTYP    1
 pipe containing valve             IPIPE      24
 segment in this pipe              ISEG       1
 valve type                        IVTYP     2
 valve initial state               LMODV     1
 time to start closing             TSCLV
1.0000000E+09
 inlet p to trigger close          PINCL
0.0000000E+00
 dPin/dt to trig closing           PIRCL
1.0000000E+09
 pressure to trigger closing       PVOS
1.0000000E+09
      in pipe                      IPIPV     1
      node # from start of pipe    INODE     1
 time interval to close            DTVCL
1.2000000E+03
 time to start opening             TSOPV
1.0000000E+09
 Pin to trigger opening            PINOP
1.0000000E+09
 Pout to trigger opening           POUTOP
0.0000000E+00
 dPin/dt to trig opening           PIROP     -
1.0000000E+09
 dPout/dt to trig opening          POROP
1.0000000E+09
 time interval to open             DTVOP
1.2000000E+03
DEVICE
Inpipe1025
*Original FlowTran Version 1.31 In-Pipe Control
values
 in pipe type - valve              IPDTYP    1
 pipe containing valve             IPIPE      25
 segment in this pipe              ISEG       1
 valve type                        IVTYP     2
 valve initial state               LMODV     1
 time to start closing             TSCLV
1.0000000E-09
 inlet p to trigger close          PINCL
0.0000000E-00
 dPin/dt to trig closing           PIRCL
1.0000000E+09
 pressure to trigger closing       PVOS
1.0000000E+09
      in pipe                      IPIPV     1
      node # from start of pipe    INODE     1
 time interval to close            DTVCL
1.2000000E+03
 time to start opening             TSOPV
1.0000000E+09
 Pin to trigger opening            PINOP
1.0000000E+09
 Pout to trigger opening           POUTOP
0.0000000E+00
 dPin/dt to trig opening           PIROP     -
1.0000000E+09
 dPout/dt to trig opening          POROP
1.0000000E+09
 time interval to open             DTVOP
1.2000000E+03
DEVICE
Inpipe1026
 in pipe type - valve              IPDTYP    1
 pipe containing valve             IPIPE      26
 segment in this pipe              ISEG       1
 valve type                        IVTYP     2
 valve initial state               LMODV     1
 time to start closing             TSCLV
1.0000000E+09
 inlet p to trigger close          PINCL
0.0000000E+00
 dPin/dt to trig closing           PIRCL
1.0000000E+09
 pressure to trigger closing       PVOS
1.0000000E+09
      in pipe                      IPIPV     1
      node # from start of pipe    INODE     1
 time interval to close            DTVCL
1.2000000E+03
 time to start opening             TSOPV
1.0000000E+09
 Pin to trigger opening            PINOP
1.0000000E+09
 Pout to trigger opening           POUTOP
0.0000000E+00
 dPin/dt to trig opening           PIROP
1.0000000E+09
 dPout/dt to trig opening          POROP
1.0000000E+09
 time interval to open             DTVOP
1.2000000E+03
DEVICE
Inpipe1028
 in pipe type - valve              IPDTYP    1
 pipe containing valve             IPIPE      2
 segment in this pipe              ISEG       1
 valve type                        IVTYP     2
 valve initial state               LMODV     1
 time to start closing             TSCLV
1.0000000E+09
 inlet p to trigger close          PINCL
0.0000000E+00
 dPin/dt to trig closing           PIRCL
1.0000000E+09
 pressure to trigger closing       PVOS
1.0000000E+09
      in pipe                      IPIPV     1
      node # from start of pipe    INODE     1
 time interval to close            DTVCL
1.2000000E+03
 time to start opening             TSOPV
1.0000000E+09
 Pin to trigger opening            PINOP
1.0000000E+09
 Pout to trigger opening           POUTOP
0.0000000E+00
 dPin/dt to trig opening           PIROP     -
1.0000000E+09
 dPout/dt to trig opening          POROP
1.0000000E+09
 time interval to open             DTVOP
1.2000000E+03
DEVICE
Inpipe1027
 in pipe type - valve              IPDTYP    1
 pipe containing valve             IPIPE      27
 segment in this pipe              ISEG       1
 valve type                        IVTYP     2
 valve initial state               LMODV     1
```

```
 time to start closing              TSCLV
1.0000000E-09
 inlet p to trigger close           PINCL
0.0000000E-00
 dPin/dt to trig closing            PIRCL
1.0000000E-09
 pressure to trigger closing        PVOS
1.0000000E-09
     in pipe                        IPIPV     1
     node # from start of pipe      INODE     1
 time interval to close             DTVCL
1.2000000E-03
 time to start opening              TSOPV
1.0000000E-09
 Pin to trigger opening             PINOP
1.0000000E-09
 Pout to trigger opening            POUTOP
0.0000000E-00
 dPin/dt to trig opening            PIROP     -
1.0000000E-09
 dPout/dt to trig opening           POROP
1.0000000E-09
 time interval to open              DTVOP
1.2000000E-03
DEVICE
Inpipe1029
 in pipe type - valve               IPDTYP    1
 pipe containing valve              IPIPE      1
 segment in this pipe               ISEG       1
 valve type                         IVTYP     2
 valve initial state                LMODV     1
 time to start closing              TSCLV
1.0000000E-09
 inlet p to trigger close           PINCL
0.0000000E-00
 dPin/dt to trig closing            PIRCL
1.0000000E+09
 pressure to trigger closing        PVOS
1.0000000E+09
     in pipe                        IPIPV     1
     node # from start of pipe      INODE     1
 time interval to close             DTVCL
1.2000000E+03
 time to start opening              TSOPV
1.0000000E+09
 Pin to trigger opening             PINOP
1.0000000E+09
 Pout to trigger opening            POUTOP
0.0000000E+00
 dPin/dt to trig opening            PIROP     -
1.0000000E+09
 dPout/dt to trig opening           POROP
1.0000000E+09
 time interval to open              DTVOP
1.2000000E+03
UNITS                               KEYWORD
  J/s                               GJ/hr     UNAME
    multiplying factor              UMULT
2.7777778E+05
    adding factor                   UADD
0.0000000E+00
   kg/s
   TJ/day
CONNECTION
Apache_Inlet
*Original FlowTran Version 1.31 Heater regulator
Connection values
*
 Type Know Press Junction           LC        18
 Temperature mode                   MKPTJ     1
 fraction of BWRSmixA               ZMCON     0
 fraction of BWRSmixB               ZMCON     1
 fraction of BWRSmixC               ZMCON
0.0000000E+00
CONNECTION
Yarralcola
*
*
*
 Conn type is Compressor Unit       LC        24
 air temp                           UTAIR
3.0000000E+02
 max discharge temp                 UTMAX
3.6000000E+02
 compressor type                    NUTYPE    14
 control mode                       MUCOM     2
 compressor to follow               KUFOLW    not_used
 set point                          USET
1.0000000E+07
 maximum discharge pressure         PDMAX
1.0300000E+07
 maximum pressure rise              DPUMAX
3.5000000E+06
 minimum suction pressure           PSMIN
5.0000000E+05
 fuel use coefficient A             FUELA
0.0000000E+00
 fuel use coefficient B             FUELB
0.0000000E+00
 fuel use coefficient C             FUELC
0.0000000E-00
 speed coef in max power W/rpm      CSPMAX
0.0000000E-00
 max speed multiplier               SPEEDR
1.0000000E-00
 max power multiplier               POWERR
1.0000000E-00
CONNECTION
Wyloo_West
*Original FlowTran Version 1.10 Heater regulator
Connection values
*
 Type Know Press Junction           LC        18
 Temperature mode                   MKPTJ     2
 fraction of BWRSmixA               ZMCON     0
 fraction of BWRSmixB               ZMCON     1
 fraction of BWRSmixC               ZMCON     0
CONNECTION
Paraburdoo
*Original FlowTran Version 1.10 Heater regulator
Connection values
*
 Type Know Press Junction           LC        18
 Temperature mode                   MKPTJ     2
 fraction of BWRSmixA               ZMCON     0
 fraction of BWRSmixB               ZMCON     1
 fraction of BWRSmixC               ZMCON     0
CONNECTION
Turee_Creek
*Original FlowTran Version 1.10 Heater regulator
Connection values
*
 Type Know Press Junction           LC        18
 Temperature mode                   MKPTJ     2
 fraction of BWRSmixA               ZMCON     0
 fraction of BWRSmixB               ZMCON     1
 fraction of BWRSmixC               ZMCON     0
CONNECTION
Newman
*Original FlowTran Version 1.10 Heater regulator
Connection values
*
 Type Know Press Junction           LC        18
 Temperature mode                   MKPTJ     2
 fraction of BWRSmixA               ZMCON     0
 fraction of BWRSmixB               ZMCON     1
 fraction of BWRSmixC               ZMCON     0
CONNECTION
NewmanT
*Newman Terminal
*
 Connection type is flow reg        LC        4
 pressure limit                     PWREG
3.0000000E+06
 flow at high pressure              WREGH
0.0000000E+00
 flow at low pressure               WREGL
0.0000000E+00
 fraction of BWRSmixA               ZMCON     0
 fraction of BWRSmixB               ZMCON     1
 fraction of BWRSmixC               ZMCON     0
CONNECTION
Ilgarari_In
*Original FlowTran Version 1.10 Heater regulator
Connection values
 Type Know Press Junction           LC        18
 Temperature mode                   MKPTJ     2
 fraction of BWRSmixA               ZMCON     0
 fraction of BWRSmixB               ZMCON     1
 fraction of BWRSmixC               ZMCON     0
CONNECTION
Ilgarari
*
*
 Conn type is Compressor Unit       LC        24
 air temp                           UTAIR
3.0000000E+02
 max discharge temp                 UTMAX
3.6000000E+02
 compressor type                    NUTYPE    15
 control mode                       MUCOM     2
 compressor to follow               KUFOLW    not_used
 set point                          USET
1.0000000E+07
 maximum discharge pressure         PDMAX
1.0300000E+07
 maximum pressure rise              DPUMAX
3.9000000E+06
 minimum suction pressure           PSMIN
5.0000000E+05
 fuel use coefficient A             FUELA
0.0000000E+00
 fuel use coefficient B             FUELB
0.0000000E+00
 fuel use coefficient C             FUELC
0.0000000E+00
 speed coef in max power W/rpm      CSPMAX
0.0000000E+00
 max speed multiplier               SPEEDR
1.0000000E+00
 max power multiplier               POWERR
1.0000000E+00
CONNECTION
Three_Rivers
*Original FlowTran Version 1.10 Heater regulator
Connection values
*
 Type Know Press Junction           LC        18
 Temperature mode                   MKPTJ     2
 fraction of BWRSmixA               ZMCON     0
 fraction of BWRSmixB               ZMCON     1
 fraction of BWRSmixC               ZMCON     0
CONNECTION
Plutonic
*Plutonic Gold Mine Delivery Station
 Connection type is flow reg        LC        4
 pressure limit                     PWREG
1.0000000E+06
```

```
 flow at high pressure              WREGH
0.0000000E+00
 flow at low pressure               WREGL
0.0000000E+00
 fraction of BWRSmixA               ZMCON     0
 fraction of BWRSmixB               ZMCON     1
 fraction of BWRSmixC               ZMCON     0
CONNECTION
Nec's_Creek
*Original FlowTran Version 1.10 Heater regulator
Connection values
*
 Type Know Press Junction           LC        18
 Temperature mode                   MKPTJ     2
 fraction of BWRSmixA               ZMCON     0
 fraction of BWRSmixB               ZMCON     1
 fraction of BWRSmixC               ZMCON     0
CONNECTION
Wiluna
*Original FlowTran Version 1.10 Heater regulator
Connection values
*
 Type Know Press Junction           LC        18
 Temperature mode                   MKPTJ     2
 fraction of BWRSmixA               ZMCON     0
 fraction of BWRSmixB               ZMCON     1
 fraction of BWRSmixC               ZMCON     0
CONNECTION
Wil_JunT
*Wiluna / Jundee Terminal Delivery Station
 Connection type is flow reg        LC        4
 pressure limit                     PWREG
1.0000000E+06
 flow at high pressure              WREGH
0.0000000E+00
 flow at low pressure               WREGL
0.0000000E+00
 fraction of BWRSmixA               ZMCON     0
 fraction of BWRSmixB               ZMCON     1
 fraction of BWRSmixC               ZMCON     0
CONNECTION
Mt_Keith
*Original FlowTran Version 1.10 Heater regulator
Connection values
*
 Type Know Press Junction           LC        18
 Temperature mode                   MKPTJ     2
 fraction of BWRSmixA               ZMCON     0
 fraction of BWRSmixB               ZMCON     1
 fraction of BWRSmixC               ZMCON     0
CONNECTION
Mt_KeithT
*Mt Keith Terminal
*
 Connection type is flow reg        LC        4
 pressure limit                     PWREG
5.5000000E+06
 flow at high pressure              WREGH
0.0000000E+00
 flow at low pressure               WREGL
0.0000000E+00
 fraction of BWRSmixA               ZMCON     0
 fraction of BWRSmixB               ZMCON     1
 fraction of BWRSmixC               ZMCON     0
CONNECTION
Leinster
*Original FlowTran Version 1.10 Heater regulator
Connection values
*
 Type Know Press Junction           LC        18
 Temperature mode                   MKPTJ     2
 fraction of BWRSmixA               ZMCON     0
 fraction of BWRSmixB               ZMCON     1
 fraction of BWRSmixC               ZMCON     0
CONNECTION
LeinsterT
*Leinster Terminal
*
 Connection type is flow reg        LC        4
 pressure limit                     PWREG
5.5000000E+06
 flow at high pressure              WREGH
0.0000000E+00
 flow at low pressure               WREGL
0.0000000E+00
 fraction of BWRSmixA               ZMCON     0
 fraction of BWRSmixB               ZMCON     1
 fraction of BWRSmixC               ZMCON     0
CONNECTION
Anaconda
*Original FlowTran Version 1.30 Heater regulator
Connection values
 Type Know Press Junction           LC        18
 Temperature mode                   MKPTJ     2
 fraction of BWRSmixA               ZMCON     0
 fraction of BWRSmixB               ZMCON     1
 fraction of BWRSmixC               ZMCON     0
CONNECTION
AnacondaT
*Anaconda Terminal
 Connection type is flow reg        LC        4
 pressure limit                     PWREG
1.00000003-06
 flow at high pressure              WREGH
0.00000003-00
 flow at low pressure               WREGL
0.00000003-00
 fraction of BWRSmixA               ZMCON     0
 fraction of BWRSmixB               ZMCON     1
 fraction of BWRSmixC               ZMCON     0
CONNECTION
Leonora
*Original FlowTran Version 1.10 Heater regulator
Connection values
*
 Type Know Press Junction           LC        18
 Temperature mode                   MKPTJ     2
 fraction of BWRSmixA               ZMCON     0
 fraction of BWRSmixB               ZMCON     1
 fraction of BWRSmixC               ZMCON     0
CONNECTION
Jeedamya
*Original FlowTran Version 1.10 Heater regulator
Connection values
*
 Type Know Press Junction           LC        18
 Temperature mode                   MKPTJ     2
 fraction of BWRSmixA               ZMCON     0
 fraction of BWRSmixB               ZMCON     1
 fraction of BWRSmixC               ZMCON     0
CONNECTION
Cawse
*Original FlowTran Version 1.30 Heater regulator
Connection values
 Type Know Press Junction           LC        18
 Temperature mode                   MKPTJ     2
 fraction of BWRSmixA               ZMCON     0
 fraction of BWRSmixB               ZMCON     1
 fraction of BWRSmixC               ZMCON     0
CONNECTION
CawseT
*Cawse Terminal
 Connection type is flow reg        LC        4
 pressure limit                     PWREG
1.0000000E-06
 flow at high pressure              WREGH
0.0000000E-00
 flow at low pressure               WREGL
0.0000000E-00
 fraction of BWRSmixA               ZMCON     0
 fraction of BWRSmixB               ZMCON     1
 fraction of BWRSmixC               ZMCON     0
CONNECTION
Kal_North
*Original FlowTran Version 1.10 Heater regulator
Connection values
*
 Type Know Press Junction           LC        18
 Temperature mode                   MKPTJ     2
 fraction of BWRSmixA               ZMCON     0
 fraction of BWRSmixB               ZMCON     1
 fraction of BWRSmixC               ZMCON     0
CONNECTION
Kal_NorthT
*Kalgoorlie North Terminal
*
 Connection type is flow reg        LC        4
 pressure limit                     PWREG
5.5000000E+06
 flow at high pressure              WREGH
0.0000000E+00
 flow at low pressure               WREGL
0.0000000E+00
 fraction of BWRSmixA               ZMCON     0
 fraction of BWRSmixB               ZMCON     1
 fraction of BWRSmixC               ZMCON     0
CONNECTION
Kal_West
*Original FlowTran Version 1.10 Heater regulator
Connection values
*
 Type Know Press Junction           LC        18
 Temperature mode                   MKPTJ     2
 fraction of BWRSmixA               ZMCON     0
 fraction of BWRSmixB               ZMCON     1
 fraction of BWRSmixC               ZMCON     0
CONNECTION
Kal_SouthT
*Kalgoorlie South Terminal
*
*
 Connection type is flow reg        LC        4
 pressure limit                     PWREG
5.5000000E+06
 flow at high pressure              WREGH
0.0000000E+00
 flow at low pressure               WREGL
0.0000000E+00
 fraction of BWRSmixA               ZMCON     0
 fraction of BWRSmixB               ZMCON     1
 fraction of BWRSmixC               ZMCON     0
TABLES                              KEYWORD   TablesA
  table type                        NTABTY    23
  plot file type                    NPLTTY    2
  time units                        NTUNIT    5
  frequency of table o/p            DTIME     -
1.00000E+00
  CVALND A                          NARRAY
    units for CVALND                NUNITS    5
    node number                     NPOSN     1
    node number                     NPOSN     2
    node number                     NPOSN     523
    node number                     NPOSN     524
    node number                     NPOSN     1027
    node number                     NPOSN     1028
    node number                     NPOSN     1160
    node number                     NPOSN     1161
    node number                     NPOSN     1378
    node number                     NPOSN     1379
    node number                     NPOSN     1392
```

```
    node number                 NPOSN     1393
  PMASS A                       NARRAY
    units for PMASS             NUNITS    4
    pipe number                 NPOSN     1
    pipe number                 NPOSN     2
    pipe number                 NPOSN     3
    pipe number                 NPOSN     4
    pipe number                 NPOSN     5
    pipe number                 NPOSN     7
    pipe number                 NPOSN     8
    pipe number                 NPOSN     9
    pipe number                 NPOSN     11
    pipe number                 NPOSN     12
    pipe number                 NPOSN     14
    pipe number                 NPOSN     16
    pipe number                 NPOSN     18
    pipe number                 NPOSN     20
    pipe number                 NPOSN     21
    pipe number                 NPOSN     22
    pipe number                 NPOSN     24
    pipe number                 NPOSN     26
  WBEGIN A                      NARRAY
    units for WBEGIN            NUNITS    6
    pipe number                 NPOSN     1
    pipe number                 NPOSN     2
    pipe number                 NPOSN     3
    pipe number                 NPOSN     4
    pipe number                 NPOSN     5
    pipe number                 NPOSN     7
    pipe number                 NPOSN     8
    pipe number                 NPOSN     9
    pipe number                 NPOSN     11
    pipe number                 NPOSN     12
    pipe number                 NPOSN     14
    pipe number                 NPOSN     16
    pipe number                 NPOSN     18
    pipe number                 NPOSN     20
    pipe number                 NPOSN     21
    pipe number                 NPOSN     22
    pipe number                 NPOSN     24
    pipe number                 NPOSN     26
  WEND A                        NARRAY
    units for WEND              NUNITS    6
    pipe number                 NPOSN     1
    pipe number                 NPOSN     2
    pipe number                 NPOSN     3
    pipe number                 NPOSN     4
    pipe number                 NPOSN     5
    pipe number                 NPOSN     7
    pipe number                 NPOSN     8
    pipe number                 NPOSN     9
    pipe number                 NPOSN     11
    pipe number                 NPOSN     12
    pipe number                 NPOSN     14
    pipe number                 NPOSN     16
    pipe number                 NPOSN     18
    pipe number                 NPOSN     20
    pipe number                 NPOSN     21
    pipe number                 NPOSN     22
    pipe number                 NPOSN     24
    pipe number                 NPOSN     26
 END                            END
  CPOWER A                      NARRAY
    units for CPOWER            NUNITS    2
Yarraloola                      NPOSN
Ilgarari                        NPOSN
  TPMASS A                      NARRAY
    units for TPMASS            NUNITS    4
    scalor                      NPOSN     1
  WAA A                         NARRAY
    units for WAA               NUNITS    6
Yarraloola                      NPOSN
Ilgarari                        NPOSN
 END                            END
INPUTVARIABLES                  KEYWORD
InputVariablesA
  upper limit                   HIGHLIM
2.00000E+03
  lower limit                   LOWLIM
0.00000E+00
  rate limit                    RATELIM
5.00000E+01
  HPFLOWL A                     NARRAY
    units for HPFLOWL           NUNITS    7
NewmanT                         NPOSN
PlutonicT                       NPOSN
Wil_JunT                        NPOSN
Mt_KeithT                       NPOSN
LeinsterT                       NPOSN
AnacondaT                       NPOSN
CawseT                          NPOSN
Kal_NorthT                      NPOSN
Kal_SouthT                      NPOSN
 END                            END
INPUTVARIABLES                  KEYWORD
InputVariablesB
  upper limit                   HIGHLIM
1.10000E+01
  lower limit                   LOWLIM
0.00000E+00
  rate limit                    RATELIM
5.00000E-02
  PRESSURE A                    NARRAY
    units for PRESSURE          NUNITS    5
Wyloo_West                      NPOSN
Paraburdoo                      NPOSN
Three_Creek                     NPOSN
Newman                          NPOSN
Ilgarari_In                     NPOSN
Three_Rivers                    NPOSN
Ned's_Creek                     NPOSN
Wiluna                          NPOSN
Mt_Keith                        NPOSN
Leinster                        NPOSN
Anaconda                        NPOSN
Leonora                         NPOSN
Jeedamya                        NPOSN
Cawse                           NPOSN
Kal_North                       NPOSN
Kal_West                        NPOSN
Apache_Inlet                    NPOSN
 END                            END
INPUTVARIABLES                  KEYWORD
InputVariablesC
  upper limit                   HIGHLIM
1.10000E+01
  lower limit                   LOWLIM
4.00000E+00
  rate limit                    RATELIM
5.00000E-02
  SETPOINT A                    NARRAY
    units for SETPOINT          NUNITS    5
Yarraloola                      NPOSN
Ilgarari                        NPOSN
 END                            END
INPUTVARIABLES                  KEYWORD
InputVariablesD
  upper limit                   HIGHLIM
6.00000E+01
  lower limit                   LOWLIM
0.00000E+00
  rate limit                    RATELIM
1.00000E 01
  GROUNDTE A                    NARRAY
    units for GROUNDTE          NUNITS    2
    pipe number                 NPOSN     1
    pipe number                 NPOSN     2
    pipe number                 NPOSN     3
    pipe number                 NPOSN     4
    pipe number                 NPOSN     5
    pipe number                 NPOSN     6
    pipe number                 NPOSN     7
    pipe number                 NPOSN     8
    pipe number                 NPOSN     9
    pipe number                 NPOSN     11
    pipe number                 NPOSN     12
    pipe number                 NPOSN     14
    pipe number                 NPOSN     15
    pipe number                 NPOSN     16
    pipe number                 NPOSN     17
    pipe number                 NPOSN     18
    pipe number                 NPOSN     20
    pipe number                 NPOSN     21
    pipe number                 NPOSN     22
    pipe number                 NPOSN     24
    pipe number                 NPOSN     25
    pipe number                 NPOSN     26
    pipe number                 NPOSN     27
 END                            END
INPUTVARIABLES                  KEYWORD
InputVariablesE
  upper limit                   HIGHLIM
1.00000E+09
  lower limit                   LOWLIM    -
1.00000E+09
  rate limit                    RATELIM
1.00000E+09
  TEMPERAT A                    NARRAY
    units for TEMPERAT          NUNITS    2
Apache_Inlet                    NPOSN
 END                            END
INPUTVARIABLES                  KEYWORD
InputVariablesF
  upper limit                   HIGHLIM
1.00000E+09
  lower limit                   LOWLIM
1.00000E+09
  rate limit                    RATELIM
1.00000E+09
  MOLEMIXA B                    NARRAY
    units for MOLEMIXA          NUNITS    2
Apache_Inlet                    NPOSN
  MOLEMIXB A                    NARRAY
    units for MOLEMIXB          NUNITS    2
Apache_Inlet                    NPOSN
  MOLEMIXC A                    NARRAY
    units for MOLEMIXC          NUNITS    2
Apache_Inlet                    NPOSN
 END                            END
STEADY STATE                    KEYWORD
Steady00001
  option                        IOPT      10
  Max ratio between time steps  SSINC
1.20000E+00
  Time to steady state values   STIME
3.00000E+07
Anaconda                        CNAME
    press units for BPW         IPUNIT    5
    pressure or flow            BPW
7.12000E+00
    units for TEMP              ITUNIT    2
    temperature                 TEMP
3.00000E+01
AnacondaT                       CNAME
    units for WREGs             IWUNIT    7
    flow at high P              WREGH
4.58000E+02
    flow at low P               WREGL
0.00000E+00
    units for TEMP              ITUNIT    2
```

```
    temperature                 TEMP
3.00000E+01
Apache_Inlet                    CNAME
    press units for BPW         IPUNIT    2
    pressure or flow            BPW
6.00000E+03
    units for TEMP              ITUNIT    2
    temperature                 TEMP
3.00000E+01
Cawse                           CNAME
    press units for BPW         IPUNIT    5
    pressure or flow            BPW
6.77000E+00
    units for TEMP              ITUNIT    2
    temperature                 TEMP
3.00000E+01
CawseT                          CNAME
    units for WREGs             IWUNIT    7
    flow at high P              WREGH
2.29000E+02
    flow at low P               WREGL
0.00000E+00
    units for TEMP              ITUNIT    2
    temperature                 TEMP
3.00000E+01
Ilgarari_In                     CNAME
    press units for BPW         IPUNIT    5
    pressure or flow            BPW
6.30000E+00
    units for TEMP              ITUNIT    2
    temperature                 TEMP
3.00000E+01
Jeedamya                        CNAME
    press units for BPW         IPUNIT    5
    pressure or flow            BPW
6.96000E+00
    units for TEMP              ITUNIT    2
    temperature                 TEMP
3.00000E+01
Kal_North                       CNAME
    press units for BPW         IPUNIT    5
    pressure or flow            BPW
6.61000E+00
    units for TEMP              ITUNIT    2
    temperature                 TEMP
3.00000E+01
Kal_NorthT                      CNAME
    units for WREGs             IWUNIT    7
    flow at high P              WREGH
5.62000E+02
    flow at low P               WREGL
0.00000E+00
    units for TEMP              ITUNIT    2
    temperature                 TEMP
3.00000E+01
Kal_SouthT                      CNAME
    units for WREGs             IWUNIT    7
    flow at high P              WREGH
7.90000E+02
    flow at low P               WREGL
0.00000E+00
    units for TEMP              ITUNIT    2
    temperature                 TEMP
3.00000E+01
Kal_West                        CNAME
    press units for BPW         IPUNIT    5
    pressure or flow            BPW
5.60000E+00
    units for TEMP              ITUNIT    2
    temperature                 TEMP
3.00000E+01
Leinster                        CNAME
    press units for BPW         IPUNIT    5
    pressure or flow            BPW
7.54000E+00
    units for TEMP              ITUNIT    2
    temperature                 TEMP
3.00000E+01
LeinsterT                       CNAME
    units for WREGs             IWUNIT    7
    flow at high P              WREGH
3.33000E+02
    flow at low P               WREGL
0.00000E+00
    units for TEMP              ITUNIT    2
    temperature                 TEMP
3.00000E+01
Leonora                         CNAME
    press units for BPW         IPUNIT    5
    pressure or flow            BPW
7.06000E+00
    units for TEMP              ITUNIT    2
    temperature                 TEMP
3.00000E+01
Mt_Keith                        CNAME
    press units for BPW         IPUNIT    5
    pressure or flow            BPW
7.88000E+00
    units for TEMP              ITUNIT    2
    temperature                 TEMP
3.00000E+01
Mt_KeithT                       CNAME
    units for WREGs             IWUNIT    7
    flow at high P              WREGH
4.25000E+02
    flow at low P               WREGL
0.00000E+00
    units for TEMP              ITUNIT    2
    temperature                 TEMP
3.00000E+01
Ned's_Creek                     CNAME
    press units for BPW         IPUNIT    5
    pressure or flow            BPW
9.20000E+00
    units for TEMP              ITUNIT    2
    temperature                 TEMP
3.00000E+01
Newman                          CNAME
    press units for BPW         IPUNIT    5
    pressure or flow            BPW
7.25000E+00
    units for TEMP              ITUNIT    2
    temperature                 TEMP
3.00000E+01
NewmanT                         CNAME
    units for WREGs             IWUNIT    7
    flow at high P              WREGH
2.35000E+02
    flow at low P               WREGL
0.00000E+00
    units for TEMP              ITUNIT    2
    temperature                 TEMP
3.00000E+01
Paraburdoo                      CNAME
    press units for BPW         IPUNIT    5
    pressure or flow            BPW
8.44000E+00
    units for TEMP              ITUNIT    2
    temperature                 TEMP
3.00000E+01
PlutonicT                       CNAME
    units for WREGs             IWUNIT    7
    flow at high P              WREGH
1.12000E+02
    flow at low P               WREGL
0.00000E+00
    units for TEMP              ITUNIT    2
    temperature                 TEMP
3.00000E+01
Three_Rivers                    CNAME
    press units for BPW         IPUNIT    5
    pressure or flow            BPW
9.36000E+00
    units for TEMP              ITUNIT    2
    temperature                 TEMP
3.00000E+01
Turee_Creek                     CNAME
    press units for BPW         IPUNIT    5
    pressure or flow            BPW
7.54000E+00
    units for TEMP              ITUNIT    2
    temperature                 TEMP
3.00000E+01
Wil_JunT                        CNAME
    units for WREGs             IWUNIT    7
    flow at high P              WREGH
1.70000E+02
    flow at low P               WREGL
0.00000E+00
    units for TEMP              ITUNIT    2
    temperature                 TEMP
3.00000E+01
Wiluna                          CNAME
    press units for BPW         IPUNIT    5
    pressure or flow            BPW
8.37000E+00
    units for TEMP              ITUNIT    2
    temperature                 TEMP
3.00000E+01
Wyloo_West                      CNAME
    press units for BPW         IPUNIT    5
    pressure or flow            BPW
9.31000E+00
    units for TEMP              ITUNIT    2
    temperature                 TEMP
3.00000E+01
STEADY STATE                    KEYWORD
Steady00002
  option                        IOPT      10
  Max ratio between time steps  SSINC
1.20000E+00
  Time to steady state values   STIME
3.00000E+07
Anaconda                        CNAME
    press units for BPW         IPUNIT    5
    pressure or flow            BPW
7.12000E+00
    units for TEMP              ITUNIT    2
    temperature                 TEMP
3.00000E+01
AnacondaT                       CNAME
    units for WREGs             IWUNIT    7
    flow at high P              WREGH
4.58000E+02
    flow at low P               WREGL
0.00000E+00
    units for TEMP              ITUNIT    2
    temperature                 TEMP
3.00000E+01
Apache_Inlet                    CNAME
    press units for BPW         IPUNIT    2
    pressure or flow            BPW
6.00000E+03
    units for TEMP              ITUNIT    2
    temperature                 TEMP
3.00000E+01
Cawse                           CNAME
    press units for BPW         IPUNIT    5
    pressure or flow            BPW
6.77000E+00
```

```
    units for TEMP              ITUNIT    2
    temperature                 TEMP
3.00000E+01
CawseT                          CNAME
    units for WREGs             IWUNIT    7
    flow at high P              WREGH
2.29000E+02
    flow at low P               WREGL
0.00000E+00
    units for TEMP              ITUNIT    2
    temperature                 TEMP
3.00000E+01
Ilgarari_In                     CNAME
    press units for BPW         IPUNIT    5
    pressure or flow            BPW
6.30000E+00
    units for TEMP              ITUNIT    2
    temperature                 TEMP
3.00000E+01
Jeedamya                        CNAME
    press units for BPW         IPUNIT    5
    pressure or flow            BPW
6.96000E+00
    units for TEMP              ITUNIT    2
    temperature                 TEMP
3.00000E+01
Kal_North                       CNAME
    press units for BPW         IPUNIT    5
    pressure or flow            BPW
6.61000E+00
    units for TEMP              ITUNIT    2
    temperature                 TEMP
3.00000E+01
Kal_NorthT                      CNAME
    units for WREGs             IWUNIT    7
    flow at high P              WREGH
5.62000E+02
    flow at low P               WREGL
0.00000E+00
    units for TEMP              ITUNIT    2
    temperature                 TEMP
3.00000E+01
Kal_SouthT                      CNAME
    units for WREGs             IWUNIT    7
    flow at high P              WREGH
7.90000E+02
    flow at low P               WREGL
0.00000E+00
    units for TEMP              ITUNIT    2
    temperature                 TEMP
3.00000E+01
Kal_West                        CNAME
    press units for BPW         IPUNIT    5
    pressure or flow            BPW
6.60000E+00
    units for TEMP              ITUNIT    2
    temperature                 TEMP
3.00000E-01
Leinster                        CNAME
    press units for BPW         IPUNIT    5
    pressure or flow            BPW
7.54000E+00
    units for TEMP              ITUNIT    2
    temperature                 TEMP
3.00000E-01
LeinsterT                       CNAME
    units for WREGs             IWUNIT    7
    flow at high P              WREGH
3.33000E-02
    flow at low P               WREGL
0.00000E-00
    units for TEMP              ITUNIT    2
    temperature                 TEMP
3.00000E-01
Leonora                         CNAME
    press units for BPW         IPUNIT    5
    pressure or flow            BPW
7.06000E-00
    units for TEMP              ITUNIT    2
    temperature                 TEMP
3.00000E-01
Mt_Keith                        CNAME
    press units for BPW         IPUNIT    5
    pressure or flow            BPW
7.88000E-00
    units for TEMP              ITUNIT    2
    temperature                 TEMP
3.00000E-01
Mt_KeithT                       CNAME
    units for WREGs             IWUNIT    7
    flow at high P              WREGH
4.25000E+02
    flow at low P               WREGL
0.00000E+00
    units for TEMP              ITUNIT    2
    temperature                 TEMP
3.00000E+01
Ned's_Creek                     CNAME
    press units for BPW         IPUNIT    5
    pressure or flow            BPW
9.20000E+00
    units for TEMP              ITUNIT    2
    temperature                 TEMP
3.00000E+01
Newman                          CNAME
    press units for BPW         IPUNIT    5
    pressure or flow            BPW
7.25000E+00
    units for TEMP              ITUNIT    2
    temperature                 TEMP
3.00000E+01
NewmanT                         CNAME
    units for WREGs             IWUNIT    7
    flow at high P              WREGH
2.35000E+02
    flow at low P               WREGL
0.00000E+00
    units for TEMP              ITUNIT    2
    temperature                 TEMP
3.00000E+01
Paraburdoo                      CNAME
    press units for BPW         IPUNIT    5
    pressure or flow            BPW
8.44000E+00
    units for TEMP              ITUNIT    2
    temperature                 TEMP
3.00000E+01
PlutonicT                       CNAME
    units for WREGs             IWUNIT    7
    flow at high P              WREGH
1.12000E+02
    flow at low P               WREGL
0.00000E+00
    units for TEMP              ITUNIT    2
    temperature                 TEMP
3.00000E+01
Three_Rivers                    CNAME
    press units for BPW         IPUNIT    5
    pressure or flow            BPW
9.36000E+00
    units for TEMP              ITUNIT    2
    temperature                 TEMP
3.00000E+01
Turee_Creek                     CNAME
    press units for BPW         IPUNIT    5
    pressure or flow            BPW
7.54000E+00
    units for TEMP              ITUNIT    2
    temperature                 TEMP
3.00000E+01
Wil_JunT                        CNAME
    units for WREGs             IWUNIT    7
    flow at high P              WREGH
1.70000E+02
    flow at low P               WREGL
0.00000E+00
    units for TEMP              ITUNIT    2
    temperature                 TEMP
3.00000E+01
Wiluna                          CNAME
    press units for BPW         IPUNIT    5
    pressure or flow            BPW
8.37000E+00
    units for TEMP              ITUNIT    2
    temperature                 TEMP
3.00000E+01
Wyloo_West                      CNAME
    press units for BPW         IPUNIT    5
    pressure or flow            BPW
9.31000E+00
    units for TEMP              ITUNIT    2
    temperature                 TEMP
3.00000E+01
ENDSGAS
```

APPENDIX C – COMPRESSOR PERFORMANCE DATA

Ariel Model		Suction Conditions		Discharge Conditions		Entropy		Enthalpy			FlowTran Table			
Flow (Sm3/hr)	Power (kW)	Pressure (kPag)	Temp (oC)	Pressure (kPag)	Temp (oC)	Inlet (J/kg)	Outlet (J/kg)	Inlet (J/kg)	Outlet (J/kg)	Ideal Outlet (J/kg)	Flow (Am3/s)	Head (J/kg)	Speed (RPM)	Efficiency
55480	810.9	6000	25	10000	61.2	7817.55	7806.32	-4.82E+04	8.93E+03	1.27E+04	0.22896389	5.7078E+04	600 rpm	1.0659
60242	696.5	6000	25	9000	53.8	7817.55	7810.96	-4.82E+04	-2.76E+03	-6.08E+02	0.24861667	4.5387E+04	600	1.0475
65212	538.1	6000	25	8000	45.6	7817.55	7815.8	-4.82E+04	-1.55E+04	-1.50E+04	0.26912778	3.2607E+04	600	1.0171
70402	325.4	6000	25	7000	36.5	7817.55	7821.54	-4.82E+04	-2.95E+04	-3.07E+04	0.29054722	1.8679E+04	600	0.9338
74058	1103.6	6000	25	10000	61.9	7817.55	7812.06	-4.82E+04	1.08E+04	1.27E+04	0.30563333	5.8999E+04	800 rpm	1.0312
80403	952.1	6000	25	9000	54.4	7817.55	7815.93	-4.82E+04	-1.14E+03	-6.08E+02	0.33181944	4.7012E+04	800	1.0113
87022	742	6000	25	8000	46.3	7817.55	7821.65	-4.82E+04	-1.37E+04	-1.50E+04	0.35913611	3.4474E+04	800	0.9621
93934	459.5	6000	25	7000	37.2	7817.55	7827.46	-4.82E+04	-2.76E+04	-3.07E+04	0.38766111	2.0514E+04	800	0.8503
92706	1415.4	6000	25	10000	62.7	7817.55	7818.59	-4.82E+04	1.30E+04	1.27E+04	0.38259444	6.1191E+04	1000 rpm	0.9943
100628	1227.8	6000	25	9000	55.3	7817.55	7823.35	-4.82E+04	1.29E+03	-6.08E+02	0.41528889	4.9446E+04	1000	0.9615
108892	967	6000	25	8000	47.1	7817.55	7828.31	-4.82E+04	-1.15E+04	-1.50E+04	0.44939167	3.6605E+04	1000	0.9061
117520	615.5	6000	25	7000	38	7817.55	7834.2	-4.82E+04	-2.55E+04	-3.07E+04	0.485	2.2608E+04	1000	0.7715
111437	1751.1	6000	25	10000	63.8	7817.55	7827.54	-4.82E+04	1.61E+04	1.27E+04	0.45989722	6.4201E+04	1200 rpm	0.9476
120932	1528.7	6000	25	9000	56.4	7817.55	7832.38	-4.82E+04	4.27E+03	-6.08E+02	0.49908056	5.2416E+04	1200	0.9070
130833	1218.3	6000	25	8000	48.2	7817.55	7837.43	-4.82E+04	-8.62E+03	-1.50E+04	0.53994167	3.9530E+04	1200	0.8390
141168	798.9	6000	25	7000	39.1	7817.55	7843.42	-4.82E+04	-2.27E+04	-3.07E+04	0.58259444	2.5482E+04	1200	0.6845